REACTOR MATERIALS

A Quarterly Technical Progress Review

Prepared for DIVISION OF TECHNICAL INFORMATION, USAEC, by
R. W. DAYTON, E. M. SIMONS, and ASSOCIATES, BATTELLE MEMORIAL INSTITUTE

Fall 1965

● VOLUME 8

● NUMBER 3

TECHNICAL PROGRESS REVIEWS

To meet the needs of industry for concise summaries of current atomic developments, the Atomic Energy Commission is publishing this series, Technical Progress Reviews. Issued quarterly, each of the reviews digests and evaluates the latest findings in a specific area of nuclear technology and science.

The five journals published in this series are:

Isotopes and Radiation Technology, P. S. Baker, A. F. Rupp, and associates, Oak Ridge National Laboratory

Nuclear Safety, Wm. B. Cottrell, W. H. Jordan, and associates, Oak Ridge National Laboratory

Power Reactor Technology, Argonne National Laboratory

Reactor Fuel Processing, Stephen Lawroski and associates, Chemical Engineering Division, Argonne National Laboratory

Reactor Materials, R. W. Dayton, E. M. Simons, and associates, Battelle Memorial Institute

Each journal may be purchased from the Superintendent of Documents, U. S. Government Printing Office, Washington, D. C., 20402. *Isotopes and Radiation Technology* at $2.00 per year for subscription or $0.55 for individual issues; the other four journals at $2.50 per year and $0.70 per issue. See back cover for remittance instructions and foreign postage requirements.

The views expressed in this publication do not necessarily represent those of the United States Atomic Energy Commission, its divisions or offices, or of any Commission advisory committee or contractor.

Availability of Reports Cited in This Review

Unclassified AEC reports are available for inspection at AEC depository libraries and are sold by the Clearinghouse for Federal Scientific and Technical Information, National Bureau of Standards, U. S. Department of Commerce, 5285 Port Royal Road, Springfield, Va., 22151. Some of the reports cited are not available owing to their preliminary nature; however, the information contained in them will eventually be made available in formal progress or topical reports.

Unclassified reports issued by other Government agencies or private organizations should be requested from the originator.

Unclassified British and Canadian reports may be inspected at AEC depository libraries. British reports are sold by the British Information Service, 45 Rockefeller Plaza, New York, N. Y.; Canadian reports (AECL series) are sold by the Scientific Document Distribution Office, Atomic Energy of Canada, Ltd., Chalk River, Ontario, Canada.

Classified U. S. and foreign reports identified in this journal as Classified may be purchased by properly cleared Access Permit Holders from the Division of Technical Information Extension, U. S. Atomic Energy Commission, P. O. Box 1001, Oak Ridge, Tenn., 37831. Such reports may be inspected at classified AEC depository libraries.

REACTOR MATERIALS

A REVIEW OF RECENT DEVELOPMENTS

Prepared for DIVISION OF TECHNICAL INFORMATION, USAEC,
by R. W. DAYTON, E. M. SIMONS, and ASSOCIATES,
BATTELLE MEMORIAL INSTITUTE

FALL 1965

VOLUME 8

NUMBER 3

Foreword

Reactor Materials is one of a series of quarterly technical progress reviews broadly covering the field of nuclear science and technology. Under the auspices of the USAEC Division of Technical Information, *Reactor Materials* is prepared by Battelle personnel from worldwide literature. It covers properties, behavior, and fabrication processes of materials applicable to nuclear reactor components and associated equipment.

The reader will recognize that the scope of this Review is too broad to permit detailed coverage of every topic. Rather, the authors and editors attempt to combine the highlights of significant new developments into an information summary of current research for both management and the technical specialist. As a rule, enough of the results are presented to define the research and summarize the findings. For readers desiring more information on any particular topic, a complete set of references is provided at the end of each section.

Each quarter, a number of bibliographies, monographs, and books appear on subjects within the scope of *Reactor Materials*. Although the main purpose of this Review is to call attention to findings that are new and significant, such publications are noted in the text because they often represent excellent compilations of available information on important materials topics.

R. W. DAYTON
E. M. SIMONS
R. W. ENDEBROCK
Battelle Memorial Institute

DEPOSITED BY THE
UNITED STATES OF AMERICA

Contents

I Fuel and Fertile Materials 119
Uranium Metal and Alloys 119
Plutonium 121
Thorium Compounds 124
Metal-Ceramic Fuels 124
Coated-Particle Fuel Materials 125
Uranium Oxides 127
Uranium and Thorium Carbides, Nitrides, and Phosphides 129
Basic Studies of Irradiation Effects in Fuel Materials 130
References 132

II Moderator Materials 135
Graphite 135
Beryllium Metals and Alloys 136
Beryllium Oxide 137
Solid Hydrides 137
References 138

III Nuclear Poisons 139
Metallic Poison Materials 139
Dispersions and Nonmetallic Poison Materials 140
References 141

IV Cladding and Structural Materials . 142
Corrosion 142
Selected Mechanical Properties of Structural and Cladding Materials . . 147
Metallurgical Aspects of Cladding and Structural Materials 149
Diffusion Studies 153
Ceramic Technology 154
Radiation Effects in Nonfuel Materials . . 155
References 160

V Special Fabrication Techniques . . . 163
Melting, Casting, and Hot and Cold Working 163
Cladding 164
Explosive Forming 167
Welding and Brazing 167
Nondestructive Testing 171
References 172

Issued quarterly by the U. S. Atomic Energy Commission. Use of funds for printing this publication approved by the Director of the Bureau of the Budget on October 14, 1963.

Section

I

Reactor Materials

Fuel and Fertile Materials

Uranium Metal and Alloys

Unalloyed Uranium

The first volume[1] of the Materials Division of the International Monograph Series on Nuclear Energy has a significant portion devoted to uranium. Information is presented on: the history, occurrence, and uses of uranium; extraction from its ores; fabrication; properties; alloy studies; and toxic hazards and safety precautions.

The proceedings[2] of a meeting on the X-ray analysis of uranium have been published. The papers discuss techniques for the measurement of grain orientation in uranium and for the prediction of irradiation growth in uranium fuel elements because of preferred grain orientation. Presentations on X-ray diffraction describe intersite exchange of standards, X-ray diffraction from highly radioactive materials, techniques for measuring texture gradients, and the measurement of grain size from statistical fluctuation in X-ray diffraction intensity. The papers on preferred-orientation measurements include the effects of various heat-treatments and fabrication procedures on the texture, texture gradients, and grain size of uranium fuel elements of various geometrical shapes. Other papers are concerned with the development of theories for predicting irradiation growth. These cover the strain-tensor theory for irradiation growth, the form of theory that would include the interaction between grains during growth, deformation modes of uranium single crystals, and crystal-structure variations in uranium at low temperatures.

Investigations of the sintering mechanisms of powdered uranium[3] and in-pile swelling of unalloyed uranium[4] have been reported by the French.

Alpha-Phase Uranium Alloys

Investigators at Mallinckrodt Chemical Works[5] have determined the boundaries and phase fields in uranium alloys containing 80 to 4000 ppm aluminum at temperatures from 600 to 1200°C. Differential thermal, metallographic, and microprobe analyses were employed in arriving at the diagram shown in Fig. I-1.

A uranium-alloy-development study was performed by Nuclear Metals Division of Textron Inc.[6] to develop a suitable metallic fuel for heavy-water power reactors. It was hypothesized that the fuel should (1) contain a large number of finely dispersed particles that would be stable at reactor temperatures, (2) have high strength, and (3) be capable of being fabricated into fuel elements. Promising alloys, based on U–350 ppm Fe–900 ppm Al, were prepared by vacuum-induction melting and then extruded as rod. The materials were evaluated by metallographic and hot-hardness tests to assess the effects of composition and heat-treatment.

The microstructure of U–350 ppm Fe–900 ppm Al was responsive to heat-treatment. The alloying elements could be dissolved at temperatures in the beta and gamma phases, as predicted by the binary-equilibrium diagrams. Oil quenching from the solution temperatures was adequate to inhibit precipitation of the alloy phases U_6Fe and UAl_2. Slower cooling, such as air cooling from the gamma phase (and the cooling of a casting), allowed precipitation to occur at high-temperature phase boundaries,* thereby forming a network structure. A uni-

*The 900 ppm aluminum exceeds the solubility limit in beta-phase uranium.

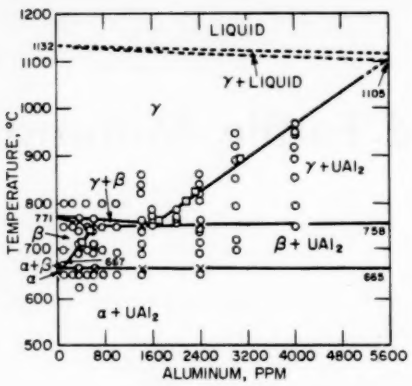

Fig. I-1 Uranium-aluminum equilibrium-phase diagram.[5] ○, optical metallography; □, electron microprobe analysis; ×, differential-thermal-analysis arrests.

form distribution of precipitated particles was observed in U-Fe-Al that had been extruded in the alpha phase and then beta treated and oil quenched. The particles are most probably UAl_2, and the iron is believed to be held in supersaturated solution. The concentration of particles about 0.1 μ in diameter was about 2×10^8 particles/cm^2. Subsequent alpha-phase aging of the beta-quenched alloy allows precipitation of the U_6Fe. The fine UAl_2 particles are stable during aging treatments as severe as 100 hr to 600°C, whereas the U_6Fe particles readily grow in size to several microns and tend to locate at the alpha-phase grain boundaries.

In extruded and beta-treated U–350 ppm Fe–900 ppm Al, additions of up to 1100 ppm silicon or up to 500 ppm chromium have no significant effect on the size and distribution of the fine precipitates (particles in the 0.1-μ range). Aging a U–800 ppm Si alloy for 100 hr at 600°C increases the fine-particle population. This does not occur, however, in the above U-Fe-Al alloy to which up to 1100 ppm silicon has been added. After aging of the chromium-bearing U-Fe-Al alloys for 100 hr at 600°C, a coarse boundary phase is observed that is believed to be chromium. This suggests that the solubility of chromium at 600°C is less than 150 ppm.

The hot hardness of uranium is related to the impurity and/or alloy content and heat-treatment. In unalloyed uranium that has been beta treated, impurities such as iron and silicon cause a marked hardening, particularly in the 200 to 400°C range. The hardening due to these impurities can be substantially reduced by aging treatments in the high alpha phase.

The addition of 350 ppm iron and 900 ppm aluminum increases the hardness of beta-treated uranium. Subsequent aging in the high alpha phase causes only softening. After an aging treatment of 100 hr at 600°C, the U-Fe-Al is still harder than unalloyed uranium. During aging, precipitation of alloy phases occurs concurrently with softening and indicates that the beta-treated alloy is hardened primarily by solid-solution hardening. In contrast to beta-treated U-Fe-Al, the gamma-treated alloy experienced precipitation hardening during aging.

The addition of 200 ppm silicon increases the hot hardness of beta-treated U-Fe-Al. Higher silicon contents (to 1100 ppm) have no further effect. Aging of beta-treated U-Fe-Al containing silicon softens the alloy; however, some of the hardening is retained.

The hot hardness of beta-treated U-Fe-Al increases with increasing chromium contents to at least 500 ppm. Aging for 100 hr at 600°C reduces the hardness of the chromium-bearing alloys to that of U-Fe-Al; the chromium additions gave no residual hardening.

The addition of 350 ppm iron and 900 ppm aluminum to uranium contributes to the formation of fine grains in the as-cast material and in extruded and beta-treated material. Further grain refinement is obtained with the addition of silicon and chromium to the U-Fe-Al.

Uranium alloys containing additions of iron, aluminum, and silicon can be fabricated by methods developed for unalloyed uranium. Additions of 700 ppm silicon and greater to U–350 ppm Fe–900 ppm Al resulted in cracking upon quenching from the beta phase. No cracks developed in U-Fe-Al alloys containing additions of chromium up to 500 ppm. However, if silicon is present, 150 ppm chromium results in cracking of U-Fe-Al alloys upon quenching.

Several French reports concerned with alpha uranium containing chromium,[7] molybdenum,[8,9] niobium,[10] and various other alloying additions[11] have been published.

Gamma-Phase Uranium Alloys

The irradiation performance of the U–10 wt.% Mo alloy was evaluated by experimenters

at Atomics International.[12,13] Unrestrained samples 0.5 in. in diameter by 2.0 in. long were irradiated for periods up to three years to achieve substantial burnup levels at relatively low burnup rates. The specimens were irradiated in the fission-rate range from 2.5 to 8.0 × 10^{12} fissions/(cm^3)(sec), at average central temperatures from 750 to 1085°F. Initially the fuel-specimen structures were as-cast, partially transformed, or homogenized gamma. The results obtained are given in Table I-1. An almost linear relation between swelling and burnup was obtained in the burnup range from 3000 to 12,000 Mwd per metric ton of uranium. Intergranular cracking and operation at excessively high central temperatures, 1300 to 1500°F, are responsible for deviations from the linear relation between swelling and burnup.

The metastable gamma-phase structure can be maintained in the U–10 wt.% Mo alloy at temperatures below 800°F for a fission-rate range of 10^{12} to 10^{13} fissions/(cm^3)(sec). Above this temperature the structure transforms to thermally stable alpha and gamma prime. The alpha and gamma-prime phases will revert to gamma if the irradiation temperature is lowered. (M. S. Farkas)

Plutonium

Plutonium Metal and Alloys

The French have surveyed[14] a number of alloys including U-Pu-Mo, U-Pu-Nb, U-Pu-Ti, and U-Pu-Zr for suitability as fast reactor fuels. On the basis of ease of preparation and fabrication, thermal stability, excellent behavior in air, very small amount of zeta phase, little brittleness, and high melting temperature, U-Pu-Ti alloys appear most promising.

The same conclusion was reached in a similar survey[15] at Argonne National Laboratory (ANL), where efforts to develop metallic uranium-plutonium-base fuels with higher melting temperatures than U-Pu-Fz alloys are being concentrated on U-Pu-Ti and U-Pu-Zr alloys. Compression-test results, as shown in Table I-2, indicate that a U–15 at.% Pu–40 at.% Ti alloy is relatively ductile at temperatures above about 500°C and retains appreciable strength at temperatures above 600°C. The compatibility of this alloy is good with a V–20 wt.% Ti alloy and poor with titanium, zirconium, and stainless steel. Phase studies show that plutonium can replace some of the uranium in the U_2Ti com-

Table I-1 POSTIRRADIATION-EXAMINATION DATA FOR METALLOGRAPHIC SPECIMENS[12]

Specimen* NAA 47-	Fission rate,† 10^{12} fissions/(cm^3)(sec)	Average temp.,† °F	Diameter change, %	Burnup, Mwd/metric ton	Preirradiation structure*	Postirradiation structure*	Intergranular cracking*
2-1-S	7.9	625	1.0	11,000	AC	G	
2-1-C	7.9	750	1.0		AC	G‡	
4-2-S	6.35	855	25.2	10,100	G	T	Yes
4-2-C	6.35	965	25.2		G	T & S	
4-5-S	7.1	960	23.1	11,800	G	T & S	Yes
4-5-C	7.1	1085	23.1		G	T & S	
4-9-S	5.9	805	35.3	10,900	PT	G	Yes
4-9-C	5.9	910	35.3		PT	T	
6-3-S	4.6	825	9.0	5,600	PT	T	
6-3-C	4.6	905	9.0		PT	T	
6-4-S	5.2	920	10.2	6,100	AC	T	Yes
6-4-C	5.2	990	10.2		AC	T	
6-7-S	5.3	890	10.6	6,300	AC	T & S	
6-7-C	5.3	975	10.6		AC	T & S	
6-9-S	4.2	790	12.3	4,700	PT	T	
6-9-C	4.2	810	12.3		PT	T	
7-3-C	2.5§	725§	0.8	3,000	PT	G	
7-6A-C	3.3§	1025§	5.4	4,600	PT	T & S	
7-6B-C	3.5§	1025§	15.7	4,600	PT	T & S	Yes

*Notation: S, surface; C, center; AC, as cast (segregated gamma); PT, partially transformed; G, gammatized; T, transformed; T & S, transformed and spheroidized.

†The fission-rate and average-temperature values shown in the table are for the final stages of irradiation since it was assumed that this period had the greatest effect on the observed microstructure. The fission rate at the center of the specimens is not corrected for self-shielding absorption of neutrons by the fuel.

‡Some inhomogeneity noted after irradiation.

§Average central temperature and fission rate for entire irradiation.

Table I-2 COMPRESSION PROPERTIES OF U–15 AT.% Pu–40 AT.% Ti ALLOY (AS-CAST INJECTION CASTINGS)[15]

Temperature, °C	Ultimate compressive strength, kg/mm²	Reduction in length, %
25	141	<1
405	71	<1
516	48	~10
618	34	>16*
717	11	>12

*Test was stopped when specimen deformed continuously without an increase in load.

pound and cause an expansion of the lattice. The high-temperature gamma-uranium phase cannot be retained on quenching. Thermal-expansion data for two U-Pu-Ti alloys and one U-Pu-Zr alloy are shown in Table I-3.

Mound Laboratory[16] studies of the plutonium-platinum system show that there are two congruently melting compounds, PuPt and $PuPt_2$, and one incongruently melting compound, Pu_2Pt, in the system. All three compounds have melting temperatures above 1000°C. A eutectic exists at 10 at.% plutonium.

Viscosities of molten Pu-Ce-Co alloys of various compositions have been measured at several temperatures. Data are presented as a function of composition in Fig. I-2. Melting and transformation temperatures of a number of low-melting, multicomponent plutonium alloys, determined by differential thermal analysis, are listed in Table I-4.

Differential thermal analysis of high-purity, electrorefined plutonium revealed a small transition at 110°C, prior to the alpha → beta transformation[15] at 125°C. Precision density measurements conducted at Hanford Atomic Products Operation[17] on plutonium in the temperature range 100 to 115.5°C revealed no discontinuities. Thus, if there is a phase change in this temperature range, it is not accompanied by a volume change. Other Hanford studies of the physical metallurgy of plutonium have shown that the ultimate strength and the yield strength of beta plutonium are increased by a factor of 3 and that the ductility is decreased from 400% to less than 20% if beta is formed from gamma rather than from alpha. Results of experiments on the effects of stress on the beta-to-alpha transformation infer that the diffusion of atoms is not a major mechanism for this transformation. X-ray studies have confirmed that the (0 2 0) plane lies perpendicular to the rolling direction in alpha-rolled plutonium and perpendicular to the direction of applied stress in the columnar-grained material obtained by beta-to-alpha transformation under compressive stress.

Investigators at Los Alamos Scientific Laboratory have found that segregation problems in Pu-Ce-Co alloys can be eliminated by chill casting in uncoated metal molds at pour temperatures of 600 to 945°C. The castings are sounder, have a finer-grained structure, and

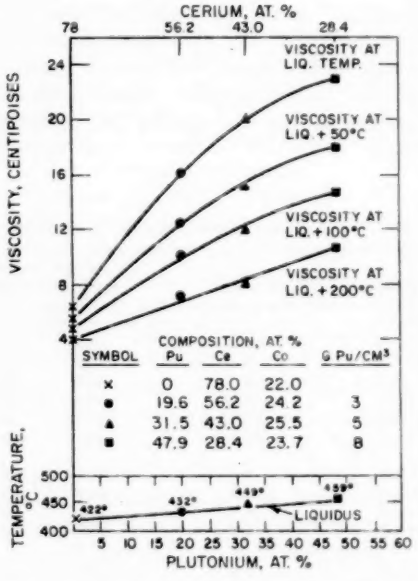

Fig. I-2 Viscosity of Pu-Ce-Co alloy as a function of composition.[16]

Table I-3 DILATOMETRIC DATA FOR U-Pu FUEL ALLOYS[15]

Alloy composition			
At.%	U–10.7 Pu–35.8 Ti	U–15 Pu–40 Ti	U–14 Pu–30 Zr
Wt.%	U–15 Pu–10 Ti	U–22.1 Pu–11.8 Ti	U–17.2 Pu–14.1 Zr
Expansion coef., 10^{-6}/°C (25°C to transformation)	20.3	16.9	18.2
Transformation range, °C	750 to 848	653 to 812	596 to 665
Expansion (Δl), %	1.09	1.14	0.58
Expansion coef., 10^{-6}/°C (transformation to 950°C)	19.7	21.3	22.3

show less tendency to oxidize or crack than do alloys cast in ceramic molds.[18]

An irradiated Pu-Ce-Co alloy and sodium were heated in contact with each other at 550°C, and the distribution of fission products was analyzed radiochemically. Results[19] are presented in Table I-5.

Table I-4 THERMAL DATA FROM MULTICOMPONENT PLUTONIUM ALLOYS[16]

Alloy	Composition, at.%						Transformations, °C		
	Pu	Ce	Co	Ni	Cu	Fe	Liquidus	Solidus	Other
100	40	37	11.5	11.5			438	400	414
101	60	20	10	10			415	400	410
102	33	30	9.5	9.5	18		430	375	395, 415
103	54	18	9	9		10	510	375	485
104	40	23		15	22		535	460	500
105	33	30		19	18		535	400	415, 465, 530
106	54	19	9	9	9		480	385	420, 445
107	37	28	11	11	13		495	380	390, 480
108	58	20	9	10		3	425	380	400

Self-diffusion in plutonium has been determined at 218.8 and 299.1°C, with the following diffusion coefficients being observed:

$$D_{218.8} = 1.13 \times 10^{-12} \text{ cm}^2/\text{sec}$$

$$D_{299.1} = 9.29 \times 10^{-12} \text{ cm}^2/\text{sec}$$

Phase-relation studies have shown that delta plutonium and beta americium form a continuous series of solid solutions. Between 5 and 85 at.% americium, the solid solution is stable at room temperature. The homogeneity range of the intermediate phase in the plutonium-scandium system has been tentatively established to be between 37 and 40 at.% scandium. The phase is formed peritectically between epsilon-plutonium solid solution (~25 at.% scandium) and alpha-scandium solid solution (~53 at.% scandium) at 753°C.

The plutonium-silicon system is characterized by five intermediate phases and three eutectics.[20] Properties of the phases are tabulated below:

Phase	Melting temp., °C	Crystal structure	Density, g/cm³
Pu_5Si_3	1377 ± 10	Body-centered tetragonal	12.00
Pu_3Si_2	1441 ± 10	Tetragonal	11.33
PuSi	1576 ± 10	Orthorhombic	10.15
Pu_3Si_5	1646 ± 10	Hexagonal	8.96
$PuSi_2$	1638 ± 10	*	

*The phase $PuSi_2$ exists over a homogeneity range. At high silicon concentrations the structure is tetragonal; as silicon is decreased the structure is deformed to orthorhombic.

The eutectics exist between epsilon plutonium and Pu_5Si_3 at 3.6 at.% silicon and 590 ± 2°C; between PuSi and Pu_3Si_5 at 54.6 at.% silicon and 1251 ± 10°C; and between $PuSi_2$ and silicon at 83.6 at.% silicon and 1232 ± 5°C.

Table I-5 RELATIVE AMOUNTS OF FISSION PRODUCTS IN FUEL AND SODIUM[19]

Fission product	Fuel (HCl-soluble), counts/(min)(g of Pu)	Sodium (butanol soluble), counts/(min)(g of Na)
Cs	2.1×10^8	5.9×10^9
Ru	3.97×10^9	7.9×10^7
Zr	3.5×10^7	1.85×10^8
Eu	9.6×10^7	7.3×10^8
Sb	1.85×10^8	3.6×10^7
Sr	3.7×10^8	3.2×10^9

The diffusion of plutonium in magnesium and magnesium alloys at temperatures of 420 to 500°C has been studied by U. K. investigators.[21] As shown in Fig. I-3, diffusion coefficients were found to vary considerably with plutonium concentration.

Preliminary results of a French study[22] reveal the existence of multiple modes of deformation in alpha plutonium. Three slip systems, cross slips, deformation bands, and at least one twinning system were found.

(V. W. Storhok)

Plutonium Compounds

Los Alamos[23,24] has developed a high-temperature nitriding process similar to that used at Battelle Memorial Institute for the preparation of stoichiometric PuN. Battelle has prepared single-phase $(U_{0.85}Pu_{0.15})N$ by interdiffusion of the physically mixed nitrides and reports the vapor pressure of PuN as 1.6×10^{-9} atm and 3.1×10^{-7} atm at 1250°C and 1550°C, respectively.[25] Microspheres of $(Th_{0.8}Pu_{0.2})O_2$ prepared by the sol-gel technique have been shown[25] to be stable in dry hydrogen at 1650°C.

New data have been reported concerning the plutonium-carbon system. Los Alamos[26]

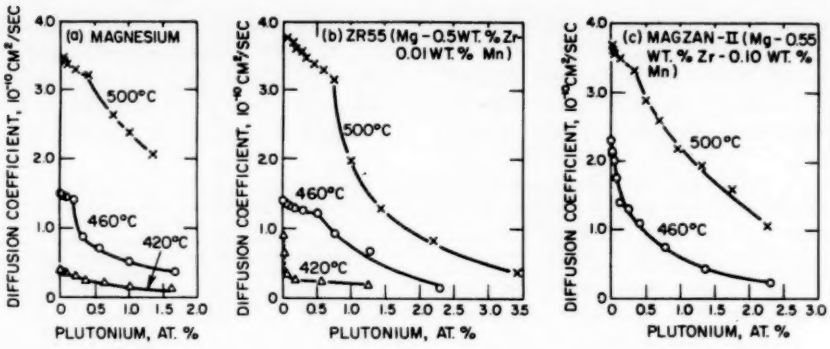

Fig. I-3 Variation of plutonium diffusion coefficient with concentration of plutonium in magnesium and two magnesium alloys.[21]

has developed a metallographic technique that greatly facilitates specimen examination and reports hardness (DPH) values of 1100 for Pu_2C_3, less than or equal to 100 for zeta, and 500 to 900 for PuC. The British indicate[27] that $(U_{0.85}Pu_{0.15})C$ is compatible with type 316L stainless steel at temperatures below 850°C for an unspecified time period.

Workers at United Nuclear Corp.[28] have prepared up to 45% of Pu(O,C) in beta Pu_2O_3 in attempts to prepare the stabilized monoxide, and Hanford[29] is attempting oxidation of the metal to PuO by use of decomposed Ag_2O as an oxygen source. British workers found[27] that for the plutonium-oxygen system above 300°C, $PuO_{1.61}$ and $PuO_{1.98-x}$ are in equilibrium, and they suggest several other modifications to the binary phase diagram of Chikalla et al.

Chalk River[30] has confirmed earlier reports that the rate of UO_2-PuO_2 solid solution is enhanced in oxidizing sintering atmospheres.

Attempts by Los Alamos[24] to synthesize PuB have not been successful, but the results indicate the existence of a "PuB_{100}" compound not previously observed. Argonne has prepared PuS and PuP powders by reaction of PuH_x with hydrogen sulfide and phosphine, respectively, followed by 1600°C vacuum homogenization. Lattice parameters reported[31] are: 5.5383 A for PuS and 5.6562 to 5.664 A for PuP. The reported average coefficient of thermal expansion (18 to 960°C) is very large, 18.54×10^{-6}/°C, for PuS. (W. M. Pardue)

Thorium Compounds

The compounds Th_2Al, ThB_4, $ThBe_{13}$, ThC, ThC_2, Th_3Si_2, and ThSi, with and without additions of their uranium counterparts, have been investigated by workers at Battelle.[32] Microstructural studies, oxidation tests in dry air and CO_2, and corrosion tests in NaK, Santowax R, and water were conducted. In addition, thermal-conductivity, hardness, compatibility, and compression tests were run. The compatibility tests revealed that, of the compounds tested, the beryllides were the most reactive with the potential cladding materials.

Except in the case of the aluminide, the uranium substituted for the thorium in solid solution in the compounds. The borides and beryllides had the greatest oxidation resistance in dry air and CO_2 up to 540°C. Above 540°C the beryllides oxidized rapidly in dry air. The borides and beryllides were not attacked in the corrosion tests. Nil-ductility strengths greater than 67,000 psi were realized for (90 Th − 10 U)C and (90 Th − 10 U)B_4 at 980°C.

A 10 mole % addition of the corresponding uranium compound is apparently soluble in ThSi and Th_2Si_3, whereas 20 mole % additions seem to go into solution in ThB_4, $ThBe_{13}$, ThC, and ThC_2. Only in the case of the Th_2Al compound, for which no corresponding uranium compound exists, is a solid-solution fuel impossible. (R. L. Martin)

Metal-Ceramic Fuels

Dispersion Fuels

Reaction kinetics of 34 wt.% U_3O_8–aluminum fuels were investigated at Georgia Institute of Technology.[33] Results indicated that the reduction of U_3O_8 occurs in two stages; first, rapid

reduction of U_3O_8 to UO_2 and, second, slower reduction of UO_2 to uranium-aluminum solutions. During the first stage approximately 15% of the U_3O_8 was reduced to uranium-aluminum solution, and about 65% of the U_3O_8 was reduced to UO_2 after the dispersion was heated for 2 min from 700 to 1090°C, with most reduction occurring between 920 and 980°C. In the second stage the remainder of the U_3O_8 was reduced at a rate of 2 to 8%/min. The energy release in the first stage was estimated to be 10 times higher than that in the second.

At Hanford, dispersions containing 20 vol. % PuO_2 in stainless steel were heat-treated at 900°C in vacuum for 408 hr and lost 2.18% in density.[34]

Battelle reports that irradiation pins containing 40 wt.% UO_2–iron dispersions clad with 2541 alloy are currently being prepared for tests[35] in-pile in flowing air at 1100°C.

At Harwell,[36] specimens containing 50 vol. % UO_2–stainless steel were thermally cycled between 800 and 50°C. After 1000 cycles no significant effect on the stainless-steel core, cladding, picture frame, and core-cladding bond was detected. A slight amount of intergranular cracking of the UO_2 spheres and development of small localized gaps at the UO_2–stainless-steel interfaces were observed after the 1000 cycles. These effects, however, did not cause any measured dimensional change. Also, a method has been developed at Harwell[27] for coating UO_2 with −400-mesh stainless-steel powders. The powder was dispersed in a solution of CCl_4 and a suitable binder and sprayed onto hot, tumbling UO_2 spheres. This technique produced dispersions containing 10 to 50 vol.% UO_2–stainless steel, and the structures showed satisfactory particle distribution as evidenced by very few UO_2-particle contacts.

In-pile tests conducted in support of the ML-1 (Mobile Low-Power Plant No. 1) fuel-element development are described.[37] Irradiation studies on the following are included: GCRE (Gas-Cooled Reactor Experiment) concentric curved plate type elements, the GCRE pin type elements, the pin type elements of the first and second cores of the ML-1, and several related capsule tests. (D. L. Stoltz)

Cermet Fuels

A cermet assembly consisting of 80 vol. % UO_2–molybdenum was fabricated by General Electric Company workers[38] for long-term irradiation-performance testing in the Vallecitos Boiling Water Reactor. Fuel pellets were hot pressed, and the 20 vol. % molybdenum additions were introduced either as fibers or as vapor coatings on the individual UO_2 particles. As a result of the unidirectional compaction, the hot-pressed fiber structures (94 to 95% of theoretical density) had their fibers oriented predominantly in the radial planes of the pellet. The vapor-coated particles had a continuous matrix and an average density of 89% of theoretical. Both sets of pellets were clad with type 304 stainless steel. The cermets will operate at high specific power levels, with surface heat fluxes of about 157 watts/cm^2 and a design life of 4.1×10^{20} fissions/cm^3.

(D. E. Kizer)

Coated-Particle Fuel Materials

Particle Coating

General Atomic Division of General Dynamics Corp.[39] has reported additional information on the structure of pyrolytic carbon (PyC) coatings applied to nuclear fuel particles. The coatings were applied to 100-g lots of fuel particles by pyrolysis of methane in a 6.3-cm-diameter fluidized-bed unit. The fluidizing gas contained 7 parts helium to 1 part methane at a total pressure of about 1 atm. Five graphite disks, 6 by 1 mm, were coated along with the spherical fuel particles. The density and preferred orientation were determined for coatings removed from the disks. The PyC coatings were prepared at 1400, 1600, 1650, 1700, 1800, 1900, 2000, and 2100°C. Coatings prepared in the range 1600 to 1700°C were the least dense. The apparent crystallite size increased uniformly with temperature. A highly oriented structure was obtained at 1400°C, and a random structure was obtained for the low-density coatings prepared at 1600 to 1700°C. Above 1800°C a gradual increase in orientation parallel to the substrate occurs. It is noted that both bed geometry and/or the partial pressure of the particular hydrocarbon used affect the preferred orientation of the coating. Other experiments are being made to gain information on the effect of bed geometry on the structure of PyC.

Workers at Oak Ridge National Laboratory[40] have also reported that the crystallite size of PyC coatings increased with increasing deposition temperature. A typical set of values follows:

PyC deposition temp., °C	Crystallite size, A
1300	35
1400	38
1700	100
1800	130

The coatings were deposited on 10-g lots of particles 150 to 250 μ in diameter in a 0.75-in.-ID graphite tube provided with a 30° included-angle cone at the bottom. Five graphite disks, $^3/_{16}$ in. in diameter by $^3/_{64}$ in. thick, were coated along with the particles. The density, preferred orientation, and hardness of coatings deposited at 1400°C were found to be quite dependent on methane partial pressure.

The propagation of cracks through the interface between laminar and columnar layers of duplex coatings is also being studied.[40] Experiments indicate that the crack will stop at the interface only if the two layers are poorly bonded. Single-layer and multilayer coatings with good bonding, i.e., PyC-SiC-PyC or duplex coatings prepared by decreasing deposition rates at 1400°C, fractured completely through the coating to the carbide particle.

A study is being made at Battelle[25,41,42] of increasing the size of porous UO_2 particles coated with PyC to take advantage of increased fuel loading. Promising in-pile performance had been shown by 460-μ UO_2 coated with about 115 μ of PyC. Other work[25] includes the coating of uranium mononitride fuel particles with PyC with the objective of extending the useful temperature range of coated particles. The mononitride is of interest since (1) it is reported to have a higher melting point than either UO_2 or UC_2 and (2) calculations indicate that the nitrogen pressure developed in a PyC-coated UN particle is less than the CO pressure in a PyC-coated UO_2 particle at the same temperature.

A study on the preparation and evaluation of alumina-coated fuel particles has been concluded.[43] The alumina coatings were applied to UO_2 fuel particles in a fluidized bed by hydrolysis of $AlCl_3$ vapor. Dense coatings were obtained in the range 1000 to 1400°C, and porous coatings were obtained in the range 500 to 900°C. The structure of the coatings is also dependent on deposition temperature. Below 700°C an amorphous structure is developed, whereas at 900 to 1150°C the structure is thought to consist of alpha Al_2O_3 in an amorphous matrix. Above 1300°C essentially 100% crystalline alpha alumina is deposited. Coatings deposited at 1000°C show a preferred orientation of the crystallographic *a* axis in a near-radial direction, whereas in the 1400°C coatings the *c* axis was radially oriented. The various structures can be deposited in successive layers on particles. Monolithic, composite (layers of alumina and other materials), and multiplex (mixed alumina structures) coatings can be made sufficiently impervious to protect the fuel from a hot-acid leach and to retain fission gases at temperatures up to 1300°C after low irradiation exposures. (N. D. Veigel)

Irradiation and Evaluation of Coated-Particle Fuels

OXIDE-BASE FUEL

Particles of UO_2 coated with PyC are being studied in in-pile experiments at Oak Ridge[40] and at Battelle.[25,41,42]

In the Oak Ridge experiments, a duplex type coating having an average thickness of 118 μ on dense UO_2 particles (229-μ average diameter) was found to resist failure to a burnup of about 2.5 at.% at 1200°C. The fission-gas-release fractions were on the order of 10^{-6}. However, failure began at 2.7 at.% burnup; it continued until the fission-gas-release fractions were on the order of 10^{-3} at 4.6 at.% burnup. Comparable coatings on dense UC_2 particles have given better performance.

Porous UO_2 particles coated with PyC have continued to exhibit good irradiation behavior at Battelle. A specimen of 78% dense, 200-μ UO_2 particles coated with 73 μ of columnar PyC is being irradiated at 1300°C. After about 8 at.% burnup, the fission-gas-release fractions are 2×10^{-7} to 1×10^{-6}, indicating failure of an estimated 0.2% of the coatings. Large, 460-μ, porous UO_2 particles coated with 112 μ of laminar PyC are also being irradiated at Battelle. One specimen has 65% dense UO_2, and another has 81% dense UO_2. These two specimens have shown no failure after 6 at.% and 1 at.% burnup, respectively, at 815°C. The fission-gas-release fractions are below 10^{-6} in both cases.

CARBIDE-BASE FUEL

Experiments at Oak Ridge continue to show that either duplex or triplex PyC coatings on UC_2 or $(Th,U)C_2$ particles can be irradiated at 1370°C to a burnup of 20 at.% of heavy metal without coating failure.[40] Recent irradiations to 16.2 at.% and 20.8 at.% burnups at 1370°C confirm this for duplex coatings on UC_2 particles. The coatings were over 100 μ thick. Metallographic examinations showed the inner, laminar PyC layer of the coating to be damaged, but no coatings were broken. The fission-gas-release fractions at the end of the irradiations were in the range of 3×10^{-6} to 1×10^{-5}, and they had increased gradually throughout the experiments. (C. W. Townley)

Uranium Oxides

Properties and Behavior

A 1960 British data manual[44] on uranium ceramics has been updated to June 1964. This manual is an excellent compilation of mechanical, physical, chemical, irradiation, and constitutional data on uranium oxides, carbides, nitrides, and silicides, considered as pure, bulk fuels.

Two recent papers are concerned with properties that influence maximum power capabilities of UO_2 fuel elements. Christensen et al.[45] made thermal-conductivity measurements on nearly stoichiometric polycrystalline UO_2 at temperatures between 1000 and 1900°C. The results of these measurements, along with other data, are summarized in Fig. I-4. The increase in thermal conductivity at about 1400°C is attributed to a high-temperature electronic contribution and not to infrared transmission that was once thought to be important. The specimen composition was found to have changed from $UO_{2.01}$ to $UO_{1.99}$ during the thermal-conductivity measurement, and the electronic contribution may involve the substoichiometric oxide. This implies that holes have a higher mobility in intrinsic UO_2 than do electrons and that doping with donors such as uranium metal may enhance the thermal conductivity of UO_2 at high temperatures. Hetzler and Zebroski[46] have studied the thermal conductivity of both stoichiometric and hypostoichiometric UO_2 out-of-pile. Below 1400°C the hypostoichiometric oxide exhibited a higher conductivity than the stoichiometric $UO_{2.00}$, as shown in Fig. I-5. In the case of the stoichiometric $UO_{2.00}$, the thermal conductivity tended to level off between 800 and 1850°C and showed no evidence of the high-temperature enhancement noted above.

The distribution of fission products in irradiated UO_2 has been studied by Bates[47] using high-resolution autoradiography and a microdrilling technique to remove microsamples for radiochemical analysis. The results are summarized in Figs. I-6 and I-7. The fission-product distribution is found to be closely related to the type of microstructure that develops during irradiation. Annular bands of

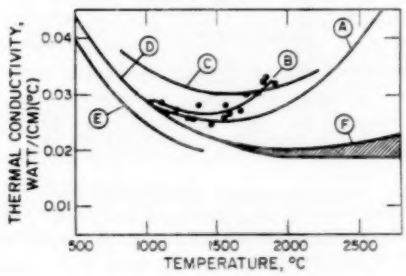

Fig. I-4 Thermal conductivity[44] of UO_2. A, lattice plus calculated maximum electronic conductivity, Transactions of the American Nuclear Society, *7(1): 128 (June 1964); B, this work; C, A. D. Feith, TID-7693 (Vol. 1), p. 162; D, J. L. Daniel, J. Matolich, Jr., and H. W. Deem, USAEC Report HW-69945, September 1962; F, deduced from irradiated fuel microstructures, Lyons et al.,* Transactions of the American Nuclear Society, *7(1): 106 (June 1964), and J. A. Christensen,* Transactions of the American Nuclear Society, *7(1): 128 (June 1964).*

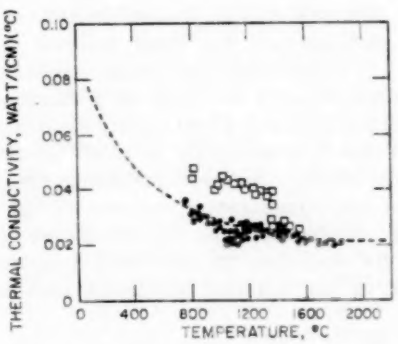

Fig. I-5 Thermal conductivity[46] of UO_2. ●, stoichiometric UO_2; □, hypostoichiometric UO_2; - - -, Lyons et al., Transactions of the American Nuclear Society, *7(1): 106 (June 1964).*

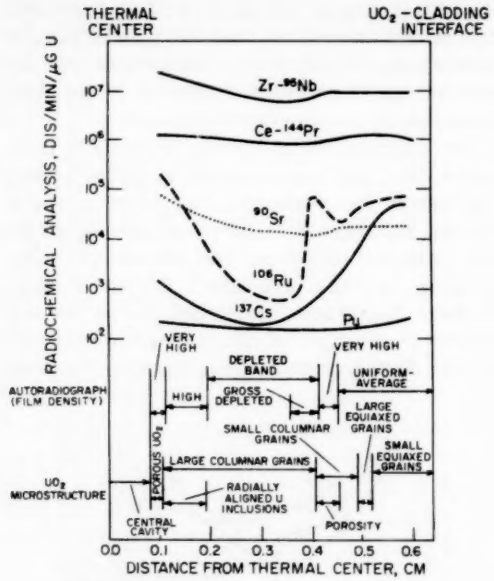

Fig. I-6 Fission-product distribution and related microstructure of irradiated UO_2 fuel rod:[47] APED-A597 (sintered UO_2 irradiated to 2×10^{19} fissions/cm³ at 0.87 to 1.23 kw/cm).

high fission-product accumulation are observed to be symmetric about the thermal center. Depletion of fission products is generally observed in the dense pore-free region of the large columnar grains. In many instances the radioactivity is observed to concentrate near the thermal center and in the small columnar grains. The distribution and concentration vary for the different fission products. Cesium and ruthenium show the greatest tendency to migrate, whereas zirconium-niobium and cerium-praseodymium are the least inclined to migrate. In some cases the cesium concentration was found to vary as much as a thousandfold across the radius of a fuel pellet. Fission products seem to concentrate in bands associated with the metallic-uranium inclusions that form in the high-temperature regions of the fuel during irradiation. The concentrations of cesium and strontium are said to be considerably higher in the uranium inclusions than in the UO_2.

Ohse[48] used the Knudsen effusion method to investigate the vapor pressure of UO_2. Over the temperature range from 2200 to 2800°K, the vapor pressure above UO_2 followed the relation

$$\log p = 12.4264 - 3.3783 \times 10^4 \, T^{-1}$$

where p is the pressure in millimeters of mercury. At temperatures from 1500 to 2000°K, the vapor pressure followed a slightly different relation:

$$\log p = 11.556 - 3.1209 \times 10^4 \, T^{-1}$$

The latent heat of sublimation at 298°K was 148.6 kcal/mole. (R. H. Barnes)

Preparation of Fuel Bodies

Australian workers[49] have recently completed an investigation on the production of spherical fuel particles having a diameter greater than 100 μ through the use of an r-f-coupled plasma. Power inputs of up to 15 kw were attempted. The spheroids produced were of a high porosity and low density owing to the formation of large center voids. It was concluded that limitations of low production rates, high porosity, surface oxidation on the spheroids, and premature torch failure at high powers rendered this method of spherical-particle production unsatisfactory.

The use of the fluidized-bed process for the preparation of dense, spheroidal uranium dioxide particles directly from UF_6 has been developed at Argonne.[50] The uranium hexafluoride is reacted with a mixture of steam

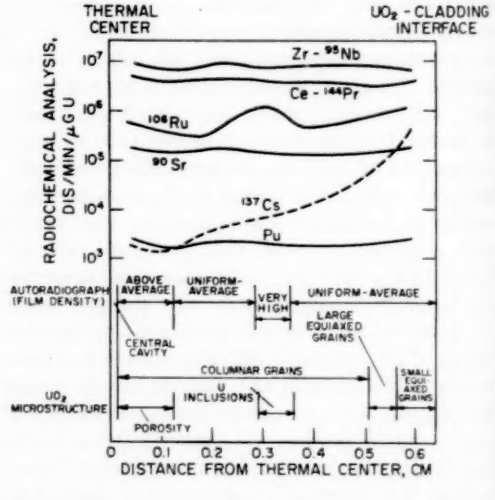

Fig. I-7 Fission-product distribution and related microstructure of irradiated UO_2 fuel capsule:[47] GEH-14-178 (swaged UO_2 irradiated to 5×10^{20} fissions/cm³ at 0.68 to 0.27 kw/cm).

and hydrogen in a bed of UO_2 fluidized by the reactant gases and maintained at 650 to 700°C. The solid reaction products deposit as dense layers on the surface of the bed particles. Uranium dioxide particles in the size range of −18 +140 mesh have been produced with densities of 89% of theoretical.

Duerrschnabel et al.[51] have melted UO_2 into 100% dense lumps having a near-stoichiometric oxygen content by direct resistance heating of stacked pellets under an argon atmosphere. The dense melted lumps are ground into various size fractions and vibratory compacted into fuel rods having a density of from 85 to 92% of theoretical.

A British patent[52] has been issued for the preparation of high-density UO_2 fuel pellets. Stoichiometric UO_2 is blended with 0.4 wt.% Nb_2O_5, 3 wt.% camphor, and 0.5 wt.% stearic acid before compacting. The pellets are calcined at 350°C for 2 hr and then sintered at 1200°C for 4 hr. Densities of the order of 96% of theoretical have been achieved.

Atomics International[53] is refabricating and encapsulating UO_2 that had previously been irradiated to burnups as high as 21,000 Mwd per metric ton of uranium. The material is fabricated into pellets by pressing and sintering. Densities obtained are of the order of 92 to 96% of theoretical. Radiochemical analysis indicated that the principal fission products removed during refabrication are cesium and the noble gases. (T. R. Wright)

Uranium and Thorium Carbides, Nitrides, and Phosphides

Properties and Behavior

Eyre and Sole[54] studied the Widmanstätten structures formed when tetragonal UC_2 platelets precipitate in cubic crystals of UC, and they determined the crystallographic nature of twinning in UC_2. Their results are in agreement with earlier data; however, they conclude that the term "martensitic" should not be applied to the precipitation of tetragonal UC_2 from the high-temperature-cubic solid solution. The change in composition required suggests that the process is more like a "bainitic" reaction.

Microstructural studies[55] of particles of UO_2 partially reduced to UC_2 by graphite show that UO_2 and UC_2 form a pseudobinary system with extensive terminal solubilities at 1800°C. The quantities of precipitates present suggest terminal solubilities of the order of 10 mole % UO_2 in UC_2 and vice versa. According to J. Henney of the United Kingdom, UC_2 can contain a maximum of 2 wt.% oxygen (about 20 mole % UO_2) at 1500 to 1600°C. He indicates that the peritectoid decomposition temperature[27] of U_2C_3 is lowered from 1800°C to 1625°C by the presence of UO_2.

Resistivity discontinuities were observed by Korbitz[56] at the composition of ThC_2 at 1440 and 1490°C. These discontinuities probably represent stages in the process of transformation of cubic ThC_2 to monoclinic ThC_2 but were interpreted in terms of two allotropic transformations. A resistivity discontinuity at the composition Th−60 at.% C, and at 1220°C, was interpreted to indicate the existence of Th_2C_3 above this temperature.

A study[57] of the Th-C-Ni system has disclosed two ternary compounds, $Th_2Ni_3C_5$ and $Th_2Ni_3C_2$, and possibly a third compound. Pseudobinary ties were found from ThC to Th_7Ni_3, ThNi, and $ThNi_2$; from $Th_2Ni_3C_2$ to ThC_2, graphite, and $ThNi_5$; and from graphite to $ThNi_5$ and Th_2Ni_{17}.

A 50 mole % mixture of ThC_2 and rhenium was observed[58] to melt at 2150°C in a graphite crucible. The solidified product contained ThC_2, rhenium, and graphite, and this suggests the existence of three-phase equilibria between these materials at high temperatures.

Argonne workers report[31] that the melting points of ThP-UP mixtures decrease from 2900°C at ThP to 2825°C at 50 wt.% UP to 2600°C at UP. The UP showed negligible weight loss[59] in vacuum at 1600°C but lost 1.6×10^{-5} g/(cm^2)(sec) at 2200°C. No solid-state reaction occurs between UP and UO_2, and the lattice constants of one are unaffected by the presence of the other.

At General Atomic[60] it was found that at 1800°C the proportional limit of UC−20 mole % ZrC in bending is about 1500 psi, whereas the limit in bending of UC−90 mole % ZrC is about 5500 psi. The latter has very little ductility at 1800°C, whereas UC−20 mole % ZrC is quite plastic.

Austrian investigators[61] have solved the crystal structure of U_2Fe_3Si. This compound is of

the $MgZn_2$ type with lattice parameters of $a = 5.14$, $c = 7.71$, and $c/a = 1.50$.

At temperatures of 1400 and 1600°C, Biddle[62] of the United Kingdom found that the rate of release of ^{133}Xe from lightly irradiated UN was slightly greater than the rate of release from similar samples of U(C,N) and UC.

Workers at Battelle[63] have obtained hot-hardness, thermal-conductivity, and electrical-resistivity data on high-purity UN prepared by consumable-electrode arc melting. The thermal conductivity of this material was 0.4 cal/(cm)(sec)(°C) at 100°C and increased to 0.06 cal/(cm)(sec)(°C) at 900°C. The electrical resistivity also increased with temperature from 157 μohm-cm at 25°C to 180 μohm-cm at 900°C. The UN-ZrN system appears to be a solid solution to 10 wt.% ZrN. The UN-TiN system contains a eutectic of about 10 wt.% TiN.

Slight reactions were observed[64] between UN and various materials as follows: with zirconium at 700°C, with nickel at 800°C, with chromium at 900°C, and with stainless steel at 1000°C. After 3000 hr at these temperatures, the reaction zones observed were 8 to 25 μ thick. (W. Chubb)

Fabrication of Refractory Fuels Other Than Uranium Oxides

Argonne[31,65] is investigating the preparation of uranium carbide powders by a gas-solid reaction. Uranium hydride powders are fluidized in a propane-hydrogen gas mixture for 2 to 5 hr at 500 to 700°C. For gas flow rates of 0.25 ft/sec, the following results are reported.

H_2, vol. %	C_3H_8, vol. %	Temp., °C	Time, hr	Carbon in product, wt.%
70	30	500 to 700	2 to 5	5.3
72	28	600	5	4.6
80	20	500 to 700	2 to 5	3.2
85	15	700	5	4.8

X-ray analyses indicated that the major product phase was UC, with minor phases of UC_2 and UH_3. The stoichiometry can be controlled by controlling the temperature, reaction time, and hydrogen concentration in the fluidizing gas.

The novelty here seems to be the fluidization of the reaction bed. Other investigators have utilized this gas-solid reaction but have found that the stoichiometry control is not straightforward because of the difficulty in producing stoichiometric UC. For a desired carbon composition to be achieved, it was necessary to determine the resulting carbon content of several batches and resort to the controlled blending of these batches. (E. O. Speidel)

Basic Studies of Irradiation Effects in Fuel Materials

Metals

Studies in the United Kingdom[66a] indicate that resistance to swelling in uranium is promoted by distributing the fission gas in the largest possible number of small bubbles and inhibiting the subsequent movement and coalescence of these bubbles. "Adjusted" uranium that contains small amounts of iron, aluminum, and carbon has swelling resistance markedly superior to that of unalloyed uranium, and the results suggest that the finely dispersed precipitates in adjusted uranium anchor the fission-gas bubbles and prevent coalescence. A U–6 at.% Mo alloy is slightly inferior to adjusted uranium in its swelling behavior. Adjusted uranium is also superior to unalloyed uranium and U–6 at.% Mo alloy in its resistance to the enhanced grain-boundary swelling observed at 400 to 500°C under high fission rates. The good mechanical properties of adjusted uranium are probably responsible for its ability to resist growth stresses; its ability to retain fission gases in a large number of small bubbles is also believed to be of importance.

The swelling hypothesis suggests that uranium in which the gas bubbles are free to move will show enhanced swelling under thermal cycling, and there is some experimental evidence to support this. The swelling of adjusted uranium is unaffected by thermal cycling of the amplitude and frequency expected in Magnox reactors, and this fact again suggests that the gas bubbles have been stabilized.

In France[66b] aluminum-lithium alloys have been irradiated with neutrons to study the part played by density and the distribution of defects on the precipitation of rare gases, in this case, helium. Observations seem to show that the growth of bubbles is governed by the diffusion of the rare gas (in volume, in the grain boundaries, or in the dislocations) or of the vacan-

cies, according to the experimental conditions. Samples heated in the microscope appear to show that the bubbles grow on the spot by diffusion in the dislocations or in volume.

In studies conducted by French workers, certain aspects of the swelling of uranium irradiated in the alpha phase, such as cavitation at the grain boundaries, do not appear to be characteristic of the uranium under irradiation. The fission-gas bubbles then act only as instigators of the intergranular cracking.

An examination conducted in France[4] deals with unalloyed uranium samples, having various structural states, cold worked and recrystallized, as cast and beta treated, and irradiated at temperatures of between 450 and 600°C and with burnups from 1300 to 5500 Mwd/ton. It is noted that these samples swelled because of precipitation of the fission gases; the porosity thus produced has a morphology depending mainly on the type of deformation (due to in-pile growth) to which the metal has been subjected. The most homogeneous distribution of pores, and thus that leading to the minimum swelling, is observed only in the material having a marked [0 1 0] texture in which growth and perhaps the thermal cycling introduce little or no strain. For other materials the deformation/swelling association causes a more rapid destruction of the samples either by cracking when the deformation is due to twinning or by pronounced swelling localized in the bands when deformation is due to slipping. Finally, the fission-gas precipitation considerably facilitates, above 500°C, the germination and growth of the intergranular cracks that can then develop at low stresses.

The form of a proposed solution for the prediction of dimensional changes in uranium fuel cores during irradiation has been set forth by The National Lead Co. of Ohio.[2] Present knowledge of relevant physical processes is reviewed and areas in which experimental data are needed are indicated.

Hudson[67] reports the determination of the orientation and Burgers vectors of the dislocation loops formed in alpha uranium by neutron irradiation. The loops lie on (0 1 0) and (1 0 0) with Burgers vectors $\frac{1}{2}\sqrt{a^2 + b^2}\langle 1\,1\,0\rangle$ and $a[1\,0\,0]$, respectively. The loops are observed to lie in sheets, the loop planes coplanar with the sheet planes. The orientation of the types of loops observed and their Burgers vectors are exactly as required to explain the irradiation-growth phenomena if the (0 1 0) loops are interstitial and the (1 0 0) loops are vacancy. The arrangement of the loops in sheets, and the lack of mutual annihilation during annealing, can be explained in terms of the elastic interactions of the loops.

Diffusion coefficients of krypton and xenon in uranium were observed[68] by the Japanese to increase during heating under an inert atmosphere. However, when highly irradiated uranium samples were heated in an inert atmosphere, the diffusion coefficients decreased. The release of gases increased suddenly at the transformation point. Gas release was also increased by thermal cycling. These effects are probably related to gas-bubble migration as a result of surface diffusion of the matrix atoms.

Ceramics

The fission-product release of spherical monogranular UC_2 particles was studied at General Atomic[69] by postirradiation annealing of neutron-activated samples and by exposing samples to a steady rate of photofission. The release of the fission products considered appears to follow the kinetics and temperature dependence of an activated diffusion process. The anomalous fast release of a portion of the ^{133}Xe in annealing experiments may be interpreted as being due to release of attached or trapped xenon atoms by a process that does not follow Fick's law. Diffusion coefficients for krypton, tellurium, iodine, xenon, and barium were obtained.

At Chalk River[66c] analyses of fission-gas behavior in UO_2 indicate that in dense sintered UO_2, all the fission gas produced up to 100,000 Mwd/ton will be retained below 800°C. Retention is completely effective to 15,000 Mwd/ton up to 1200°C. Fission-gas retention above 1600°C is quite low, and, in irradiations of several months, even more than 95% of the gas may escape if sufficient volume is available. If, however, the oxide is firmly restrained, the gas pressure may build up to the point at which irradiation-induced reentry of the gas matches the rate of release.

If the density of the sintered oxide is less than 10.3 g/cm^3, the rate of reentry at 200 atm in the cooler parts of the fuel at ratings up to $\int \lambda \, d\theta = 50$ watts/cm will exceed the rate of release at least up to 15,000 Mwd per ton of uranium. Thus, with fuel of this density or less,

it is unlikely that it will be necessary to leave any extra space for the escaped gas for burnups at least up to 15,000 Mwd per ton of uranium. For fuel of higher density at high ratings, it is necessary to provide space to allow the thermal expansion of the oxide, and for high burnup a comparable or larger space may also be needed to limit the pressure of the released fission gas. Further experiments are planned to test these conclusions.

Thin layers of irradiated UO_2 have been studied in Russia,[66d] and it is found that irradiation causes dislocation loops from 20 to 300 A in diameter and "light defects" about 10 A in size. The dislocation loops are formed by condensation of interstitial atoms around various "obstacles." "Light defects" are of vacancy character, and their sites depend on fission-fragment traces. After irradiation to 10^{19} fissions/cm^3, the density of dislocations exceeds 10^{12}/cm^2. The density in annealed UO_2 is about 10^9/cm^2. Annealing of postirradiation defects occurs in two steps. Dislocation loops are annealed at 800 to 1100°C, and light defects are annealed in the range 1200 to 1700°C. Electron diffraction reveals that stresses occur in the UO_2 and increase with the irradiation exposure. These stresses arise around dislocation loops and anneal gradually at the same time with annealing of dislocation loops.

A study was made at Westinghouse Electric Corp.[70] of the melting point of irradiated uranium dioxide using specimens representative, in terms of burnup and irradiation temperature, of contemporary power-reactor fuels. The melting point was found to decrease, during irradiation, at a rate of 32°C/(10,000 Mwd per metric ton of uranium), the decrease being nearly linear between 2000 and 52,000 Mwd per metric ton of uranium. The lowest burnup (2000 Mwd per metric ton of uranium) exceeded that found by Hanford to cause a significant increase in melting point.

The decrease in UO_2 melting temperature lowers the linear heat rating required for fuel-center melting by approximately 0.2 kw/(ft) (10,000 Mwd per metric ton of uranium).

It has been shown at Hanford[47] that gross fission-product relocation occurs during high-temperature irradiation of UO_2 fuel elements. Cesium and ruthenium show the greatest tendency to migrate, whereas zirconium-niobium and cesium-praseodymium exhibit the least tendency to migrate. Cesium concentration across the fuel-element radius varies as much as 1000 times.

Fission products concentrate in bands associated with metallic-uranium inclusions that are found at high temperatures during irradiation. The concentration of cesium and strontium in the uranium is significantly higher than in the UO_2.

Plutonium also migrates during irradiation, forming higher concentrations in the thermal center and a minimum in concentration in the large columnar grains.

The extensive migration of fission fragments during irradiation appears complex and results from more than one mechanism. (F. A. Rough)

References

1. R. G. Bellamy and N. A. Hill, Extraction and Metallurgy of Uranium, Thorium, and Beryllium, *International Series of Monographs on Nuclear Energy, Division VIII. Materials*, Vol. 1, The Macmillan Co., New York, 1963.
2. E. F. Sturcken (Ed.), Papers presented at the X-Ray Preferred Orientation Meeting at Savannah River Laboratory June 7 and 8, 1962, USAEC Report DP-904, Savannah River Laboratory, July 1964.
3. B. Pinteau, G. Cizeron, and P. Lacombe, Study of the Sintering Mechanisms for Powdered Uranium in α, β, γ Phases (in French), *Mem. Sci. Rev. Met.*, 61: 787-804 (November 1964).
4. H. Mikailoff, Some Aspects of In-Pile Swelling of Fissile Materials, Part I: Non-Alloyed α Uranium (in French), French Report CEA-R-2601, September 1964.
5. J. A. Straatmann and N. F. Neumann, Equilibrium Structures in the High Uranium-Aluminum Alloy System, USAEC Report MCW-1488, Mallinckrodt Chemical Works, Nov. 11, 1964.
6. R. W. Anderson, Metallurgical Evaluation of High-Uranium Fuel Systems, USAEC Report NMI-7292, Nuclear Metals Division of Textron Inc., June 19, 1964.
7. M. Degois, Study of the Tempering at Various Temperatures of the Beta Phase Retained by Water Quenching in Uranium-Chromium Alloys with Cadmium Concentrations of from 0.37 to 4 At.%, USAEC Report ANL-Trans-124, translated from French Report CEA-R-2340, 1963.
8. P. Grenier, Comparative Study of the Flow of Polycrystalline Uranium and Its Alloys with Molybdenum at 0.5 and 1.1% Between 415 and 630 C (in French), *Compt. Rend.*, 259: 1956-1959 (September 1964).
9. J. Lehmann and J. Decours, Properties of Uranium-Molybdenum Alloys of Low (Mo) Content Utilizable as Fuel Materials (in French), French Report CEA-R-2568, August 1964.
10. C. Collot, Study of the Transformation of Uranium-Niobium Alloys with Low Niobium Concentrations, Quenched from the Gamma and Beta + Gamma$_1$ Regions and Then Tempered at Various

Temperatures. Comparison with Uranium-Molybdenum Alloys, USAEC Report ANL-Trans-101, translated from French Report CEA-R-2341, 1963.

11. J. Laniesse, H. Aubert, and P. Lebret, Mechanical Properties of Low-Concentration Uranium Alloys (in French), *Mem. Sci. Rev. Met.*, 61: 761-767 (November 1964).
12. R. M. Willard and A. R. Schmitt, Irradiation Swelling, Phase Reversion, and Intergranular Cracking of U-10 Wt.% Mo Fuel Alloy, USAEC Report NAA-SR-8956, Atomics International, Feb. 1, 1965.
13. A. R. Schmitt, R. M. Willard, and D. K. Magnus, The NAA 47 U-10 Mo Fuel Irradiation Program for HNPF Core I, USAEC Report NAA-SR-8955, Atomics International, Feb. 1, 1965.
14. R. Boucher and P. Barthelemy, Comparison of the Alloys U-Pu-Mo, U-Pu-Nb, U-Pu-Ti, and U-Pu-Zr, USAEC Report ANL-Trans-138, translated from French Report CEA-R-2531, July 1964.
15. Argonne National Laboratory, Reactor Development Program Progress Report, February 1965, USAEC Report ANL-7017, Mar. 18, 1965.
16. L. J. Wittenberg and G. R. Grove, Reactor Fuels and Materials Development; Plutonium Research: July-September 1964, USAEC Report MLM-1220, Mound Laboratory, Sept. 30, 1964.
17. Hanford Atomic Products Operation, Metallurgy Research Operation, Quarterly Progress Report, July-September 1964, USAEC Report HW-84281, Sept. 15, 1964.
18. J. A. Leary and L. J. Mullins, Preparation of Ternary Plutonium Alloys for Core Test Facility Program, USAEC Report LA-3209, Los Alamos Scientific Laboratory, Nov. 9, 1964.
19. Los Alamos Scientific Laboratory, Quarterly Status Report on Plutonium Reactor Fuel Development for Period Ending November 20, 1964, USAEC Report LA-3208-MS, Dec. 23, 1964.
20. C. C. Land, K. A. Johnson, and F. H. Ellinger, The Plutonium-Silicon System, USAEC Report LADC-6199, Los Alamos Scientific Laboratory, 1963.
21. D. J. Hodkin and P. G. Mardon, The Diffusion of Plutonium in Magnesium and Magnesium Alloys, British Report AERE-R-4800, December 1964.
22. B. Spriet, Modes of Deformation of Alpha Plutonium, USAEC Report UCRL-Trans-1150(L), translated from *J. Nucl. Mater.*, 12: 159-166 (1964).
23. J. A. Leary (Comp.), Plutonium Fuels, USAEC Report LA-DC-6712, Los Alamos Scientific Laboratory, Oct. 20, 1964.
24. Los Alamos Scientific Laboratory, Quarterly Status Report on Advanced Reactor Technology (ART) for Period Ending January 31, 1965, USAEC Report LA-3244, Mar. 3, 1965.
25. R. W. Dayton and S. J. Paprocki, Progress Relating to Civilian Application During February 1965, USAEC Report BMI-1717, Battelle Memorial Institute, Mar. 1, 1965. (Classified)
26. K. A. Johnson, Metallographic Preparation and Observations of Some Plutonium-Carbon Alloys, USAEC Report LA-3191, Los Alamos Scientific Laboratory, Nov. 5, 1964.
27. L. E. J. Roberts and J. Williams, Atomic Energy Research Establishment, Harwell, England, unpublished.
28. D. Stahl, A. Strasser, J. Anderson, and K. Taylor, Study of Uranium-Plutonium Monoxides, Progress Report, August 1-October 31, 1964, USAEC Report UNC-5102 (EURAEC-1287), United Nuclear Corp. and The Carborundum Company, Dec. 28, 1964.
29. Hanford Atomic Products Operation, Ceramics Research and Development Operation, Quarterly Report July-September 1964, USAEC Report HW-81602, Dec. 28, 1964.
30. Atomic Energy of Canada Ltd., unpublished.
31. Argonne National Laboratory, Reactor Development Program Progress Report, November 1964, USAEC Report ANL-6977, Dec. 21, 1964.
32. N. M. Griesenauer, M. S. Farkas, and F. A. Rough, Thorium and Thorium-Uranium Compounds as Potential Thermal Breeder Fuels, USAEC Report BMI-1680, Battelle Memorial Institute, July 28, 1964.
33. J. D. Fleming, J. W. Johnson, and S. H. Bomar, Reactions in Al-34 Wt.% U_3O_8 Dispersions, USAEC Report TID-21311, Georgia Institute of Technology, July 1, 1964.
34. Hanford Atomic Products Operation, Research and Development Programs, Executed for the Division of Reactor Development, Quarterly Progress Report, April-June, 1964, USAEC Report HW-83298, November 1964.
35. General Electric Company, Advanced Technology Services, High-Temperature Materials Program, Progress Report No. 43, Part A, USAEC Report GEMP-43A, Jan. 29, 1965.
36. J. M. Davies and C. Steer, Thermal Cycling of UO_2-Stainless Steel Cermets, British Report AERE-M-1253, January 1964.
37. G. L. Vivian, A Summary Report on ML-1 Fuel Element Development In-Pile Test History, USAEC Report IDO-10040, Idaho Operations Office, June 1964.
38. S. Y. Ogawa, AEC Fuel Cycle Program—Design and Fabrication of Special Assembly 9-L. Irradiation Performance Test of UO_2-Cermet Fuel, USAEC Report GEAP-4435, Vallecitos Atomic Laboratory, March, 1964.
39. J. C. Bokros, W. V. Goeddel, J. R. Hooker, H. K. Lonsdale, J. L. White, and L. R. Zumwalt, Advanced, Graphite-Matrix, Dispersion-Type Fuel Systems, Quarterly Progress Report for the Period Ending September 30, 1963, USAEC Report GA-4617 (Part 1), General Atomic Division, General Dynamics Corp., Sept. 30, 1963.
40. Oak Ridge National Laboratory, Gas-Cooled Reactor Program Semiannual Progress Report for Period Ending September 30, 1964, USAEC Report ORNL-3731, February 1965.
41. R. W. Dayton and S. J. Paprocki, Progress Relating to Civilian Applications During December 1964, USAEC Report BMI-1707, Battelle Memorial Institute, Jan. 1, 1965. (Classified)
42. R. W. Dayton and S. J. Paprocki, Progress Relating to Civilian Applications During January 1965, USAEC Report BMI-1711, Battelle Memorial Institute, Feb. 1, 1965. (Classified)
43. M. F. Browning, V. M. Secrest, and J. M. Blocher, Jr., Preparation and Evaluation of Alumina-Coated Fuel Particles, USAEC Report BMI-1708, Battelle Memorial Institute, Jan. 20, 1965.
44. B. J. Seddon, Uranium Ceramics Data Manual, Properties of Interest in Reactor Design, British

DEG-Report-120 and Addendum, Mar. 7, 1960. Amended June 1964.
45. J. A. Christensen, A. J. Bush, H. M. Ferrari, and R. J. Allio, Uranium Oxide Thermal Conductivity, *Trans. Am. Nucl. Soc.*, 7(2): 391 (November 1964).
46. F. J. Hetzler and E. L. Zebroski, Thermal Conductivity of Stoichiometric and Hypostoichiometric Uranium Oxide at High Temperatures, *Trans. Am. Nucl. Soc.*, 7(2): 392 (November 1964).
47. J. L. Bates, Fission Product Distribution in Irradiated UO_2, *Trans. Am. Nucl. Soc.*, 7(2): 389 (November 1964).
48. R. W. Ohse, High-Temperature Vapor-Pressure Studies of UO_2 by Effusion Method, Euratom Report EUR-2166.e, 1964.
49. E. Lee, Spheroidization of Uranium Dioxide and Alumina by R. F. Coupled Plasma, Australian Report AAEC/TM-267, September 1964.
50. I. E. Knudsen, N. M. Levitz, and A. A. Jonke, Engineering Development of Fluid-Bed Fluoride Volatility Processes. Part 6. Preparation of Dense Uranium Dioxide Particles from Uranium Hexafluoride in a Fluidized Bed, USAEC Report ANL-6902, Argonne National Laboratory, December 1964.
51. W. Duerrschnabel, W. Hoppe, B. Liebmann, O. Neumann, P. Saalfeld, and L. Schikarski, Production of UO_2 Powders for High Bulk Density by Melting and Grinding and Their Processing into Fuel Elements, Quarterly Report No. 16. Special Report, July 1, 1963–June 30, 1964, USAEC-Euratom Report EURAEC-1121, 1964.
52. W. Bauschmann and R. Pascard, Improvements in or Relating to Uranium Dioxide, British Patent No. 970,735, Sept. 23, 1964.
53. J. Guon, J. E. Bodine, and R. J. Sullivan, Refabrication and Encapsulation of Highly Irradiated Uranium Dioxide, USAEC Report NAA-SR-8213, Atomics International, Dec. 1, 1964.
54. B. L. Eyre and M. J. Sole, Electron Microscope Studies of UC_2 Precipitates in UC Single Crystals, *Phil. Mag.*, 9: 545-556 (April 1964).
55. M. F. Browning, Battelle Memorial Institute, private communication, January 1965.
56. F. W. Korbitz, Electrical Resistivity and Phase Boundaries for Thorium-Carbon Alloys, Ph. D. Thesis, Iowa State University, 1964.
57. C. Brisi and P. Appendino, Equilibria in the Systems: U-Ni-C and Th-Ni-C, *Ann. Chim. (Rome)*, 54: 661-672 (July 1964).
58. Los Alamos Scientific Laboratory, Quarterly Status Report of LASL Rover Program for Period Ending November 30, 1964, USAEC Report LA-3212-MS, p. 96, December 1964. (Classified)
59. Argonne National Laboratory, Reactor Development Program Progress Report, January 1965, USAEC Report ANL-7003, Feb. 18, 1965.
60. L. Yang et al., Investigations of Carbides as Cathodes for Thermionic Space Reactors, Final Report, Report GA-4769 (Pt. I), General Atomic Division, General Dynamics Corp., Mar. 17, 1964.
61. J. Kusma and H. Nowotny, The Crystal Structure of U_2Fe_3 Si and TaNiAl (in German), *Monatsh. Chem.*, 95: 428-430 (1964).
62. P. Biddle, The Emission of Xenon-133 from Uranium Carbonitrides, British Report AERE-R-4700, September 1964.
63. R. W. Endebrock, E. L. Foster, Jr., and D. L. Keller, Preparation and Properties of Cast UN, USAEC-Euratom Report BMI-1690 (EURAEC-1206), Battelle Memorial Institute, Aug. 28, 1964.
64. D. L. Keller, Development of Uranium Mononitride, Quarterly Progress Report, April–June, 1964, USAEC Report BMI-X-10092 (EURAEC-1136), Battelle Memorial Institute, July 1, 1964.
65. Argonne National Laboratory, Reactor Development Program Progress Report, December 1964, USAEC Report ANL-6997, Jan. 18, 1965.
66. Papers presented at the Third United Nations International Conference on the Peaceful Uses of Atomic Energy, Geneva, 1964.
    a. R. S. Barnes, R. G. Bellamy, B. R. Butcher, and P. G. Mardon, The Irradiation Behavior of Uranium and Uranium Alloys Fuel, A/Conf.28/P/145.
    b. Y. Adda, J-P. Mustelier, and Y. Quere, Behavior of Uranium Under Irradiation, A/Conf. 28/P/62.
    c. W. B. Lewis, J. R. MacEwan, W. H. Stevens, and R. G. Hart, Fission Gas Behavior in UO_2 Fuel, A/Conf.28/P/19.
    d. V. M. Golyanov and N. F. Pravdyuk, Behavior of Nuclear Fuel Under Irradiation (Investigation of Thin Layers of Irradiated Uranium Dioxide), A/Conf.28/P/338.
67. B. Hudson, The Crystallography and Burgers Vectors of Dislocation Loops in α-Uranium, *Phil. Mag.*, 8: 10 (December 1964).
68. R. Nagasaki and S. Kawasaki, Behaviors of Krypton and Xenon in Uranium Metal. Release of Krypton and Xenon from Metallic Uranium, *Nippon Genshiryoku Kenkyusho Kenkyu Hokoku*, No. 4030 (1964).
69. L. R. Zumwalt, P. E. Gethard, and E. E. Anderson, Fission-Product Release from Monogranular UC_2 Particles, *Nucl. Sci. Eng.*, 21: 1-12 (January 1965).
70. J. A. Christensen, R. J. Allio, and A. Biancheria, Melting Point of Irradiated Uranium Dioxide, *Trans. Am. Nucl. Soc.*, 7(2): 390-391 (November 1964).

Section

II

Reactor Materials

Moderator Materials

Graphite

A second interim report[1] has been issued by Hanford on the long-term irradiation stability of Experimental Gas Cooled Reactor (EGCR) graphite. Samples were irradiated in a temperature range 375 to 850°C to a maximum neutron exposure equivalent to 70,000 Mwd/adjacent ton, the largest known exposure on graphite. The data in this report are too extensive to summarize, but some of the more important conclusions are presented here. Concerning possible effects of neutron-flux-intensity differences on contraction and other properties, 425 to 475°C data obtained at the minimum flux and those obtained at the maximum flux showed no statistical difference. The present data indicate that the concept of saturation of length change previously discussed in USAEC Report HW-71500A is not valid. At the highest irradiation temperatures, the results from transverse samples indicate that a mechanism causing growth with continued irradiation has become controlling. The neutron exposure at which the high-temperature contraction passes through a maximum, 6 to 8 $\times$ 10^{21} neutrons/cm^2 ($E > 0.18$ Mev), appears to be a critical point for other parameters also. The mechanism causing the increase in length also causes a decrease in apparent crystallite size, L_c, and an increase in electrical resistivity, indicating that the crystallite disorder is becoming greater.

A comprehensive program to provide fundamental information concerning various factors controlling the oxidation behavior of protective-coating systems for graphite at temperatures up to 2200°C is being conducted by Carbon Products Division of the Union Carbide Corp. for the Air Force Materials Laboratory. A recent report[2] summarizes the work accomplished on this continuing research program. The work discussed includes the evaporation of iridium in the presence of oxygen and water vapor to temperatures of 1300°C; studies involving carbon diffusion through iridium; the permeability of iridium, rhodium, ZrO_2, HfO_2, and ThO_2 to oxygen at temperatures of 2000°C; the coating of graphite with iridium, including the carbon-iridium eutectic-temperature determination; the reactions of iridium and rhodium with ZrB_2, HfB_2, ZrC, HfC, and ThC_2; the kinetics of the carbothermic reduction of ZrO_2, HfO_2, and ThO_2 to temperatures in excess of 2000°C; the chemical reactions of graphite with ZrB_2 and HfB_2; and arc-plasma tests of iridium-coated graphite.

The study has shown that iridium has high potential as a single-layer coating for the oxidation protection of graphite. It has been demonstrated that (1) iridium is virtually impervious to oxygen at temperatures up to 2200°C, (2) iridium does not react with graphite even at temperatures in excess of 2000°C, and (3) molten iridium wets graphite and forms an adherent coating that exhibits excellent thermal-shock resistance in the temperature range 25 to 2200°C. A 5-mil-thick coating of iridium submitted to an oxidation test in an arc plasma provided complete protection for the graphite substrate at 2000°C. At this temperature the ablation rate was 5.4 mils/hr in an air pressure of 1 atm and 0.5 mil/hr in a stagnation pressure of 48 torrs. The use of iridium on graphite would be limited to operational temperatures of 2110 $\pm$ 25°C, the eutectic temperature. The cost is high; at the current price it is given as $126 per square foot of 1-mil-thick coating. (M. C. Brockway)

Beryllium Metal and Alloys

Physical Metallurgy and Mechanical Properties

Bunshah,[3] at the Lawrence Radiation Laboratory, has reviewed the effects of purification on the mechanical properties of single crystals and polycrystalline beryllium. Commercial and high-purity materials prepared by distillation and/or zone refining were compared. A decrease in critical resolved shear stress for basal and prism slip, work-hardening rate, and probability of crack formation was seen with increasing purity. Crack propagation was also more difficult in higher purity material.

Schmidt[4] of the Navy Bureau of Weapons reviewed current thinking regarding increasing the ductility of beryllium. The means most likely to achieve this goal, according to the author, are selected alloying and refinement of grain size. The deformation modes in single crystals and phenomena affecting them are also discussed. Also reviewed are the effects of crystallographic orientation, purity, hot working, and grain size on mechanical properties.

An abstract of a recent Soviet article[5] concerned primarily with the mechanical properties of zone-refined beryllium was received. The abstract indicates that the Soviets are pursuing the same general approaches as in the United States for making more plastic beryllium. These approaches are as follows:

1. Hot working of ingot beryllium
2. Alloying aimed at stabilizing the beta phase
3. Grain refinement by powder metallurgy
4. Purification by distillation, thermal decomposition of halides, and zone refining

Fabrication

The Defense Metals Information Center (DMIC) issued a memorandum[6] reviewing the surface-damage effects incurred while machining beryllium. This surface damage is caused by twinning and microcracking as a result of various machining operations. The twinning is a result of surface working while microcracks initiate at various sites, often in conjunction with twinning. Causes of these phenomena, such as the effect of machining parameters, are given. The effect of machining damage on mechanical properties is also discussed.

Work on the vacuum hot pressing of electrolytic beryllium powder was reported by the Australian Atomic Energy Commission (AEC).[7] Densities in excess of 99% of the theoretical density could be attained in bodies pressed at 1080°C. Density varied with oxide content and geometry of the compact. For example, specimens with 2.3 wt.% BeO required 1500 psi for densification at 1080°C, whereas those containing 0.54 wt.% BeO required only 750 psi. A density gradient was noted in compacts with length-to-diameter ratios greater than 0.5.

Roberts at Rocky Flats has detailed a technique[8] for electroless nickel coating of beryllium shapes from an acidic solution. The coating contained approximately 7 wt.% phosphorus. The substrate was thoroughly cleaned, activated, and covered with a thin zirconate coating. It was found that complete coverage of complex beryllium shapes could be achieved. Rate of deposition could be controlled by regulating solution variables such as temperature, *p*H, composition, and application time.

Nuclear and Chemical Properties

The Australian AEC reported[9] on irradiation damage in extruded beryllium initially consolidated by hot pressing or pressureless sintering. The specimens were submitted to fast radiation doses of 5.5 to 9.0 $\times$ 10^{20} neutrons/cm^2 at temperatures of 450, 550, and 650°C. Density changes were noted only at 650°C. A loss in elevated-temperature tensile properties was noted in all the materials and was attributed to helium bubble formation in the grain boundaries. Beryllium that was hot pressed prior to extrusion was superior to that which was pressureless sintered.

Battelle reported[10] on techniques for detecting minute quantities of impurities in beryllium. The report details the development of a spark-source mass-spectrographic analytical procedure. Of primary importance was the development of techniques for specimen surface preparation prior to analyses. Emission-spectrographic methods capable of determining metallic impurities near the 1 ppm level were also developed. Carbon was determined by combustion methods.

(H. D. Hanes)

Beryllium Oxide

Since the existence of a high-temperature form of BeO was confirmed in recent years by high-temperature X-ray diffraction studies, attention has been given to the possibility of stabilizing this form of BeO. The expectation was that the high-temperature form might be less anisotropic and thus more resistant to damage by neutron irradiation than the low-temperature form.

Bannister[11] has recently reviewed the literature on the high-temperature BeO phase and reported on properties and the probability of stabilization. On the bases of the work of several investigators, he lists the most likely transformation temperature to be 2050 ± 50°C. A discrepancy exists between Austerman's (1963) measured 1.25 ± 0.25 kcal/mole heat of transformation, and Kandiba's (1960) work in which he detected no discontinuity in the heat content of BeO from 900 to 2500°C. Bannister found no evidence in the literature to suggest that the high temperature (beta BeO) has ever been stabilized sufficiently by an additive to be retained as an equilibrium phase at moderate temperatures. He also utilized the Clausins-Clapeyron equation with the heat of transformation taken to be 1.25 kcal/mole and constructed the initial part of the boundary between the alpha-plus-beta and the beta phases for a phase system BeO-*A*, where *A* is an additive that dissolves in beta BeO and not in the low-temperature alpha BeO. The results indicate that a substantial solubility of additive *A* in beta BeO could be required to stabilize it. The significance of these calculations depends on the validity of the heat of transformation used, the solubility of *A* in alpha BeO, and deviations from Raoult's law. However, from the literature survey and theoretical calculations, the author concludes that the high-temperature beta BeO is not likely to be stabilized.

(M. C. Brockway)

Solid Hydrides

Zirconium Hydride

Earlier work on zirconium hydride in Zircaloy showed that, if the hydride platelets were oriented normal to an applied tensile stress, the room-temperature ultimate tensile strength and ductility were drastically reduced.[12] However, recent studies at Chalk River[13] have demonstrated that the tensile properties of hydrided Zircaloy are restored in the range 100 to 200°C owing to plasticity of the hydrides. The mechanism is not clear, but the temperature increase may change the hydride to a ductile form, or there may exist a complex relation between the hydride phase and the zirconium matrix. For samples containing 200 ppm hydrogen, the ultimate tensile strength at 100°C was the same as that for 0 ppm hydrogen, whereas ductility and reduction of area started to recover at about 125°C and continued to improve with further temperature increase. This restoration of tensile properties cannot be attributed to re-solution of the hydrogen because the low solubility of hydrogen at these temperatures requires that 50% or more of the hydrogen exist as precipitated zirconium hydride. The effects of higher hydrogen concentrations and neutron irradiation on hydride ductility have yet to be evaluated.

The effects of hydride precipitates on the mode of fracture of Zircaloy-2 have been investigated by Louthan.[14] Metallographic examination of polished sections of ductile specimens showed that the hydride orientation in the specimen before testing was approximately random and that during deformation the hydrides rotated so that they were parallel to the major direction of deformation. Fracture occurred by the coalescence of voids. The center of the specimen fractured by ductile rupture, whereas the fracture near the edges occurred by ductile shear. Hydride orientation in brittle specimens was normal to the stress axis and did not change during fracture because only limited deformation occurred. Fracture occurred by discontinuous cleavage.

Other Hydrides

The terminal solubility of hydrogen in Zr–2.5 wt.% Nb has been measured at Chalk River.[15] Over the range 375 to 500°C, the solubility was found to be 276 to 627 ppm hydrogen. These results indicate that the extent of hydrogen solution and hydride formation in zirconium is not influenced by niobium addition.

The systems Li-Rh-H and Li-Ir-H have been studied at Denver Research Institute.[16] Compounds of the compositions $(LiH)_4Rh$ and $(LiH)_4Ir$ were prepared by heating 4-to-1 molar ratio mixtures of LiH and the metal. At room temperature both compounds are grayish-black

crystalline materials. The rhodium compound melts at about 575°C, but the iridium derivative does not melt below 850°C. The rhodium compound has been found to be tetragonal, and the calculated N_H value is 5.8, based on an X-ray density to 3.17 g/cm^3. (H. H. Krause)

References

1. J. W. Helm, The H-3 Irradiation Experiment: Irradiation of EGCR Graphite, Interim Report No. 2, USAEC Report HW-71500B, Hanford Atomic Products Operation, September 1964.
2. J. M. Criscione, R. A. Mercuri, E. P. Schram, A. W. Smith, and H. F. Volk, High-Temperature Protection Coatings for Graphite, Report ML-TDR-64-173(Part II), Union Carbide Corp., Carbon Products Division, August 1964.
3. R. F. Bunshah, Effect of Purification on Some Mechanical Properties of Beryllium, *Metals Eng. Quart.*, 4: 8-17 (November 1964); also in USAEC Report UCRL-7522, University of California, Lawrence Radiation Laboratory, Apr. 3, 1964.
4. R. Schmidt, Ductile Beryllium Comes in View, *Metal Progr.*, 86(6): 134-138 (December 1964).
5. I. V. Milov, D. M. Skorov, and V. V. Nikishanov, Mechanical Properties of Zone-Refined Beryllium, *Met. i Metalloved. Chistytkh Metal.*, No. 4, 175-181 (1963).
6. S. W. Porembka and H. D. Hanes, Surface Damage in Machined Beryllium, Report DMIC-Memo-198, Defense Metals Information Center, Battelle Memorial Institute, Jan. 4, 1965.
7. T. E. Clare, P. D. Smith, and W. J. Wright, The Vacuum Hot-Pressing of Beryllium, Australian Report AAEC/E-118, March 1964.
8. W. H. Roberts, Coating Beryllium with Electroless Nickel, USAEC Report RFP-478, Dow Chemical Co., Rocky Flats Division, Dec. 29, 1964.
9. B. S. Hickman and G. Bannister, Irradiation of Beryllium at Elevated Temperatures, Part II. Irradiation of RIG X-74 in HIFAR, Australian Report AAEC/E-115, December 1963.
10. W. M. Henry, Development of Analytical Techniques for the Determination of Minute Quantities of Selected Elements in Beryllium, Battelle Memorial Institute, Final Report to Navy Bureau of Weapons, Feb. 25, 1965.
11. M. J. Bannister, The High-Temperature BeO Phase — A Review, Australian Report AAEC/TM-271, November 1964.
12. R. P. Marshall and M. R. Louthan, Jr., Tensile Properties of Zircaloy with Oriented Hydrides, *Trans. Am. Soc. Metals*, 56(3): 693-700 (1963).
13. G. W. Parry and W. Evans, Occurrence of Ductile Hydrides in Zircaloy-2, *Nucleonics*, 22(11): 65 (November 1964).
14. M. R. Louthan, Jr., Cleavage in Hydrided Zircaloy-2, *Am. Soc. Metals, Trans. Quart.*, 57: 1004-1008 (1964).
15. Atomic Energy of Canada Ltd., unpublished, 1964.
16. C. B. Magee, A Study of the Synthesis and Properties of Transition-Metal Hydryls, USAEC Report DRI-2189, Denver Research Institute, Oct. 15, 1964.

Section

III

Reactor Materials

Nuclear Poisons

Metallic Poison Materials

In a study[1] of the molybdenum-rich portion of the molybdenum-boron phase diagram, the solubility of boron in molybdenum was found to be 0.2 at.% at the eutectic temperature (2050°C) and 0.07 at.% at 1400°C. The hardness of molybdenum decreases slightly with the increase of boron in the solid-solution range, beyond which it increases steadily with further increase in boron content.

The performance of 80 wt.% Ag–15 wt.% In–5 wt.% Cd alloy was improved as a control-rod material by various additions of tin, platinum, and palladium.[2] The addition of 2.5 wt.% palladium and 0.5 wt.% tin resulted in increased elevated-temperature yield and creep strength, as well as improved resistance to oxidation in hot borated water. However, irradiation of the modified alloy resulted in larger decreases in ductility than those experienced by unmodified 80 wt.% Ag–15 wt.% In–5 wt.% Cd at comparable exposures (Table III-1). Also, the modified alloy was found to undergo larger radiation-induced dimensional changes than did the unmodified alloy.

An anisotropy of oxidation rate was found in coarse-grained hafnium samples.[3] This effect is associated with a variation in the stoichiometry of the oxide films covering the differently oriented grains. It has been found[4] that additions of oxygen and nitrogen to hafnium stabilize the alpha phase and increase the alpha → beta transformation temperature.

Results of tensile tests[5] on irradiated hafnium are shown in Table III-2. Fracture-tough-

Table III-1 EFFECT OF IRRADIATION ON TENSILE PROPERTIES OF Ag-In-Cd ALLOYS[2]

(Irradiation Temperature, 150°F)

Material*	Exposure, neutrons/cm² (> 1 Mev)	Test temp., °F	Yield strength (0.2% offset), 1000 psi	Ultimate tensile strength, 1000 psi	Total elongation, %
Ag-In-Cd-Sn	Nonirradiated	Room	21.6	50.3	44.0
Ag-In-Cd-Sn	2.8×10^{21}	Room	48.2	49.9	8.1
Ag-In-Cd-Sn	Nonirradiated	600	14.2	15.3	61.0
Ag-In-Cd-Sn	2.8×10^{21}	550	30.8	32.9	0.6
Ag-In-Cd	Nonirradiated	Room	12.2	44.2	53.0
Ag-In-Cd	9.1×10^{20}	Room	39.8	50.2	31.3
Ag-In-Cd	Nonirradiated	550	9.0	26.0	27.0
Ag-In-Cd	9.1×10^{20}	550	30.3	39.0	6.6

*All material was extruded, then stress relieved at 750°F for 1 hr.

Table III-2 TENSILE PROPERTIES OF IRRADIATED HAFNIUM[5]

Exposure, neutrons/cm² (> 0.625 Mev)	Ultimate tensile strength, 1000 psi	Yield strength (0.2% offset), 1000 psi	Elongation in 1 in., %	Uniform elongation, %	Reduction in area, %
0	58.6	27.5	34.2	28.1	32.5
7×10^{21}	89.0	81.0	15.0	4.0	22.5
15×10^{21}	102.5	96.0	13	4.0	21.5

ness tests were performed on four specimens irradiated to 7×10^{21} neutrons/cm^2 (>0.625 Mev) and on four specimens irradiated to 15×10^{21} neutrons/cm^2 (>0.625 Mev). These tests were performed from −320 to 80°F. The tests revealed that (1) irradiated hafnium possesses adequate toughness for current control-rod application and (2) there is essentially no difference in the brittle-fracture resistance of the material at the two levels of irradiation.

(M. Kangilaski)

Dispersions and Nonmetallic Poison Materials

A German publication[6] describes the fabrication and testing of boron carbide and copper absorbers for shutdown control rods and presents the methods used to consolidate and fabricate the absorbers. A diffusion study conducted at 900°C, using couples of copper plus Nimonic-75 and copper plus V2A stainless steel, indicated that the former results in a wide diffusion zone, whereas the latter couple produces a narrow zone.

Thermal-conductivity values reported[7] for boronated graphite at 1000°F are:

Boron content, wt.%	k, Btu/(hr)(ft)(°F)	
	Perpendicular	Parallel
6.2	16.6 ± 1.8	26.7 ± 1
9.3	17.5 ± 1.2	19.6 ± 1.5

Similar measurements on powdered boron carbide gave:

Bulk density, lb/cu ft	Temp., °F	k, Btu/(hr)(ft)(°F)
73.9	500	0.18
73.9	1000	0.28
84.4	500	0.25
84.4	1000	0.35

Elevated-temperature tensile tests, performed by the Bureau of Mines[8] on hafnium-carbon alloys, gave the results shown in Table III-3. It was also found that the emissivity of hafnium carbide decreases from 0.97 at 1000°C to 0.70 at 2800°C.

Table III-3 TENSILE-TEST DATA ON HAFNIUM-CARBON ALLOYS[8]

Test temp., °C	Carbon content, wt.%	Strength, psi
2100	8.88	3160
2070	8.32	4000
2420	8.17	2380
2040	9.62	1130

Measurements of the linear-thermal-expansion coefficients of fused hafnium carbide–carbon alloys at temperatures up to 900°C were made by the Bureau of Mines[9] (see Table III-4). The carbon contents of these alloys varied from 5.1 wt.% (stoichiometric) to 12.3 wt.%. The coefficient values increased with increasing temperature range and decreased with increasing carbon content, with the exception that the lowest coefficient was for the single-phase hafnium carbide (5.1 wt.% carbon). The coefficients for fused hafnium carbide were very nearly the same as the maximum values reported in the literature for the powder-metallurgy product.

Atomics International[10] fabricated a control-rod assembly consisting of a central graphite rod surrounded by an annulus of dysprosium oxide and clad on the outside with Hastelloy X. The maximum heat-generation rate in the absorber column is calculated to be 15 kw/ft. Under this condition the absorber material will reach a temperature of 2000°F, and the Hastelloy X will reach 1800°F. On the basis of a gap distance of 0.035 in. between the outside of the cladding and the inside of the stainless-steel thimble, the thimble will reach 1050°F with a sodium coolant at 1000°F circulating through the gap.

Short-term (1000- and 2600-hr) elevated-temperature compatibility tests have been com-

Table III-4 THERMAL-EXPANSION COEFFICIENTS FOR HAFNIUM-CARBON-ALLOY CASTINGS[9]

Temp. range, °C	Average linear-expansion coefficient, 10^{-6}/°C, at indicated carbon content, wt.%			
	12.3	10.4	7.7	5.1*
100 to 200	6.42	6.38	6.48	6.33
100 to 300	6.42	6.47	6.62	6.38
100 to 400	6.49	6.57	6.77	6.42
100 to 500	6.57	6.70	6.87	6.52
100 to 600	6.70	6.79	6.94	6.58
100 to 700	6.75	6.88	7.01	6.70
100 to 800	6.82	6.92	7.05	6.66
100 to 900	6.83	6.93	7.03	6.60

*The specimen was found cracked after the test.

pleted. At 1850°F a 0.0004-in. layer of dysprosia adhered to the Hastelloy component. This layer was rich in chromium, but it was later found that the reaction was restricted to the surface of the Hastelloy and that chromium had not migrated from the interior of the cladding. Further compatibility, thermal-cycling, and irradiation tests are planned.

(E. G. Smith, Jr.)

References

1. T.-L. Chuang and C.-H. Wu, Phase Diagram of the Molybdenum-Rich Portion of the Molybdenum-Boron System, *Sci. Sinica*, 13: 1851-1860 (November 1964).
2. W. R. Smalley and D. B. Scott, Metallurgical Evaluation of Silver-Indium-Cadmium Control-Rod Alloys, USAEC Report WCAP-3269-29, Westinghouse Electric Corp., Atomic Power Division, August 1964.
3. J. P. Pemsler, Studies on the Oxygen Gradients in Oxidizing Metals: II, Hafnium, *J. Electrochem. Soc.*, 111: 1339-1342 (December 1964).
4. N. H. Krikorian and T. C. Wallace, The Effect of Oxygen and Nitrogen on the Hafnium α-β Transformation, *J. Electrochem. Soc.*, 111: 1431-1433 (December 1964).
5. D. F. Mowbray, Fracture Toughness of Irradiated PWR Hafnium, USAEC Report KAPL-3076, Knolls Atomic Power Laboratory, Sept. 10, 1964.
6. O. Ruediger, G. Lohrke, and J. Willbrand, Composite Materials of BC and Copper as Neutron Absorbers for Shutdown Rods, *Tech. Mitt. Krupp*, 22: 41-47 (August 1964).
7. C. F. Bonilla and A. J. Friedland, Thermal Conductivity of Boronated Graphite and Powdered Boron Carbide, *Nucl. Struct. Eng.*, 1: 7-13 (January 1965).
8. Bureau of Mines, Albany Metallurgy Research Center, Metallurgical Quarterly Progress Report No. 25, October 1–December 31, 1964, USAEC Report USBM-RC-1150.
9. Bureau of Mines, Albany Metallurgy Research Center, Coefficients of Thermal Linear Expansion of Fused Hafnium Carbide–Carbon Alloys, USAEC Report USBM-RC-1119, October 1964.
10. Atomics International, Annual Technical Progress Report, AEC Unclassified Programs, Fiscal Year 1964, USAEC Report NAA-SR-9999, Aug. 31, 1964.

Section

IV

Reactor Materials

Cladding and Structural Materials

Corrosion

Corrosion of Zirconium Alloys

GENERAL

The effect of oxygen and nitrogen on the aqueous-corrosion behavior of consolidated Zircaloy-2 powder has been studied at Knolls Atomic Power Laboratory.[1] Greater than 2700 ppm oxygen and 100 ppm nitrogen additions to Zircaloy-2 had deleterious effects on the alloy's corrosion resistance in 680°F water and 750°F steam. Increasing nitrogen content (100 to 400 ppm) in the Zircaloy resulted in a decrease in the fraction of theoretical hydrogen absorbed (ratio of hydrogen absorbed to that produced by the corrosion reaction).

The behavior of zirconium alloys in Santowax organic coolants is being studied in Canada.[2] Despite the findings that hydriding was enhanced by neutron irradiation, a Zircaloy-4 in-reactor test section did not exhibit excessive hydriding after more than 5000 hr of exposure to Santowax OM at 320 to 400°C.

OXIDE STUDIES

The results of microprobe studies on the distribution of alloying elements in the oxide and bulk metal of zirconium alloys have been summarized by Savannah River Laboratory.[3] Iron-chromium aggregates and occasional iron-nickel aggregates were found in the oxide of Zircaloy-2. Chromium concentrations were low in the metal matrix and in the oxide matrix, and iron and nickel concentrations were higher in the oxide matrix than in the metal matrix. Niobium and copper were found to be uniformly distributed in the metal and oxide of Zr–2.5 wt.% Nb–0.5 wt.% Cu alloys except for a thin layer enriched in copper at the metal-oxide interface.

Tritium, T_2O vapor, and autoradiography have been used[4] to determine the distribution of hydrogen during oxidation and hydrogenation of zirconium alloys at Chalk River. Hydrogen distribution was studied in the oxide, at the oxide-metal interface, and in the metal (as functions of the heat-treatment). Among the interesting results was the suggestion that a discrete barrier restricted hydrogen diffusion into the metal. This was based on the presence of large quantities of hydrogen uniformly distributed in the oxide but very low concentrations in the oxygen-rich metal (Zircaloy-2) beneath the oxide film.

RADIATION EFFECTS

The effect of preoxidizing nickel-free Zircaloy-2 in dry oxygen gas at 750°F on subsequent in-reactor corrosion behavior has been studied by Westinghouse Electric Corp.[5] The results of exposure in the Saxton core to a burnup of 9500 Mwd per metric ton of uranium with a fast dosage (>1 Mev) of 1.2×10^{21} neutrons/cm^2 revealed black lustrous films, normal weight gains, and normal hydrogen pickup in the Zircaloy.

Dissolution of the oxide formed on Zircaloy during corrosion in water under irradiation and reducing conditions may have occurred in an experiment conducted at Chalk River.[6] This suggested to the Canadian scientists that the apparently normal oxidation behavior of Zircaloy cladding in pressurized-water reactors might be the result of the oxide film reaching an equilibrium thickness in which the rate of film growth equals the rate of dissolution.

Measurements of electrical potentials across corroding oxides on zirconium alloys and calculation of ionic and electronic transference numbers have been performed at Chalk River.[7] The results of the study indicated that the high

in-reactor weight gain of unalloyed zirconium could not be accounted for by a decrease in the electronic resistivity of the oxide.

(W. E. Berry)

Corrosion of Stainless Steel

The effect of short-term overheating and film boiling on the surfaces of type 304 stainless steel and Zircaloy-2 has been studied at Vallecitos Atomic Laboratory.[8] Tests of up to 1-hr duration at 2000°F in a water-steam environment indicated that cladding rupture would not be expected to occur during short-term overheating but that grain growth within the cladding, surface oxidation, and reactions between the cladding and UO_2 could possible shorten the life of the fuel element.

The addition of 1 wt.% yttrium to Fe–25 wt.% Cr–4 wt.% Al alloy resulted in improved oxidation resistance under cyclic conditions in research conducted at General Electric Company.[9] The alloy exhibited oxidation life in excess of 2000 hr at 2300°F. Its oxidation rate at 2300°F was comparable to that of Hastelloy X at 2000°F.

Factors relating to the chloride stress-corrosion cracking of stainless steel were reported by Rideout and Mittelberg.[10] Cited were service failures resulting from chlorides (1) leached from wet insulation, PVC labels, and neoprene gaskets or (2) concentrated at leaks in heat-exchanger tube sheets. Laboratory studies demonstrated that cathodic protection and certain nitrate additions inhibited the initiation and propagation of cracking.

(W. E. Berry)

Corrosion of Base Metals

Oxidation and carburization of Hastelloy X-280 and Haynes 25 at 2050°F are being studied at Hanford Atomic Products Operation.[11] The oxidation rate of Hastelloy X-280 was found to be dependent on the one-fifth power of oxygen pressure. Data for Haynes 25 were too random to yield a numerical value for oxygen-pressure dependence, although there were indications of a slight increase in oxidation rate with increasing oxygen pressure. Carburization was found to occur readily in static methane at 25-torr pressure. The rate-controlling step appeared to be the mass transfer of methane from reservoirs at room temperature to the reaction tube at 2050°F.

In studies conducted at Vallecitos,[12] Incoloy and Inconel cladding did not exhibit localized corrosion after 120 days' exposure to the same in-reactor nuclear superheat conditions that caused failure of type 304 stainless steel within 29 days. Type 348 stainless steel and low-nitrogen vacuum-melted types 304 and 310 stainless-steel cladding performed satisfactorily at relatively low heat ratings and low stress levels.

(W. E. Berry)

Oxidation and Protection of Refractory Metals

Reaction rates of the binary Nb–10 wt.% Mo alloy with oxygen at 1-atm pressure were determined[13] gravimetrically at temperatures between 400 and 1200°C for times ranging from 6¾ to 200 hr. The temperature dependence of reaction rate was found to be very irregular. Oxidation was slow at 400°C but catastrophic at 450 to 550°C. A marked minimum in the oxidation rate occurred at 600°C. Between 600 and 800°C the oxidation rate increased with increasing temperature. A second minimum was observed at 900°C, after which the oxidation rate again increased with increasing temperature. At temperatures above 600°C the binary alloy was more oxidation resistant than pure niobium.

In Russia, eight W-Nb alloys[14] containing 1 to 50 wt.% niobium were oxidation tested in air for 6 hr at 900, 1000, 1100, and 1200°C and for 5 hr at 1300°C. The alloys containing up to 10 wt.% niobium oxidized at linear rates. Parabolic oxidation rates were obtained at 1300°C for alloys containing 15, 20, and 30 wt.% niobium. The 30 wt.% niobium alloy showed the slowest oxidation rate.

Tem-Pres Research, Inc., is conducting a study of metal-W-O reactions and equilibria and is determining the properties of any intermediate phases that result.[15] Work on five systems has been completed. These systems are: W-O, Ti-W-O, Ca-W-O, Sm-W-O, and Co-W-O. The W-O system has been investigated up to 1700°C. Isothermal sections of the ternary systems were determined at 1400 and 1700°C.

Stanford Research Institute[16] has completed an intensive study of the interactions of nitrogen, oxygen, and nitrogen-oxygen mixtures with niobium in vacuums in the range of 10^{-6} torr. The kinetics of adsorption, absorption, and degassing were investigated. Also, the thermo-

dynamic equilibrium for solution of nitrogen in niobium was determined. Detailed mechanisms for these processes were formulated to explain the experimental results.

Phosphide coatings on unalloyed niobium, tantalum, tungsten, and molybdenum were found to improve their oxidation resistance in air at 800°C. The phosphide coatings used in a study at Ames Laboratory[17] were a few microns thick. Weight changes of coated tungsten, tantalum, and molybdenum were less than 10 mg/cm^2 after 10 hr of exposure at 800°C. Phosphide-coated niobium was not as oxidation resistant as the other coated metals in this investigation. Samples containing sharp edges did not resist oxidation as well as samples having rounded edges.

Thompson Ramo Wooldridge Inc. has developed a coating process for the application of Si-W and Ti + Zr + Si-W coatings to tungsten sheet.[18] The average life of these coatings in air at atmospheric pressure is illustrated in Fig. IV-1 for temperatures from 1600 to 3600°F. Exposure of coated tungsten specimens at static air pressures below 15 mm Hg at 3400 to 3500°F resulted in varying degrees of deterioration of the coatings. Under dynamic low-pressure conditions of 2000 to 2800 ft/sec simulated air flow at 16 to 20 mm Hg, both coatings were protective to tungsten and resisted erosion in the temperature range 2900 to 3400°F [180 to 325 Btu/(sec)(sq ft) heat-flux range] for up to 60 min without failure. In stress-oxidation tests the coated tungsten specimens were loaded to 20% of the yield strength and showed essentially no creep after 1 hr at 3350°F in air. The coatings are completely protective at this stress level.

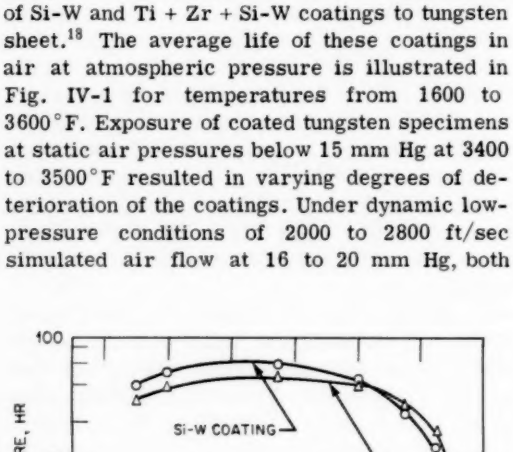

Fig. IV-1 Average life of Si-W and Ti + Zr + Si-W coatings[18] to failure in air at temperatures from 1600 to 3600°F. Five specimens of each coating system were exposed at each temperature, and all specimens were thermally cycled as follows: 1600°F, one cycle for each hour of exposure; 1800, 2500, and 3000°F, one cycle for each 5 hr of exposure; and 3300 to 3650°F, one cycle for each hour of exposure.

Solar, a division of International Harvester Co., recently published[19] the second year's results of their evaluation of coated-refractory-metal foils. The program objective was to evaluate the capabilities of coated-refractory-metal foils for multicycle reentry vehicles. The Thompson Ramo Wooldridge Cr-Ti-Si coating on B-66 niobium-alloy foil was judged as having the best potential for use in this application. For a peak reentry temperature of 2500°F, this coating system would be expected to survive numerous reentries without failure.

Two coating-research programs are in progress at Sylvania Electric Products Inc.[20,21] The first program deals with the scale-up of Sylvania's Sn-Al coating facilities. It is reported that T-111 tantalum alloy and corrugated panels of Ta–10 wt.% W are being coated. In the second program, slurry coatings are being developed for niobium, tantalum, and molybdenum alloys.

Illinois Institute of Technology Research Institute (IITRI) reported[22] that their pack-cementation silicide coating protects 20-mil sheet of V–60 wt.% Nb–1 wt.% Ti from oxidation for twenty-five 4-hr cycles at temperatures up to 2300°F in static air. These oxidation exposures generally did not affect the room-temperature tensile ductility of the siliconized alloy. At reduced air pressures of 0.1 to 1 torr, the siliconized alloy survived a 20-hr oxidation exposure at temperatures up to 2300°F without coating failure.

Solar and IITRI are jointly conducting a coatings-development program to improve the ductility of oxidation-resistant coatings.[23] Their approach to this problem will be to provide at least one layer in the coating with some ductility and oxidation resistance.

The development of processes for applying oxidation-resistant coatings to refractory metals by the fluidized-bed technique is being conducted at Boeing Co.[24] The coating process was initially developed for the X-20 program. The

coating-substrate combinations to be studied in this program will include:

1. Disilicide coating on C-129Y niobium alloy
2. Vanadium-modified disilicide coating on Ta-10 wt.% W and C-129Y niobium alloys
3. Cr-Ti-Si coating on FS-85 and Cb-752 niobium alloys

Process-development studies will be conducted in a 4-in.-diameter bed, with beds 8 and 18 in. in diameter being used for the more advanced evaluation. (J. J. English)

Corrosion by Liquid Metals

Figures IV-2 to IV-4 present information relative to the utilization of steels in large-scale sodium-cooled reactor systems. Figure IV-2 is extrapolated from 5000-hr tests with type 316 stainless steel;[25] the data are considered conservative. The influence of corrosion factors on design stresses is reflected in Figs. IV-3 and IV-4. The values represented here are also tagged as conservative.[26] For example, the design stresses for Croloy $2\frac{1}{4}$ alloy steel are based on the strength of completely decarburized material, whereas the curve for type 316 stainless steel presumes no enhanced strength as a result of carburization during exposure to flowing sodium.

A series of V-Ti alloys with ternary additions of chromium was evaluated at Argonne National Laboratory[27] for resistance to corrosion by 650°C flowing sodium containing about

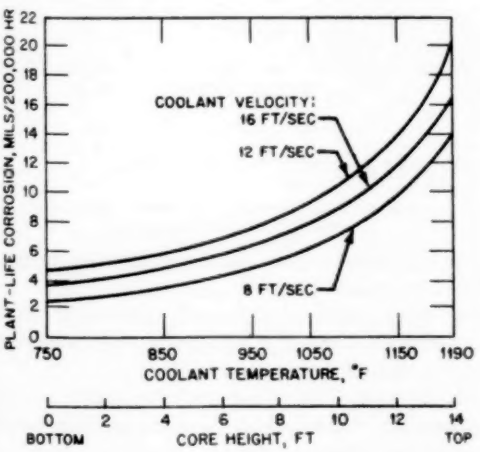

Fig. IV-2 Corrosion of austenitic stainless-steel process tubes in sodium.[25]

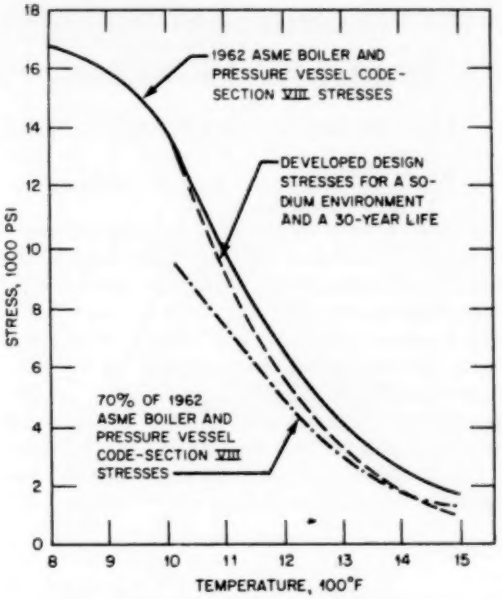
1962 ASME BOILER AND PRESSURE VESSEL CODE-SECTION VIII STRESSES
DEVELOPED DESIGN STRESSES FOR A SODIUM ENVIRONMENT AND A 30-YEAR LIFE
70% OF 1962 ASME BOILER AND PRESSURE VESSEL CODE-SECTION VIII STRESSES
STRESS, 1000 PSI
TEMPERATURE, 100°F

Fig. IV-3 Developed design stresses for type 316 stainless steel in a sodium environment and a 30-year life.[26]

50 ppm oxygen. Results from one-week-long experiments indicated some benefit from 5 to 10 wt.% chromium additions. For example, a loss of thickness of 0.0092 cm was observed for a sample of V–20 wt.% Ti, as compared with losses of 0.0028 and 0.0048 cm for samples of V–30 wt.% Ti–5 wt.% Cr. Of this pair of materials, the ternary alloy is considerably more difficult to fabricate.[28]

Figure IV-5 summarizes part of the data obtained from a study[29] to determine the effects of 1100 and 1200°F sodium exposures on the mechanical properties of type 316 stainless steel (and $2\frac{1}{4}$ wt.% Cr–1 wt.% Mo steel). It is seen that increased carbon content in sodium tends to increase the creep-rupture life of type 316 stainless steel. Recent preliminary data indicate that fatigue life, impact strength, and ductility are correspondingly reduced.

The equilibrium solubility of tantalum in 600 to 1000°C tin can be expressed by the following equation, according to information from Argonne:[30]

Solubility (μg of tantalum/g of tin) =

$$(2.274 \pm 0.214) \times 10^4 \exp \frac{-(7210 \pm 870)}{T(^\circ\mathrm{K})}$$

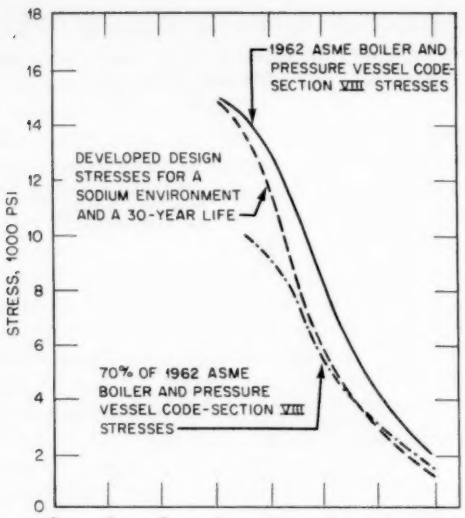
1962 ASME BOILER AND PRESSURE VESSEL CODE-SECTION VIII STRESSES
DEVELOPED DESIGN STRESSES FOR A SODIUM ENVIRONMENT AND A 30-YEAR LIFE
70% OF 1962 ASME BOILER AND PRESSURE VESSEL CODE-SECTION VIII STRESSES
STRESS, 1000 PSI
TEMPERATURE, 100°F

Fig. IV-4 Developed design stresses for Croloy 2¼ alloy steel in a sodium environment and a 30-year life.[26]

owing to grain-growth effects; these lost all their silver, although helium leak checks did not reveal any leaks.

The resistance of 11 refractory materials to attack by liquid lithium and by cesium vapor in the 2500 to 3400°F range has been studied at Battelle Memorial Institute[32] in static capsule experiments utilizing TZM (Mo–0.5 wt.% Ti–0.08 wt.% Zr) containers. The results are summarized in Table IV-1.

Pumping loops for NaK, fabricated from a variety of materials located in series as follows in the flow circuit, have been operated at Oak Ridge National Laboratory.[33]

Hastelloy N, chromized (heater zone)
Type 347 stainless steel
Type 316 stainless steel
Croloy 9M (cooler zone)
Hastelloy C
Type 316 stainless steel

The maximum fluid-side wall temperatures were 1325 or 1425°F, with a fluid-temperature differential from 200 to 300°F. Several 2000-

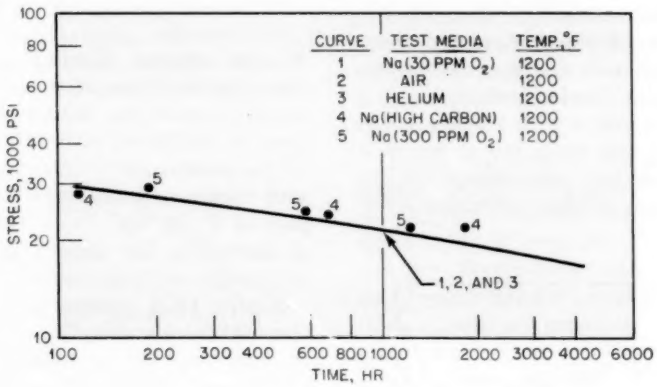

Fig. IV-5 Creep to rupture of type 316 stainless-steel specimens[29] *in air, helium, and sodium at 1200°F.*

Los Alamos Scientific Laboratory[31] is examining materials for heat-pipe containment at temperatures above 1500°C. Five containers constructed from tantalum were tested for 1000 hr at 1800°C. The test fluids were silver, indium, lead, bismuth, and a Pb-Bi alloy. No corrosion was detectable by metallographic examination. Other containers fabricated of Ta–5 wt.% W alloy were similarly exposed using silver as the test fluid. Two failed at 580 hr hr experiments have produced results such as the following:

1. Very little metal migration occurred in low-oxygen-content (< 30 ppm in NaK) systems; carbon migration was quite severe.

2. In these systems the corrosion of the chromized Hastelloy N was about five times that of the other materials.

3. An increased oxygen content (to 80 ppm) accelerated the corrosion rates of all ma-

terials, although the rate for the chromized Hastelloy N was least affected. On the other hand, high corrosion rates occurred in some low-oxygen-content systems.

4. Considerable decarburization of the Croloy 9M occurred under all conditions.

5. Additions of hydrogen to the NaK did not produce any particular effect, either on corrosion rates or on carbon migration.

Examples of approximate weight-change values pertaining to the above are shown in Table IV-2.

Attention is called to an unclassified compilation[34] of information relating to the corrosion of stainless steels by NaK and to a summary[35] of structural-materials recommendations for the Fast Reactor Test Facility sodium-cooled reactor. (J. H. Stang)

Selected Mechanical Properties of Structural and Cladding Materials

Nickel-Base Alloys

Tensile creep properties of Ni-W alloys containing up to about 10 at.% tungsten were studied by Japanese workers.[36] Tests were carried out in an argon atmosphere over the temperature range from 750 to 1200°C and the stress range from 1.4 to 9 kg/mm^2. The steady-state creep rate, ϵ_s, was shown to decrease with increasing tungsten content. Temperature and stress dependencies of the steady-state creep rate were analyzed using Dorn's equation, $\epsilon_s = C^n \exp(-Q_s/RT)$. The activation energy for creep, Q_s, which was independent of applied stress, increased with tungsten content from 66 kcal/mole for pure nickel to a maximum of 84 kcal/mole for the alloy with 5 at.% tungsten; it decreased with further increases in tungsten content. The stress exponent, n, increased with the tungsten content from a value of 5.0 for pure nickel to the maximum value of 7.2 for the alloy with 1.7 at.% tungsten. Above 1.7 at.% tungsten, n decreased with increasing tungsten content to values that were less than the value for pure nickel.

Table IV-1 CORROSION OF REFRACTORY METALS BY LITHIUM AND CESIUM[32]

Test specimen	Test period, hr	Results of exposure to liquid lithium	Results of exposure to cesium vapor
W W–0.9 wt.% Nb W–15 wt.% Mo W–10 wt.% Re W–25 wt.% Re	1000	No attack at 2500°F; fairly extensive surface dissolution and grain-boundary penetration at 2800 and 3000°F; W–15 wt.% Mo alloy was most resistant	No attack to 3100°F; surface dissolution at 3400°F; W–25 wt.% Re alloy was most resistant
TZM	1000	No attack (maximum temperature of 3000°F)	No attack (maximum temperature of 3400°F)
Re	1000 (except where noted)	Dissimilar-metal attack was characterized by transport of molybdenum (from the TZM) to the rhenium; at 3000°F this occurred in 100 hr	Dissimilar-metal attack at 3100 and 3400°F was similar to that for lithium exposures
Ta–12 wt.% W Ta–8 wt.% W–2 wt.% Hf (T-111)	100	Surface dissolution at 2500°F	Unattacked at 2500°F; surface dissolution and grain-boundary leaching at 2800°F
Nb–5 wt.% Mo–5 wt.% V–1 wt.% Zr (B-66)	100 (except where noted)	Unattacked at 2500°F; heavy grain-boundary attack at 2800°F	Unattacked at 2500 and 2800°F; surface dissolution at 2500°F (1000 hr)

Table IV-2 WEIGHT CHANGES OF MATERIALS IN MULTIMETALLIC NaK CORROSION LOOP[33]

Material	Weight change* in 2000 hr, mg/cm^2	
	For 1425°F, <30 ppm oxygen	For 1425°F, 80 ppm oxygen
Hastelloy N	−2 to −9	−2½ to −8
Type 347 S.S.	−1	−3
Type 316 S.S.	−0.3	−1
Croloy 9M	+0.3	+0.1 to +0.3

*Adjusted for carbon migration.

Refractory Metals

Stress relaxation, i.e., the drop in load due to plastic flow at constant strain, was used by workers at Mellon Institute[37] to study the phenomenon of plastic strain in the preyield region of the load-elongation curve. Results from experiments on niobium and molybdenum were interpreted to mean that, at room temperature, some dislocations are free to move at very low stresses. The amount of plastic strain due to the movement of these free dislocations at any given stress level, below the upper yield stress, was found to be a function of loading rate. The movement of the free dislocations was inhibited by the presence of interstitial impurity atoms, defects produced by radiation damage, and by debris and dislocation tangles produced by cold work. It was also concluded that the defects produced by radiation damage, which anneal out in the temperature range 140 to 200°C, form clusters on annealing rather than condensing onto dislocation lines. It was inferred from these experiments that the yield-point phenomenon results from dislocation multiplication rather than unpinning from impurity atmospheres.

Workers at the National Aeronautics and Space Administration's Lewis Research Center[38] studied the effects of selected alloying additions on the high-temperature creep and tensile strength and the ductile-brittle transition behavior of arc- and electron-beam-melted tungsten. Two of the conclusions reached are: (1) the tensile and creep strength of tungsten above 2500°F can be significantly increased by additions of hafnium, tantalum, niobium, and rhenium (in order of decreasing effectiveness); and (2) the addition of 2.11 and 6.64 at.% rhenium to electron-beam-melted tungsten resulted in 4T bend-transition temperatures below room temperature for 0.40-in.-thick sheet in the stress-relieved condition.

Zirconium Alloys

Long-term creep-rupture tests of sintered-aluminum-powder (SAP) materials and Zircaloy-2 alloys were conducted at Battelle.[39] The reports include data for SAP materials M-583, M-257, SAP-915, and SAP-895 at 700, 800, and 900°F. Selected tests were carried out in excess of 20,000 hr. Creep tests of annealed and 15% cold-worked Zircaloy-2 were carried out at 450 to 750°F and, in two cases, for times in excess of 50,000 hr. Effects of cycling temperature and of cycling both temperature and stress were studied. Cold-worked Zircaloy-2 was found to have about twice the creep-rupture strength of annealed material at 550°F. At 750°F, strength differences were slight. Both types of cycling accelerated creep, with the temperature cycling having the greater effect.

Miscellaneous Alloys

A review of fracture modes and fracture mechanics was performed in a study on the likelihood of pipe ruptures in water-cooled reactor systems by investigators at General Electric.[40] The review leads to the following conclusions:

1. With the proper application of present knowledge, fracture by fibrous ductile fracture due to gross overstress or by brittle cleavage can be virtually ruled out as credible events, except where cyclic strain aging is found to raise the brittle-ductile transition temperature above the service temperature for carbon steels.

2. With the proper application of present knowledge, fracture by creep rupture at 500 to 650°F can be virtually ruled out, although combined creep fatigue should be studied further with respect to superheat plant piping.

3. Relations exist which could be used to eliminate any possibility of impact-erosion failures if the critical velocity parameters were determined for the specific piping steels.

4. The remaining possible fracture modes (fatigue, low-energy ductile fracture, and localized corrosion cracking) are not well enough understood to permit prediction of complete immunity from their occurrence.

Important questions that could not be answered on the basis of present knowledge are: (1) whether long, shallow, cracklike defects can develop undetected due to fatigue or localized corrosion, and whether such defects, if they develop, can propagate to large-area fractures by unstable ductile rupture; (2) whether the time for serious fatigue- or corrosion-crack (or lead) propagation, in the specific materials of interest, is fast or slow compared to the inherent response time for flaw- and leak-detection procedures; (3) whether service experience thus far, and short-term experimental results showing freedom

from localized corrosion fracture, can be taken to imply complete immunity from attack over a 10- to 40-year service exposure.

(J. A. DeMastry)

Metallurgical Aspects of Cladding and Structural Materials

Nickel and Iron Alloys

The recrystallization behavior of 93% cold-rolled TD nickel was investigated[41] by workers at Pratt & Whitney Aircraft Division, United Aircraft Corp. It was found that annealing for 1 hr at 600°C caused the hardness to decrease to one-half of the cold-worked value. The hardness remained practically constant during further annealing at temperatures up to the melting point. The decrease in hardness was related to recrystallization and grain growth, as shown by optical and transmission electron micrographs. The crystallographic orientation of grains in cold-rolled and recrystallized material was established by pole-figure determinations.

Nickel alloys[42] containing 8 to 10 wt.% additions of tungsten and molybdenum were quenched and aged at 600 to 900°C. Analyses were made of creep strength, fatigue, ductility, hardness, impact strength, and phase composition as affected by tungsten and molybdenum concentrations and aging temperatures.

Investigators at General Electric[43] have found that an yttrium content of about 0.5 wt.% in Fe-Cr-Al-Y alloys produces ductile-brittle transition temperatures about 150°C higher than those of the same alloys without yttrium. This loss of ductility is attributed to the presence of the YFe_9 phase in the alloy matrix, an effect that diminishes with decreasing chromium content. The resulting poor ductility of the welds can be improved by postweld annealing.

The United States Steel Corporation[44] is developing high-yield-strength quenched and tempered steels containing a maximum of 0.25 wt.% carbon. Because weldability considerations dictate the lowest possible carbon content, five selected steels containing varying amounts of chromium, molybdenum, nickel, niobium, and vanadium with 0.22 to 0.27 wt.% carbon were evaluated after being tempered at appropriate temperatures to determine their suitability as HY-180/210 steels. Generally, the five steels had adequate hardenability for 4-in.-thick plates. Yield strengths of about 185 ksi were attained at a carbon content of 0.25 wt.%, when the steels were tempered at temperatures in the range of 400 to 1000°F. None of the steels was significantly embrittled by tempering. At a yield strength of 185 ksi, none of the steels met the tentative minimum toughness (50 ft-lb at 0°F) for an HY-180/210 base metal. However, the 3 wt.% Ni-Cr-Mo-Nb steel and the 5 wt.% Ni-Cr-Mo-V steel appear capable of meeting the toughness requirement at a yield strength of about 182 ksi in ½-in.-thick plates and of about 175 ksi in 4-in.-thick plates.

Savannah River Laboratory has issued an informative up-to-date stainless-steel information manual for the Savannah River Plant in two volumes, one covering properties and the other fabrication. The fabrication volume[45] has extensive coverage of the fabrication, heat-treatment, and testing and inspection of austenitic, ferritic, martensitic, and precipitation-hardenable stainless steels.

Zirconium Alloys

Investigators at Argonne have shown[46] that the critical resolved shear stress of crystals of zone-refined zirconium was increased as much as 500% by hydrogen in the form of finely dispersed hydride needles. The combined strength increment due to hydrogen and the oxygen impurity is expressed by $\Delta\tau = (\tau_H^2 + \tau_O^2)^{1/2}$, where $\tau_O \approx (A - BT^{1/2})^{1/2}$ and $\tau_H \approx KG$ (A, B, and K are constants, and G is the shear modulus). Thus the overcoming of the oxygen barriers by glide dislocations can be thermally activated but the overcoming of the hydride barriers cannot.

Inert-particle-strengthening concepts were extended to zirconium-base alloys by investigators[47] at General Electric. Particles of Y_2O_3 were mechanically dispersed in a Zircaloy-2 matrix by powder-metallurgy techniques. Hot-hardness, elevated-temperature tensile, 343°C creep, and 400°C steam corrosion tests were run on the resulting materials. The elevated-temperature yield strength of Zircaloy-2 was increased. Although much of this increase was related to oxygen contamination, significant strengthening was shown to be caused by particle dispersion. The 343°C steady-state creep rates of dispersion-strengthened Zircaloy-2

were markedly lower than those for the wrought alloy. Yttria dispersants were noted to have some adverse effect on corrosion resistance in 400°C steam. Oxygen contamination was the major technological problem with regard to the development of dispersion-strengthened zirconium-powder-metallurgy materials. Alloy additions of beryllium are suggested as a means of minimizing both the corrosion and oxygen-contamination problems.

The transformation kinetics in a series of Zr-Mo alloys and in a Zr–0.9 wt.% Fe alloy were studied[48] by electrical-resistivity measurements and by metallography. The Zr-Mo alloys behaved much like the Zr-Nb alloys previously reported.[49] The iron-containing alloy results were difficult to interpret because three phases are observed over an appreciable temperature range.

Refractory Metals

Investigators at the University of California[50] have measured the heat contents of niobium over the temperature range 298 to 1415°K, using a diphenyl-ether calorimeter. Smoothed values of the thermal properties of niobium, $H_T^\circ - H_{298}^\circ$, C_P, $S_T^\circ - S_{298}^\circ$ and $(F_T^\circ - H_{298}^\circ)/T$, were derived and tabulated at 100°K intervals. Within an average deviation of 0.10%, the tabular heat-content values are given by the expression

$$H_T^\circ - H_{298.15}^\circ = 5.885T + 4.044 \times 10^{-4}\, T^2 + 2.194 \times 10^4\, T^{-1} - 1864$$

Researchers at ORNL[48] have shown, by transmission electron microscopy of deformed foils of body-centered cubic (bcc) metals and alloys, that the effect of solid-solution alloying is similar to that of a lowered temperature of deformation. In both cases microstructures are dominated by straight jogged screw dislocations. It is felt that a frictional stress, composed of an inherent Peierls-Nabarro stress and the effects of mismatch in atomic size and modulus, increases the resistance to motion of screw dislocations.

Annealing studies have revealed an unusual nonsteady-state grain growth occurring in early stages of annealing in aluminum. A model was proposed based on interactions between point defects and grain boundaries. Annealing of deformation twins in niobium single crystals showed that the twins can either contract or expand by the migration of noncoherent twin boundaries. Recrystallization occurred at 1000°C at twin intersections.

The weldability of sheet specimens of the advanced Nb-Ta alloys D-43, B-66, FS-85, C-129Y, and T-111 was evaluated by measuring bend-transition temperatures after fusion welding by either gas tungsten-arc or electron-beam methods. Transition temperatures were generally below room temperature, which testified to the good weldability of these materials. Postweld aging treatments demonstrated that D-43, B-66, and C-129Y were susceptible to embrittlement under certain conditions. A study of the systems Nb-V-Ti and Ta-V-Ti had indicated that several compositions in these ternaries are useful for brazing of refractory metals to produce joints capable of high service temperatures.

The contamination of refractory metals and alloys by the residual gases in vacuum systems has been systematically studied as a function of pressure, temperature, time, alloy composition, and ratio of metal surface to volume. Empirical equations were developed to represent the effects of these variables on the contamination of Nb–1 wt.% Zr over the temperature range 750 to 1200°C. Low-partial-pressure additions of CH_4 (approximately 10^{-7} torr) to the vacuum system reduced the contamination of TZM and unalloyed niobium but not that of the Nb-Zr alloy. Measured weight losses of several stainless steels and superalloys were caused by evaporation in high vacuums at 760 to 980°C, and it was found that they depended on temperature and the chromium and manganese contents of the alloys. Postevaporation creep testing of type 316 stainless steel demonstrated that thermally induced structural changes within the alloy, rather than evaporation, controlled the creep behavior. No aging effects were observed in Cb-752, but D-43 showed a marked aging tendency, which was attributed to changes in the morphology and composition of carbide precipitates in this alloy.

The electrical resistivity and total hemispherical emittance of rhenium, T-111, D-43, and Nb–1 wt.% Zr have been measured up to 1500°C.

That Nb-Ti alloys exhibit clustering type local order was demonstrated[51] by researchers at Battelle by means of X-ray diffuse scattering. The states of local order that have been

determined in bcc group A alloys, Ti-Nb, Ti-Mo, and Mo-W, are compared and discussed in relation to phase diagram, solution thermodynamics, lattice parameter, and elastic-modulus behavior. It is also shown that Fisher-mechanism solution strengthening adequately accounts for the Nb-Ti alloy strength.

The effect of rhenium additions on the occurrence of faulting in niobium and tantalum alloys was studied at Yale University,[52] principally by analyses of the X-ray diffraction peak profile and fracture characteristics. It was found that the addition of rhenium to niobium, forming the terminal bcc solid solution, raises the ductile-brittle transition temperature from less than −196°C for pure niobium to room temperature for a Nb−14 at.% Re alloy. These brittle alloy compositions are observed to fracture by transgranular cleavage on surfaces parallel to the {100} planes. The analysis of the line broadening from powders of these alloys is consistent with a picture of a powder containing small {100} oriented cleavage platelets. Similar results were obtained with Ta-Re alloys. The line broadening from the ductile low-rhenium niobium-base alloys is interpreted in terms of (1) faulting on the {112} planes in the bcc lattice, (2) the small size of the coherently diffracting domains, and (3) the lattice strains within these regions. The addition of rhenium to niobium does not enhance the observed fault density for pure niobium and hence does not lower the stacking-fault energy of the Nb-Re alloys.

As part of a study of the mechanical properties of a niobium alloy containing 20 wt.% tantalum, 15 wt.% tungsten, and 5 wt.% molybdenum, some yield-point-return experiments were performed by investigators[53] at Pratt & Whitney. The alloy was deformed in tension at a constant strain rate to the end of the Lüders strain and was aged in baths of oil or Wood's metal at temperatures between 90 and 200°C until a slight yield drop was observed. The yield point failed to return after several days at room temperature but returned within a few seconds after aging at 200°C.

Coworkers from the Massachusetts Institute of Technology and the International Nickel Company, Inc., have proposed[54] a constitution diagram for the Nb-Ru system above 1100°C. Solidus, metallographic, X-ray, and diffusion-couple data were utilized. A minimum melting point, maximum melting point, and eutectic occur in order of increasing ruthenium content. The minimum melting point occurs at 29 at.% ruthenium and 1870°C, and the maximum, at 50 at.% ruthenium and 1942°C. The maximum solubility of ruthenium in niobium is 58 at.%, but the bcc terminal solid solution exists at room temperature only up to 40 at.% ruthenium. From 40 to 58 at.% ruthenium, the structure is body-centered tetragonal (bct), which suggests the existence of a martensitic transformation. The maximum solubility of niobium in ruthenium is 29 at.%. A hexagonal close-packed (hcp) intermediate phase forms peritectoidally at 1540°C and 75 at.% ruthenium. The eutectic reaction between the terminal solid solutions occurs at 1774°C and 65 at.% ruthenium.

Russian investigators[55] have constructed the phase diagram of the Nb-N system from the results of studies made of the density, ductility, microhardness, thermoelectric force, Hall constants, and thermal and electrical conductivities of a number of alloys.

A discussion[56] of the research now in progress at the University of Sheffield on the metallurgy of niobium includes such subjects as the rate-controlling mechanisms in the creep of niobium alloys, the mode of precipitation of niobium carbide on stacking faults present in austenitic steels, and the growth of ferrite grains in mild steels when niobium carbide is present. Special attention is given to research concerning the use of niobium in steels and superalloys, alloys based on niobium, and the importance of niobium in the development of alloys for service at high temperatures.

Some relations were established among crystallographic orientation, rollability, deformation texture, annealing behavior, slip planes, and ductile-brittle bend-transition temperature of molybdenum single crystals by researchers[57] at the Bureau of Mines. Six large molybdenum single crystals obtained from an electron-beam-melted ingot were oriented by X-ray diffraction and rolled on crystallographic planes of low indices in a known direction. During room-temperature rolling, cleavage occurred on {100} type planes. At 300°C the crystals were rolled to 95% reduction in thickness. The crystals (001)[110] and (011)[100] were most easily rolled. Pole figures were used to correlate the deformation textures of the rolled crys-

tals with the initial crystallographic orientation. Several of the textures which developed could be explained as a rotation about a ⟨1 1 0⟩ axis of symmetry. The cube crystal (0 0 1) [1 0 0] retained much of its "cubic" orientation. The (0 0 1) [1 1 0] crystal developed the simplest texture, whereas the (2 1 1) [1 1 $\bar{3}$] and (2 1 1) [1 $\bar{2}$ 0] crystals developed the most complex textures. The 1-hr recrystallization temperature of the crystal (2 1 1) [1 1 $\bar{3}$] was 700°C, which is about 300°C lower than that of commercial polycrystalline molybdenum. The poles of the slip planes (as determined from gross slip lines at low magnifications) tended to lie within 20 to 60° of the pole of the rolling plane. The ductile-brittle bend-transition temperature was dependent upon the rolling orientation and the dislocation density.

The observation of dislocation loops in quenched molybdenum has been reported[58] by researchers at the Franklin Institute. This is thought to be the first direct evidence of defect structures produced by the aggregation of quenched-in vacancies in a bcc metal.

That the ductility of electron-beam-melted ingots of molybdenum is greatly improved by the addition of small amounts of boron has been demonstrated by researchers[59] at Fansteel Metallurgical Corporation. Ingots containing boron in concentrations from 10 to 500 ppm by weight were sufficiently ductile that they could be directly forged at temperatures of 1200 to 1320°C without cracking. Improved forgeability was related to the fine grain structure induced by the boron. Grain refinement was evident in castings with 10 ppm or less and was further enhanced by boron additions up to 230 ppm, with little further refinement above this concentration. Ductility in sheet produced from experimental forgings was greatest at boron levels between 60 and 230 ppm. Tensile strength and recrystallization temperature were equivalent to those reported for commercial unalloyed molybdenum. The stress rupture of molybdenum containing small amounts of boron was substantially above that reported for commercial unalloyed molybdenum and roughly twice that of high-purity electron-beam-melted molybdenum. Boron in amounts greater than 230 ppm appeared to cause embrittlement in finished sheet.

Kossowsky[60] at the University of Pennsylvania has studied the nature of the basic mechanism that controls flow and yield in bcc metals by analyzing the dependence of the initial yield on temperature, strain history, and purity. Seven specimens of iron and 10 specimens of molybdenum of three different purities were tested in tension. Tests were conducted at temperatures between 5 and 298°K. The characteristics of the following parameters were investigated: (1) the elastic limit, which is the stress above which a hysteresis loop is first observed upon loading and unloading; (2) the anelastic limit, which is the stress at which a permanent strain can be first detected; and (3) the frictional stress, which is defined as half the slope in a plot of loops area as a function of loops width. The results indicated an almost identical behavior of the iron and molybdenum. The elastic and frictional stress were independent of prestrain and strain rate. The temperature dependence was the same for all purities down to 77°K. At 5°K an increase in the temperature dependence of the elastic limit and the frictional stress was observed for the less pure specimens. The anelastic limit was independent of prestraining strain rate but exhibited a significant dependence upon prestraining temperature and test strain rate.

Sigma-phase precipitates in Mo–35 at.% Re alloy were studied[61] by researchers at the University of Pennsylvania using transmission electron microscopy. The sigma-phase precipitate in this alloy system has the platelet shape, and its habit plane is {1 1 0} of the matrix. The orientation relation is such that ⟨1 0 0⟩ of the precipitate is parallel to ⟨1 0 0⟩ of the matrix. The edges of the platelet were found to be along ⟨1 1 1⟩ of the matrix. More patterns were observed in thin precipitates, and the electron-diffraction reflections from the $(h\,k\,O)$ plane of the sigma phase are missing when the sum of the indices h and k is odd. This implies the existence of a diagonal glide plane normal to the tetrad axis of the sigma phase.

The effect of nitrogen on the strain aging and brittle-ductile transition of vanadium has been investigated[62] at Ames Laboratory. All of the mechanical effects generally associated with strain aging were observed. A study of the dynamic effects was characterized by the occurrence of a strain-aging peak, and, from the activation energy determined from the strain-rate dependence of this peak, it was concluded that the diffusion of nitrogen with the moving dislocations was responsible for this peak. The return of the yield point after straining and

aging led to the conclusion that nitrogen was also responsible for the occurrence of the yield point observed in vanadium. It was found that nitrogen does not embrittle vanadium when present in amounts below about 2000 ppm, whereas alloys containing greater than this amount exhibit a brittle-ductile transition temperature that increases with increasing nitrogen content. Carbon does not promote cleavage fracture in vanadium, but, when present as a carbide phase, it suppresses the occurrence of mechanical twinning.

A phase diagram of the Ti-Al (Mo: V = 1 : 1) system with up to 50 wt.% aluminum, molybdenum, and vanadium was constructed by Russian investigators.[63] Isothermal cross sections were plotted for 1100, 800, and 600°C, and curves of hardness and electrical conductivity as functions of composition were drawn.

Thermochemical properties of the Laves phase, Cr_2Ta, have been determined by British investigators.[64] The transformation temperature from the C15 to the C14 type of the Cr_2Ta was found to lie between 1600 and 1640°C. X-ray work indicated that the solubility of chromium in tantalum was greater than that of tantalum in chromium. The heat of formation of Cr_2Ta was determined at 1420°C in a high-temperature calorimeter to be -2040 ± 120 cal/gram atom. The activities of chromium in various Cr-Ta alloys were measured by means of an effusion technique. The free energy of formation of Cr_2Ta at 1200°C is -2200 ± 120 cal/gram atom. The entropy of formation is thus slightly positive, namely, $+0.11 \pm 0.16$ cal/(gram atom) (°C).

An internal-friction profile induced by nitrogen in Cr–35 at.% Re was studied at Battelle[65] as a function of nitrogen concentration and heat-treatment. These studies indicated that the equilibrium solubility of nitrogen in this alloy does not differ significantly from that in chromium, as determined by internal-friction techniques. However, the precipitation kinetics of nitrogen from solution appear to be slower in the alloy than in chromium. If the precipitate approximates Cr_2N in composition, it is suggested that the function of the rhenium may be to act as a buffer between chromium and nitrogen.

Miscellaneous

Researchers at Los Alamos[66] have studied the cerium-rich part of the system cerium-manganese up to 20 at.% manganese between 500 and 800°C by differential thermal analysis, augmented by metallography and an X-ray identification of the phases. No compounds were detected. A eutectic was found at about 16.1 at.% manganese and 622°C. The cerium side of the eutectic showed an invariant effect at 638°C, at which temperature the following phases were indicated to coexist: liquid of about 14 at.% manganese, delta cerium containing about 5 at.% manganese, and gamma cerium containing about 2 at.% manganese.

(N. M. Griesenauer)

Diffusion Studies

In a continuing program to develop fuel-element materials for use at high temperatures in air, steam, and other oxidizing coolants,[67] selected iron cladding alloys containing chromium, aluminum, and yttrium were examined by X-ray fluorescence analysis for uranium diffusion through the claddings. No uranium diffusion was detectable on the cladding surfaces of specimens containing UO_2 after being tested for 5035 hr at 950°C and for 3660 hr at 1100°C. Nearly all the specimens containing UN in either an iron matrix or a chromium matrix showed significant diffusion through alloy claddings after being tested for 1600 hr at 1100°C. One specimen containing UN showed no detectable diffusion through the cladding. The investigators presumed that the oxygen content of the core matrix was high enough to form an effective oxide diffusion barrier between the fuel and the cladding of this specimen.

A survey of hydrogen-permeation data through selected metals has been made by Atomics International.[68] Flux data were determined experimentally and combined with data from other references listed in the bibliography. The flux data were fitted to the equation

$$\phi = (CP^{1/2}/\chi) \exp(-Q/RT)$$

where ϕ = flux at standard temperature and pressure, cm/(hr)(cm^2)
C = permeation constant
P = hydrogen pressure, atm
χ = membrane (metal) thickness, mm
Q = activation energy, cal/mole
R = gas constant
T = absolute temperature

In the area of basic diffusion studies, major achievements of a program to study surface-diffusion phenomena on low-index planes of face-centered cubic (fcc) metals were reported.[69] A quantitative autoradiographic technique was developed to obtain accurate surface-diffusion profiles. A theoretical approach was used to study the parasitic effect of volume diffusion at elevated temperatures. Extensive measurements were made on Ni-Ni, Ni-Ag, and Ag-Ag systems between 400 and 1000°C. The value of 0.60 ev determined for the activation energies on the (1 1 1) and (1 1 0) planes was compared to 0.62 ev reported for diffusion on (1 1 1) planes obtained by mass-transport techniques. Also of basic interest is a review of evidence by Gibbs[70] supporting the theory that diffusion in titanium, zirconium, and uranium occurs entirely through equilibrium vacancy-atom exchange.

Two reports published recently on the interdiffusion of zirconium and aluminum included an examination for intermediate alloy phases in the diffusion zone. Kidson and Miller[71] studied the system as a function of time and temperature. One intermediate alloy phase, $ZrAl_3$, was detected and grew according to the empirical relation

$$W(T,t) \leq [2.22 \times 10^9 \exp - (46{,}000/RT)]t^{1/2}$$

In a report from the Atomic Energy Establishment in India,[72] the Zircaloy-Al system, as well as the Zr-Al system, was studied. X-ray analysis and metallographic techniques were used to examine the diffusion zone. The authors reported the existence of two phases identified as $ZrAl_3$ and Zr_3Al. The $ZrAl_3$ phase predominated in the zone and apparently is more brittle. The predominance of $ZrAl_3$ was attributed to interstitial diffusion of aluminum atoms in the fcc tetragonal lattice of the $ZrAl_3$. Interdiffusion rates in the Zircaloy-Al system were comparatively higher than those in the Zr-Al system. (A. N. Ashurst)

Ceramic Technology

A number of ultrahigh-purity ceramics have been formed by the decomposition of selected organometallic compounds[73] by the Air Force Materials Laboratory. Borides, carbides, nitrides, and oxides have been prepared. The thermal decomposition of organometallic compounds in the vapor phase produces high-purity fine-particle-size powders and coatings and thin films, or fibers, by controlled pyrolysis conditions. Compounds of the type $M(OR)_3$ and $M(OR)_4$, where M is titanium, zirconium, hafnium, thorium, yttrium, ytterbium, and dysprosium, and various alkyl groups such as C_4H_9 and C_5H_{11} have been studied. The metal-oxygen bond in these compounds is very stable, and thermal decomposition is complete to the oxides. A method has been developed to produce, on a continuous basis, ZrO_2 and HfO_2 with an average particle size of less than 100 A and a purity of 99.95+%. Adherent coatings of refractory oxides on graphite have been made by thermal decomposition of the alkoxides at the substrate surface.

The densification of fine-grained Al_2O_3 in vacuum hot pressing has been attributed by Rossi[74] to particle rearrangement in the initial stage and to diffusional creep in the final stage. Under hot-pressing temperatures from 1150 to 1350°C and pressures from 3000 to 6000 psi, the extent of the densification that takes place in the initial stage depends upon the amount of sliding, fragmentation, and plastic flow that occurs. In the final stage, the densification by diffusional creep is controlled by aluminum-ion diffusion. The activation energy for this stage is 115 kcal/mole, which agrees with the activation energy for diffusion of aluminum ions. Gases entrapped within pores of the hot-pressed compact will produce end-point porosities.

As part of a broad program of studies of phase-equilibrium relations of selected metal carbides at high temperatures, Union Carbide Corporation has prepared diagrams of the Hf-C, Ta-C, and B-C systems.[75] The only intermediate phase observed in the Hf-C system was HfC. This phase was found to be homogeneous between 34.0 and 48.0 at.% carbon at 2200°C and between 36.0 and 49.3 at.% carbon at 3150°C. The most refractory composition, with a melting point of 3830°C, was established at 47.5 at.% carbon. Solidus temperatures of 2240 and 3150°C occur on the high-hafnium and high-carbon sides of the monocarbide, respectively. The Ta-C system is characterized by two high-temperature phases, TaC and Ta_2C. A eutectic is observed at 2825°C and 12.5 at.% carbon between TaC and Ta_2C. The Ta_2C has low-carbon limits of 26.5 and 29.0 at.% at 2850 and 3150°C, respectively. The Ta_2C phase-field boundary apparently does not deviate from

the stoichiometric composition on the high-carbon side. A peritectic reaction at 3240°C leads to formation of Ta_2C from tantalum-rich liquid and TaC. The TaC is face-centered cubic and has boundary limits of 41.7 and 49.5 at.% carbon at 2250°C. The phase field broadens at higher temperatures. The eutectic formed between TaC and carbon corresponds to 3375°C and 61.2 at.% carbon. The highest melting temperature for TaC is above 3800°C, when the carbon content is approximately 48.5%. In the B-C system, a solid solution of boron in carbon was found, with a maximum solubility of about 2.35 at.% boron at 2350°C.

Phase diagrams have been established for the systems alpha Fe_2O_3-NiO, La_2O_3-NiO, and alpha Fe_2O_3-NiO-La_2O_3 by Cassedanne.[76] The binary diagrams were established up to a temperature of 1550°C; the ternary diagram was studied at the isotherms of 800, 1000, 1300, and 1400°C.

Weber has prepared an annotated bibliography[77] of research on the structural and physical properties of ZrO_2. It covers the literature of the past 35 years and provides a critical analysis of the information, rather than a simple review. Evaluated references (307) are listed.

The behavior of ZrO_2 at elevated temperatures[78] has been studied by Materiadyne, a division of Pfaudler Permutit Inc. The investigations included the effects of isostatic pressure on the tetragonal-monoclinic inversion of ZrO_2 and studies of the destabilization of MgO-stabilized ZrO_2. Using a matrix of SiO_2 glass to apply an isostatic pressure during heating, it was found that high pressures, predicted to be about 95,000 psi at 1025°C by the Lundin-Selsing equation, accelerated the inception of the monoclinic-tetragonal inversion and inhibited the completion of the tetragonal-monoclinic transformation. In the study of the destabilization of cubic ZrO_2-MgO, the monoclinic phase was found to form between 1000 and 1200°C, and the tetragonal phase, between 1200 and 1400°C. Above 1400°C the cubic phase was redeveloped. Monoclinic ZrO_2 resulting from destabilization of cubic ZrO_2 + MgO was transformed to the tetragonal phase between 1200 and 1300°C, and the monoclinic phase, developed by inversion from tetragonal ZrO_2, inverted to the tetragonal phase between 1050 and 1160°C. With ZrO_2 alone there was no evidence of any inversion between 1250 and 1600°C. Destabilization of a ZrO_2 + 15.5 mole % MgO composition affected the thermal conductivity. The thermal conductivity of the destabilized material was about 90% higher than that of the cubic material at 100°C and about 45% higher at 600°C.

Russian workers report[79] ZrO_2 bodies with superior high-temperature characteristics through the use of 99.5% pure ZrO_2 stabilized with 10 mole % of either CaO or MgO; MgO provided the better sinterability.

(D. J. Bowers)

Radiation Effects in Nonfuel Materials

Stainless Steels

The severe loss of ductility of austenitic stainless steel as a result of elevated-temperature irradiation has been the subject of study for several laboratories. Hanford[80] reports that the radiation-induced property changes in types 304 and 348 stainless steel are greater when the irradiation is done at 290°C than when done at 50°C. American Iron and Steel Institute (AISI) type 348 stainless steel, in both the annealed and 25% cold-worked conditions, was irradiated at temperatures between 700 and 775°C and then tested at room temperature. Both yield strength and ductility were found to be lower than for unirradiated annealed material. Workers at Hanford[11] are also studying the in-reactor creep properties of type 304 stainless steel at 500, 550, and 600°C. Some tests are in progress, and the results are shown in Table IV-3.

Table IV-3 IN-REACTOR CREEP RATES FOR ANNEALED AISI 304 STAINLESS STEEL[11]

Temp., °C	Stress, 1000 psi	In-reactor creep rate per hour	Time, hr	Out-of-reactor creep rate per hour	Time, hr
500	20	$< 2.5 \times 10^{-7}$	2000	$< 2.5 \times 10^{-7}$	2000
500	30	6.0×10^{-7}	300	7.6×10^{-7}	1000
550	20	1.1×10^{-6}	600	9.3×10^{-7}	1000
				7.6×10^{-7}	1000
600	20	8.9×10^{-6}	800	2.1×10^{-5}	1000

Nickel-Base Alloys

Studies in progress at General Electric[43] on Hastelloy X and A-286 show significant re-

ductions in both the time to rupture under an applied stress and in the ductility as the result of irradiation. They attributed this degradation in properties to the thermal neutrons and, more specifically, to the helium resulting from the $^{10}B(n,\alpha)^{7}Li$ reaction. Other gaseous elements formed by other (n,p) and (n,α) reactions are considered. The data for these alloys are shown in Tables IV-4 and IV-5.

The effect of 740°C irradiation on the room-temperature properties of Incoloy 800, Inconel 600, Inconel 625, and Inconel 718 is being investigated[11] by Hanford workers. The data showing the effect of irradiation are shown graphically in Figs. IV-6 to IV-9.

Zircaloy-2

The tensile behavior at room temperature and 300°C of notched Zircaloy-2 containing 0, 100, 200, 400, 500, and 600 ppm hydrogen was studied[81] by Canadian researchers. Specimens were irradiated at reactor ambient temperatures to approximately 1×10^{20} neutrons/cm^2 and tested at room temperature and 300°C. Unirradiated specimens having 600 ppm hydrogen and irradiated ones having 500 ppm hydrogen and greater were notch sensitive at room temperature; none of the specimens were notch sensitive at 300°C.

Table IV-4 STRESS-RUPTURE TEST RESULTS OF SHIELDED-UNSHIELDED HASTELLOY X SPECIMENS[43]

Specimen*	Test temp., °C	Stress, kg/mm^2	Rupture time, hr	Elongation in 3.8-cm gauge length, %	Reduction of area, %
			Control		
34 HCS	650	31.6	99.8	26.5	20.8
35 HCS	650	24.6	509.1	23.3	47.8
134 HS	732	19.7	42.1	40.8	59.1
			Unshielded†		
25 HCS	650	28.1	136.8	17.1	28.9
123 HS	650	24.6	215.4	9.0	28.2
125 HS	650	31.6	44.2	8.2	27.8
130 HS	732	15.5	123.8	10.6	36.2
135 HS	732	19.7	15.7	5.3	20.1
136 HS‡	732	19.7	38.4	29.9	34.6
			Shielded§		
39 HCS	650	28.1	88.9	14.7	25.9
40 HCS	650	31.6	65.1	19.5	28.0
41 HCS	650	24.6	329.9	20.5	26.8
122 HS	732	24.6	5.2	11.0	16.8
128 HS	732	19.7	30.3	19.9	30.2
137 HS	732	15.5	85.6	5.3	18.4

*Smooth-bar specimens from heat E-9500 which were heat-treated at 1175°C for 1 hr and then rapidly cooled in air.

†Irradiated in capsule 33MT-104A; 3.6×10^{19} neutrons/cm^2 ($E_n \geq 1$ Mev), 11.0×10^{19} thermal neutrons/cm^2.

‡Postirradiation annealed at 732°C in air for 119 hr.

§Irradiated in capsule 33MT-104B shielded with 0.5-mm cadmium-coated steel jacket; 3.5×10^{19} neutrons/cm^2 ($E_n \geq 1$ Mev), 2.3×10^{19} thermal neutrons/cm^2.

Table IV-5 STRESS-RUPTURE TEST RESULTS OF SHIELDED-UNSHIELDED A-286 SPECIMENS[43]

Specimen*	Test temp., °C	Stress, kg/mm^2	Rupture time, hr	Elongation in 3.8-cm gauge length, %	Reduction of area, %
			Control		
36 ACS	650	38.7	181.2	13.5	20.1
185 ACS	650	35.2	237.5	13.6	17.1
191 AS	650	42.2	111.7	11.9	14.2
192 AS	732	24.6	36.3	33.0	60.8
194 AS	732	17.7	211.3	37.5	44.4
			Unshielded†		
186 AS	650	35.2	6.8	1.1	6.44
187 AS	650	28.1	23.8	2.8	11.6
188 AS	650	21.1	125.6	1.4	11.2
189 AS	732	12.7	38.5	2.3	4.49
190 AS	732	18.3	4.0	0.4	5.41
193 AS‡	732	18.3	4.7	6.3	29.7
			Shielded§		
28 ANS	650	35.2	39.5	1.2	5.20
29 ACS	650	38.7	14.5	1.2	3.99
33 ACS	650	28.1	89.8	3.2	2.79
34 ACS	732	21.1	3.1		12.2
183 AS	732	18.3	6.8	0.7	
184 AS	732	12.7	50.7	1.3	11.6

*Smooth-bar specimens from heat C-2527 which were heat-treated as follows: 900°C for 2 hr and water cooled, 720°C for 16 hr and air cooled, and 650°C for 16 hr and air cooled.

†Irradiated in capsule 33MT-104A; 3.6×10^{19} neutrons/cm^2 ($E_n \geq 1$ Mev), 11.0×10^{19} thermal neutrons/cm^2.

‡Postirradiation annealed at 732°C in air for 9.1 hr.

§Irradiated in capsule 33MT-104B shielded with a 0.5-mm cadmium-coated steel jacket; 3.5×10^{19} neutrons/cm^2 ($E_n \geq 1$ Mev), 2.3×10^{19} thermal neutrons/cm^2.

Refractory Alloys

Studies by General Electric[43] on the effects of radiation on the high-temperature properties of refractory metals and alloys have included creep-rupture tests of irradiated and unirradiated tungsten, W–25 wt.% Re, and molybdenum at temperatures of 1100°C or greater. For tungsten irradiated at reactor ambient temperatures, the radiation was found to increase the strength without affecting the ductility. The increase in strength appears to be a function of the fast-neutron dose. Irradiation strengthening was still evident at temperatures as high as 1700°C, where it was believed that recoverable defects should be completely removed. Typical test results for tungsten are given in Table IV-6.

The increase in creep-rupture strength of irradiated tungsten specimens tested at temperatures below 900°C was found to be much greater than for specimens tested above 900°C.

Additional strengthening was noted in irradiated specimens by annealing at 1050 and 1200°C for 1 hr prior to creep testing. Some increase in creep strength at 1700°C was attributed to transmutation products.

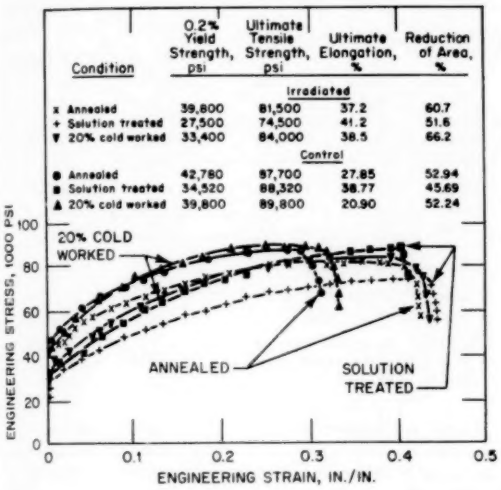
Condition
0.2% Yield Strength, psi
Ultimate Tensile Strength, psi
Ultimate Elongation, %
Reduction of Area, %
Irradiated
x Annealed 39,800 81,500 37.2 60.7
+ Solution treated 27,500 74,500 41.2 51.6
▼ 20% cold worked 33,400 84,000 38.5 66.2
Control
● Annealed 42,780 97,700 27.85 52.94
■ Solution treated 34,520 88,320 38.77 45.69
▲ 20% cold worked 39,800 89,800 20.90 52.24
20% COLD WORKED
ANNEALED
SOLUTION TREATED
ENGINEERING STRESS, 1000 PSI
ENGINEERING STRAIN, IN./IN.

Fig. IV-6 Effects of 740°C irradiation on the room-temperature properties of Incoloy 800 in the annealed, solution-treated, and cold-worked condition.[11] [Irradiated at 9×10^{19} neutrons/cm^2 (E > 1 Mev).]

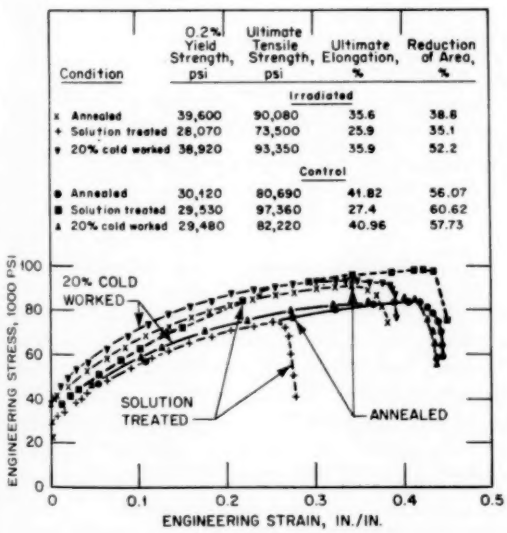
Condition
0.2% Yield Strength, psi
Ultimate Tensile Strength, psi
Ultimate Elongation, %
Reduction of Area, %
Irradiated
x Annealed 39,600 90,080 35.6 38.8
+ Solution treated 28,070 73,500 25.9 35.1
▼ 20% cold worked 38,920 93,350 35.9 52.2
Control
● Annealed 30,120 80,690 41.82 56.07
■ Solution treated 29,530 97,360 27.4 60.62
▲ 20% cold worked 29,480 82,220 40.96 57.73
20% COLD WORKED
SOLUTION TREATED
ANNEALED
ENGINEERING STRESS, 1000 PSI
ENGINEERING STRAIN, IN./IN.

Fig. IV-7 Effects of 740°C irradiation on the room-temperature properties of Inconel 600 in the annealed, solution-treated, and cold-worked condition.[11] [Irradiated at 9×10^{19} neutrons/cm^2 (E > 1 Mev).]

No significant changes in creep-rupture properties were shown in W–25 wt.% Re alloys irradiated at reactor ambient temperatures to neutron doses of about 3.7×10^{19} fast neutrons/cm^2 and tested at 1100°C. However, specimens subjected to about 8×10^{19} fast neutrons/cm^2 showed about a 50% increase in rupture life at 1100°C and about half the ductility of unirradiated control specimens. These data are shown in Table IV-7. The shape of the time-deformation curve was altered slightly after irradiation.

A molybdenum specimen irradiated under somewhat the same reactor environment as the

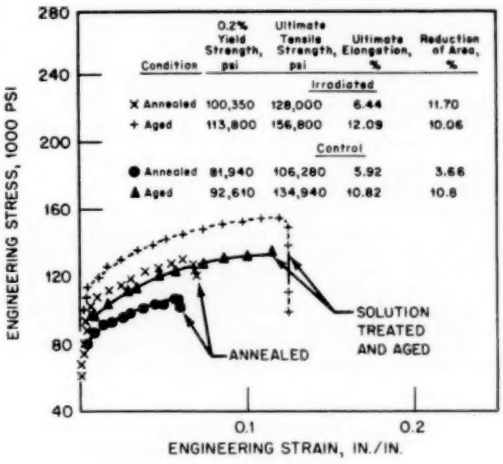

Fig. IV-8 Effects of irradiation on the room-temperature properties of Inconel 625 in the annealed and solution-treated-and-aged condition[11] irradiated at 740°C to an exposure of 9×10^{19} neutrons/cm^2 (E > 1 Mev).

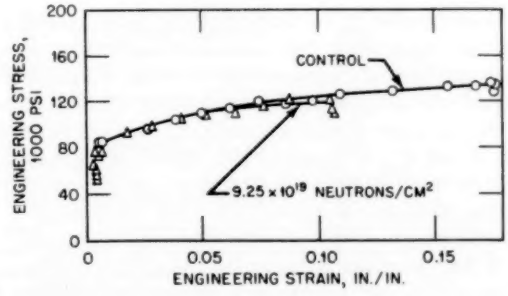

Fig. IV-9 Effects of irradiation on the room-temperature properties of Inconel 718 irradiated at 740°C to an exposure[11] of 9.25×10^{19} neutrons/cm^2 (E > 1 Mev).

Table IV-6 SUMMARY OF CREEP-RUPTURE DATA ON TUNGSTEN SPECIMENS, ROD J MATERIAL[43]

Specimen*	Condition	Postirradiation anneal: Temp., °C	Time, hr	Atmosphere	Temp., °C	Stress, kg/mm²	Rupture life, hr	Linear creep rate per second	Elongation in 4.54 cm, %	Reduction of area, %
1265	Control				900	22.64	12.45	2.32×10^{-6}	36.2	96.6
1256	Irradiated 33MT-137†				900	22.64	148.00	1.72×10^{-7}	21.7	68.1
1255	Irradiated 33MT-137				900	22.64	77.30	2.80×10^{-7}	19.5	62.1
1257	Irradiated 33MT-137				900	22.64	140.00	3.07×10^{-8}	4.5	23.3
1268	Irradiated ORM-17‡				900	22.64	47.48	5.46×10^{-7}	26.8	96.5
1263	Irradiated ORM-17	1050	1	H_2	900	22.64	77.04	5.08×10^{-7}	32.5	96.8
1271	Irradiated ORM-17	1200	1	H_2	900	22.64	124.60	1.96×10^{-7}	30.0	96.6
1264	Irradiated ORM-17	1300	1	H_2	900	22.64	36.65	8.97×10^{-7}	33.6	96.2
1266	Irradiated ORM-17	1400	1	H_2	900	22.64	32.20	1.01×10^{-6}	35.3	93.7
1267	Irradiated ORM-17	1700	1	H_2	900	22.64	24.12	1.26×10^{-6}	33.9	94.8
1272	Control				1400	10.55	19.33	2.92×10^{-7}	12.7	35.5
1258	Irradiated ORM-19§				1400	10.55	26.71	2.74×10^{-7}	15.1	26.7
1273	Control				1400	9.84	33.67	1.59×10^{-7}	11.4	33.3
1259	Irradiated ORM-19				1400	9.84	41.93	1.23×10^{-7}	11.1	17.4
1278	Control				1400	8.44	83.63	3.97×10^{-8}	9.2	23.8
1274	Control				1500	8.44	18.28	2.07×10^{-7}	8.7	21.5
1261	Irradiated ORM-19				1500	8.44	20.10	1.90×10^{-7}	6.1	16.2
1277	Control				1700	4.22	38.90	1.09×10^{-7}	4.4	11.8
1276	Control				1700	4.92	22.71	1.67×10^{-7}	6.1	15.8
1260	Irradiated ORM-19				1700	4.92	24.61	1.43×10^{-7}	5.4	13.6
1275	Control				1700	5.62	12.57	2.39×10^{-7}	7.5	8.0
1262	Irradiated ORM-19				1700	5.62	13.67	2.07×10^{-7}	5.4	10.4

*Specimens from 0.508-cm-diameter tungsten rod which were annealed at 1750°C in hydrogen for 1 hr prior to fabrication; stress relieved at 1600°C for 1 hr in hydrogen following grinding.

†Capsule 33MT-137 irradiated at approximately 7×10^{19} neutrons/cm² ($E_n \geq 1$ Mev) at elevated temperatures, 1000°C < T < 1350°C, in the Engineering Test Reactor.

‡Capsule ORM-17 irradiated at approximately 1.6×10^{19} neutrons/cm² ($E_n \geq 1$ Mev) and reactor ambient temperature in the Oak Ridge Research Reactor F2 facility.

§Capsule ORM-19 irradiated at approximately 8.2×10^{19} neutrons/cm² ($E_n \geq 1$ Mev) and reactor ambient temperature in the Oak Ridge Research Reactor F2 facility.

Table IV-7 SUMMARY OF CREEP-RUPTURE DATA[43] ON W-25 WT.% Re SPECIMENS AT 1100°C

Specimen	Condition	Stress kg/mm²	Rupture life, hr	Linear creep rate per second	Elongation in 2.54-cm gauge length, %
723*	Control	47.5	2.90	2.28×10^{-5}	57.10
724*	Control	45.7	3.94	1.65×10^{-5}	49.80
726*	Control	43.9	7.03	9.23×10^{-6}	53.30
716*	Irradiated ORM-16†	47.5	3.13	2.03×10^{-5}	45.60
717*	Irradiated ORM-16	45.7	3.61	1.73×10^{-5}	47.20
718*	Irradiated ORM-16	43.9	10.70	6.22×10^{-6}	45.10
719*	Irradiated ORM-16	42.2	13.05	5.00×10^{-6}	54.00
745‡	Irradiated ORM-20§	47.5	5.30	1.37×10^{-5}	47.09
748‡	Control	43.9	6.20	1.18×10^{-5}	60.31
742‡	Irradiated ORM-20	43.9	9.62	5.67×10^{-6}	26.70
746‡	Control	40.0	17.09	4.54×10^{-6}	66.06
743‡	Irradiated ORM-20	40.0	25.07	2.99×10^{-6}	37.72
750‡	Control	34.0	63.41	1.10×10^{-6}	63.40

*Specimens from 0.051-cm sheet (powder batch RWS-9, ingot No. 2) recrystallized by vendor at 1600°C for 0.5 hr in hydrogen and annealed at 1900°C for 1 hr in hydrogen after fabrication.

†Capsule ORM-16 irradiated [~3.7×10^{19} neutrons/cm² ($E_n \geq 1$ Mev)] at reactor ambient temperature in the Oak Ridge Research Reactor F9 facility.

‡Specimens from 0.051-cm sheet (powder batch RWS-9, ingot No. 4) recrystallized by vendor at 1600°C for 0.5 hr in hydrogen and annealed at 1750°C for 1 hr in hydrogen after fabrication.

§Capsule ORM-20 irradiated [~8×10^{19} neutrons/cm² ($E_n \geq 1$ Mev)] at reactor ambient temperature in the Oak Ridge Research Reactor F2 facility.

tungsten and W-Re samples showed accelerated creep when tested at about 580°C. At the temperatures investigated, irradiated molybdenum showed a slight reduction in rupture life and an increase in creep rate when compared with control samples. The ductility of the irradiated molybdenum is not appreciably different from that of unirradiated material. These data are given in Table IV-8.

Table IV-8 SUMMARY OF CREEP-RUPTURE DATA[43] ON MOLYBDENUM* SPECIMENS AT A CONSTANT STRESS OF 21.09 kg/mm²

Specimen	Sheet†	Condition	Temp., °C	Rupture life, hr	Linear creep rate per second	Elongation in 2.54-cm gauge length, %
1037	8	Control	580	68.20	5.78×10^{-7}	53.4
1042	8	Irradiated ORM-23‡	580	2.25	$\sim 2.16 \times 10^{-6}$	50.9
1038	8	Irradiated ORM-23	580	3.62	1.47×10^{-6}	51.4
1040	8	Irradiated ORM-23; annealed at 757°C§	580	110.48	4.22×10^{-7}	42.2
1043	8	Irradiated ORM-23; annealed at 779°C¶	580	75+**	4.16×10^{-7}	
1045	8	Control	600	13.50	2.91×10^{-6}	60.0
1041	8	Control	620	2.15	1.49×10^{-5}	53.8
1039	8	Control	650	0.27	1.19×10^{-4}	53.4
850	1	Control	560	487.90	1.01×10^{-7}	56.9
692	1	Irradiated ORM-16††	560	237.70	2.14×10^{-7}	51.9
851	1	Control	580	115.60	3.59×10^{-7}	52.3
690	1	Irradiated ORM-16	580	41.30	1.13×10^{-6}	53.1
699	1	Control	600	40.30	1.03×10^{-6}	49.8
693	1	Irradiated ORM-16	600	27.30	1.62×10^{-6}	49.7
698	1	Control	650	5.74	7.70×10^{-6}	51.8
853	1	Irradiated ORM-16	650	3.01	1.58×10^{-5}	55.8

*Arc-cast molybdenum sheet, 0.5 mm thick, heat KDM-515A; recrystallized by vendor.
†Sheet 8 annealed in argon for 1 hr at 1200°C after fabrication of specimens. Sheet 1 annealed in hydrogen for 1 hr at 1200°C after fabrication of specimens.
‡Capsule ORM-23 irradiated at reactor ambient temperature in the Oak Ridge Research Reactor F2 facility to about 1×10^{19} neutrons/cm² ($E_n \geq 1$ Mev).
§Annealed for 1 hr at indicated temperature in unstressed condition.
¶Annealed for 8 hr at indicated temperature in unstressed condition.
**Temperature controller malfunction at 75 hr.
††Capsule ORM-16 irradiated at reactor ambient temperature in the Oak Ridge Research Reactor F2 facility to about 3.7×10^{19} neutrons/cm² ($E_n \geq 1$ Mev).

Basic Studies of Radiation Effects

Isochronal annealing studies of neutron-induced defects in recrystallized bcc metals show that the resistivity properties recover with three resolved peaks, which occur at temperatures of 0.15, 0.22, and 0.31 times the absolute melting temperature. These various recovery peaks are attributed to defect migration.

Investigators at Hanford[11] are studying damage mechanisms related to neutron bombardment and interaction of dislocations. Initially these studies were directed toward understanding the mechanisms of plastic deformation in alpha iron. Samples were irradiated in a helium-filled capsule to an exposure of 5×10^{18} neutrons/cm² at 60°C. The two high-purity irons tested, Ferrovac E and Battelle zone-refined iron, showed the characteristic increase in yield strength. Tests were made at 298, 204, and 78°K. The results showed clearly that at and below 200°K (–100°F) the radiation produced no significant change in deformation mechanisms. Comparison of values obtained for activation volumes and activation energy suggested that the deformation mechanism was a thermally activated nucleation of double kinks to overcome the Peierls stress barrier. Annealing irradiated samples at 350°C for 3 hr increased the activation volume to that of the unirradiated samples. The lower yield strength also decreased to nearly the preirradiation value. This was believed to indicate that the defects can be annealed out and are not related to impurities or precipitates of impurity atoms.

The combined effects of neutron irradiation and impurities on the properties and structure of molybdenum are being investigated

by Hanford. The behavior of defects after annealing irradiated, 1×10^{20} neutrons/cm^2 (>1 Mev), molybdenum has been studied using electron microscopy and X-ray diffraction. The observable dislocation loop resulting from annealing has been positively identified to be interstitial in origin. Slip-line studies in bent molybdenum crystals have shown a direct relation between surface-slip traces and channels observed by transmission electron microscopy.

Lattice-parameter and line-broadening measurements were made on molybdenum foils with controlled carbon content after irradiation at several levels up to 1×10^{20} neutrons/cm^2. Comparison of these data with some determined earlier on commercial molybdenum indicated that the irradiation-induced-defect state after exposure to about 10^{20} neutrons/cm^2 is independent of impurity content and preirradiation history. The most prominent feature of the damaged material is the broadened X-ray lines.

Measurements were made of slip-line densities produced by bending on the surfaces of irradiated and unirradiated molybdenum crystals. The slip-line pattern on the irradiated sample was clear and distinct, exhibiting straight slip lines on the (110) face and irregular and branching lines on the (001) face. It was believed that the wavy slip lines resulted from extensive cross-slipping.

(F. R. Shober)

References

1. A. E. Bibb, A. P. Beard, and J. F. Fascia, Corrosion Resistance of Consolidated Zircaloy-2 Powder Containing Oxygen and Nitrogen, USAEC Report KAPL-3060, Knolls Atomic Power Laboratory, June 1964.
2. A. Sawatzky, The Behavior of Zirconium Alloys in Santowax OM Organic Coolant at High Temperature, Canadian Report AECL-2118, October 1964.
3. K. F. J. Heinrich, Microprobe Study of Zircaloy Corrosion Films, USAEC Report DP-906, Savannah River Laboratory, November 1964.
4. C. Roy, Hydrogen Distribution in Oxidized Zirconium Alloys by Autoradiography, Canadian Report AECL-2085, September 1964.
5. D. R. McClintock, Performance of Pre-Oxidized Zircaloy Clad Fuel Rods in the Saxton Reactor, *Trans. Am. Nucl. Soc.*, 7(2): 457-458 (November 1964).
6. Atomic Energy of Canada Ltd., unpublished, 1964.
7. S. B. Dalgaard, Transference Numbers and Their Relation to In-Reactor Oxidation of Zirconium, Canadian Report AECL-2066, September 1964.
8. R. H. Leyse, Zircaloy-2 and Type-304 Stainless Steel at 2000°F in Water-Steam for Brief Times, USAEC Report APED-4413, General Electric Company, Vallecitos Atomic Laboratory, Apr. 27, 1964.
9. C. S. Wukusick and J. F. Collins, An Iron-Chromium-Aluminum Alloy Containing Yttrium, *Mater. Res. Std.*, 4(2): 637-646 (December 1964).
10. S. P. Rideout and R. F. Mittelberg, Savannah River Laboratory, Factors Controlling Chloride Stress Corrosion of Type 304 Stainless Steel, USAEC Report CONF-778-3, paper presented at ASM-AIME Metals and Materials Congress, Philadelphia, October 1964.
11. Hanford Atomic Products Operation, Metallurgy Research Operation, Quarterly Progress Report, July–September 1964, USAEC Report HW-84281, Sept. 15, 1964.
12. C. N. Spalaris, R. F. Boyle, H. J. Busboom, and V. E. Hazel, Fuel-Element Irradiations in Superheated Steam, *Trans. Am. Nucl. Soc.*, 7(2): 456-457 (November 1964).
13. T. L. Kolski, Oxidation of 90 Cb–10 Mo Alloy in the Temperature Range 400 to 1200°C, *Am. Soc. Metals, Trans. Quart.*, 57: 690-700 (September 1964).
14. D. A. Prokoshkin, E. V. Vasil'eva, and I. Yv. Lazareva, Oxidation Kinetics of Tungsten-Niobium Alloys, *Issled. Metal. v Zhidkom i Tverd. Sostoyaniyakh, Akad. Nauk SSSR, Gos. Kom. po Chern. i Tsveln. Met. pri Gosplane SSSR, Inst. Met.*, 241-247 (1964).
15. B. Phillips, L. L. Y. Chang, and M. G. Scroger, Research on Criteria for Selection of Alloys and Surface Treatments for Inhibition of Tungsten Oxidation — Part I, Report ML-TDR-64-230(Pt. I), Tem-Pres Research, Inc., August 1964.
16. R. A. Pasternak, High-Temperature Oxidation and Nitridation of Niobium in Ultrahigh Vacuum, Final Report, July 1, 1963–October 31, 1964, USAEC Report SRIA-132, Stanford Research Institute, Nov. 15, 1964.
17. J. H. Witte and H. A. Wilhelm, Oxidation Studies of Some Refractory Metals, USAEC Report IS-854, Ames Laboratory, Iowa State University, February 1964.
18. H. J. Nolting and R. A. Jefferys, Oxidation-Resistant High-Temperature Protective Coatings for Tungsten, Report ML-TDR-64-227, Thompson Ramo Wooldridge Inc., July 1964.
19. V. S. Moore and A. R. Stetson, Evaluation of Coated Refractory Metal Foils, Report RTD-TDR-63-4006(Pt. II), Solar, a division of International Harvester Co., December 1964.
20. L. Sama and B. Reznik, Development of Production Methods for High-Temperature Coating of Large Tantalum Parts, Interim Engineering Progress Report, 1 September–30 November 1964, Sylcor Division, Sylvania Electric Products Inc., November 1964.
21. S. Priceman and L. Sama, Development of Slurry Coatings for Tantalum, Columbium, and Molybdenum Alloys, Progress Report No. 3, 1 October–31 December 1964, Sylcor Division, Sylvania Electric Products Inc., Dec. 31, 1964.
22. Illinois Institute of Technology Research Institute, High-Temperature Oxidation Protective Coatings for Vanadium-Base Alloys, Report IITRI-B6019-6 (AD-611376), Dec. 1, 1964.
23. Solar, a division of International Harvester Co., Ductile Coatings for Columbium Alloys — Phase

I, Progress Report No. 2, 1 November 1964–31 January 1965, Feb. 26, 1965.
24. Boeing Co., Fluidized-Bed Techniques for Coating Refractory Metals, First Interim Progress Report, 8 December 1964–8 March 1965.
25. Atomics International, AEC Unclassified Programs, Quarterly Technical Progress Report, October–December 1964, USAEC Report NAA-SR-10850, Feb. 15, 1965.
26. R. C. Anstine, The Combined Effects of a Sodium Environment and Extended Life on Type 316 Stainless Steel and Croloy 2¼ Alloy Steel Design Stresses, USAEC Report BW-67-3, The Babcock & Wilcox Co., September 1964.
27. Argonne National Laboratory, Reactor Development Program Progress Report, February 1965, USAEC Report ANL-7017, Mar. 18, 1965.
28. Argonne National Laboratory, Reactor Development Program Progress Report, December 1964, USAEC Report ANL-6997, Jan. 18, 1965.
29. MSA Research Corp., Effect of High-Temperature Sodium on Austenitic and Ferritic Steels, Physical Properties of Materials, Progress Report No. 52, December 1964, USAEC Report MSAR-65-05, Jan. 15, 1965.
30. Argonne National Laboratory, Reactor Development Program Progress Report, January 1965, USAEC Report ANL-7003, Feb. 18, 1965.
31. Los Alamos Scientific Laboratory, Quarterly Status Report on Advanced Reactor Technology (ART) for Period Ending January 31, 1965, USAEC Report LA-3244-MS, Mar. 3, 1965.
32. J. A. DeMastry and N. M. Griesenauer, Investigation of High-Temperature Refractory Metals and Alloys for Thermionic Converters, Report AFAPL-TR-65-29, Battelle Memorial Institute, Apr. 1, 1965.
33. Oak Ridge National Laboratory, SNAP-8 Corrosion Program Quarterly Progress Report for Period Ending November 30, 1964, USAEC Report ORNL-3784, March 1965.
34. C. A. Zimmerman, Corrosion of Type 316 Stainless Steel in NaK Service—A Literature Search, USAEC Report IDO-14651, Phillips Petroleum Company, February 1965.
35. L. R. Kelman and R. J. Dunworth, Selection of the Structural Material for the FARET Liquid-Metal Systems, USAEC Report ANL-6939, Argonne National Laboratory, December 1964.
36. K. Monma, H. Suto, and H. Oikawa, High-Temperature Creep of Nickel-Tungsten Alloys, *Nippon Kinzoku Gakkaishi*, 28: 304-307 (1964).
37. B. J. Shaw and G. A. Sargent, Stress Relaxation Prior to the Yield Point in Niobium and Molybdenum, *Acta Met.*, 12: 1225-1230 (November 1964).
38. P. L. Raffo, W. D. Klopp, and W. R. Witzke, Mechanical Properties of Arc-Melted and Electron-Beam Melted Tungsten Base Alloys, Report NASA-TN-D-2561, National Aeronautics and Space Administration, Lewis Research Center, January 1965.
39. J. A. VanEcho and S. W. Porembka, Long-Term Creep Rupture of Sintered Aluminum Powder and Zircaloy-2 Alloys, USAEC Report BMI-X-10113, Battelle Memorial Institute, Jan. 25, 1965.
40. A. J. Brothers, L. F. Coffin, Jr., H. H. Klepfer, J. R. Lowe, Jr., and M. B. Reynolds, A Review of Fracture Modes as Related to Primary Coolant System Rupture Study, USAEC Report GEAP-4446, General Electric Company, Atomic Power Equipment Department, May 1964.
41. M. C. Inman, K. M. Zwilsky, and D. H. Boone, Recrystallization Behavior of Cold-Rolled TD-Nickel, *Am. Soc. Metals, Trans. Quart.*, 57: 701-713 (September 1964).
42. M. V. Pridantseo, G. V. Estulin, and L. N. Zimina, Influence of Molybdenum and Tungsten on Properties of Heat Resistant Nickel Alloys, *Stal'*, No. 4: 349-353 (1964).
43. General Electric Company, Advanced Technology Services, High-Temperature Materials and Reactor Component Development Programs, Volume I: Materials, USAEC Report GEMP-334A, Feb. 26, 1965.
44. S. J. Manganello and L. F. Porter, The Effects of Low-Temperature Tempering on the Properties of 0.25% Carbon Ni-Cr-Mo Steels, Report AD-604876, United States Steel Corporation, July 1, 1964.
45. W. C. Rion, Jr. (Comp.), Stainless Steel Information Manual for the Savannah River Plant, Volume II: Fabrication, USAEC Report DP-860(Vol. II), Savannah River Laboratory, July 1964.
46. D. G. Westlake, Precipitation Strengthening in Crystals of Zirconium-Hydrogen Alloys Containing Oxygen as an Impurity, *Acta Met.*, 12: 1373-1380 (December 1964).
47. K. C. Antony and H. H. Klepfer, Dispersion-Strengthened Zirconium Alloys, *J. Less-Common Metals*, 8: 36-46 (January 1965).
48. Oak Ridge National Laboratory, Metals and Ceramics Division Annual Progress Report for Period Ending June 30, 1964, USAEC Report ORNL-3670, October 1964.
49. Oak Ridge National Laboratory, Metals and Ceramics Division Annual Progress Report for Period Ending May 31, 1963, USAEC Report ORNL-3470, Nov. 11, 1963.
50. D. T. Hawkins and R. L. Orr, High-Temperature Heat Content of Niobium, *J. Chem. Eng. Data*, 9: 505-507 (October 1964).
51. P. S. Rudman, An X-Ray Diffuse-Scattering Study of the Niobium-Titanium BCC Solution, *Acta Met.*, 12: 1381-1388 (December 1964).
52. E. N. Aqua and C. N. J. Wagner, An X-Ray Diffraction Study on the Effect of Rhenium on the Occurrence of Faulting in Refractory Alloys, Report AD-608738, Yale University, September 1964.
53. B. Harris and D. E. Peacock, Strain Aging of a Solution-Hardened Niobium Alloy, *J. Less-Common Metals*, 8: 77-79 (January 1965).
54. G. F. Hurley and J. H. Brophy, A Constitution Diagram for the Niobium-Ruthenium System Above 1100°C, *J. Less-Common Metals*, 7: 267-277 (October 1964).
55. T. S. Verkhoglayadova, S. N. Lvov, and V. F. Nemchenco, Some Properties of the Niobium-Nitrogen System, *Ukr. Khim. Zh.*, 30: 667-670 (1964).
56. B. B. Argent, Research on the Metallurgy of Niobium at the University of Sheffield, *Sci. Progr. London*, 52: 608-627 (October 1964).
57. R. Blickensderfer, R. Siemens, G. Asai, and H. Kato, Rolled Molybdenum Single Crystals, Deformation Textures, Recrystallization, and Transition Temperature, Report BM-RI-6539, Bureau of Mines, Albany Metallurgy Research Center, March 1964.

58. J. D. Meakin, A. Lawley, and R. C. Koo, Vacancies in Quenched Molybdenum Single Crystals, *Appl. Phys. Letters*, 5: 133-135 (Oct. 1, 1964).
59. A. D. Zumbrunnen and J. M. Fitzpatrick, Grain Refinement and Improved Ductility in Molybdenum by Small Boron Additions, *J. Less-Common Metals*, 7: 356-367 (November 1964).
60. R. Kossowsky, Microstrain Studies in Iron and Molybdenum Between 5 and 298°K (thesis), University of Pennsylvania, 1963.
61. K. Ojawa and R. Maddin, Sigma-Phase Precipitates in Molybdenum-Rhenium Alloys, *Acta Met.*, 12: 1161-1165 (October 1964).
62. R. W. Thompson and O. N. Carlson, The Effect of Nitrogen on the Strain Aging and Brittle-Ductile Transition of Vanadium, USAEC Report IS-994, Ames Laboratory, Iowa State University, August 1964.
63. C. Ko, I. I. Kornilov, and E. N. Pylaeva, Phase Equilibrium Diagram for Titanium-Aluminum (Molybdenum: Vanadium = 1:1) System, *Zh. Neorgan. Khim.*, 9: 1662-1668 (July 1964).
64. P. Feschotte and O. Kubachewski, Thermochemical Properties of the Laves Phase, Cr_2Ta, *Trans. Faraday Soc.*, 60: 1941-1946 (November 1964).
65. M. J. Klein, Nitrogen-Induced Internal Friction in Chromium–35 At.% Rhenium, USAEC Report BMI-1703, Battelle Memorial Institute, Nov. 24, 1964.
66. B. J. Thamer, The System Cerium-Manganese in the Range of 0–20 At.% Manganese, *J. Less-Common Metals*, 7: 341-346 (November 1964).
67. General Electric Company, Advanced Technology Services, High-Temperature Materials Program Progress Report No. 41, Part A, USAEC Report GEMP-41A, Nov. 30, 1964.
68. R. W. Webb, Hydrogen Permeation Through Metals, USAEC Report NAA-SR-Memo-9844, Atomics International, Apr. 27, 1964.
69. J. B. Drew and J. J. Pye, Surface Diffusion Studies, USAEC Report NYO-2994-3, Franklin Institute Laboratories for Research and Development, March 1964.
70. G. B. Gibbs, The Mechanism of Diffusion in Anomalous B.C.C. Transition Metals, *Acta Met.*, 12: 1302-1303 (November 1964).
71. G. V. Kidson and G. D. Miller, A Study of the Interdiffusion of Aluminum and Zirconium, *J. Nucl. Mater.*, 12: 61-69 (May–June 1964).
72. G. P. Tiwari and B. D. Sharma, Interdiffusion in Zirconium-Aluminum and Zircaloy-Aluminum System, *Nature*, 204: 178-179 (Oct. 10, 1964).
73. K. S. Mazdiyasni and C. T. Lynch, An Approach to the Preparation of Powders, Fibers, and Films of Ultra-High Purity Ceramics, Report ML-TDR-64-269 (AD-608043), Air Force Materials Laboratory, Research and Technology Division, August 1964.
74. R. C. Rossi, The Kinetics and Mechanism of Final-Stage Densification on the Vacuum Hot Pressing of Fine-Grained Aluminum Oxide (thesis), USAEC Report UCRL-11564, University of California, Lawrence Radiation Laboratory and College of Engineering, July 20, 1964.
75. R. V. Sara and C. E. Lowell, Research Study To Determine the Phase Equilibrium Relations of Selected Metal Carbides at High Temperatures, Report WADD-TDR-60-143(Pt. V), Union Carbide Corporation, June 1964.
76. J. Cassedanne, Study of the Binary Diagrams α-Fe_2O_3-NiO and La_2O_3-NiO and the Ternary Diagram α-Fe_2O_3-NiO-La_2O_3, *Anais Acad. Brasil. Cienc.*, 36: 13-19 (1964).
77. B. C. Weber, An Annotated Bibliography of Research on the Structural and Physical Properties of Zirconia, Report ARL-64-205, Aerospace Research Laboratories, November 1964.
78. R. B. Burdick, W. R. Hoskyns, C. F. Smith, and W. B. Crandall, Research on the Thermal Properties of Zirconia, Report ARL-64-219, Materiadyne, a division of Pfaudler Permutit Inc., December 1964.
79. G. P. Kalliga and L. A. Lyutsareva, Some Properties of High-Purity Zirconium Dioxide, *Izv. Vysshikh Uchebn. Zavedenii, Khim. i Khim. Tekhnol.*, 7(1): 106-110 (1964).
80. Hanford Atomic Products Operation, Research and Development Programs Executed for the Division of Reactor Development, Quarterly Progress Report, April–June 1964, USAEC Report HW-83298, November 1964.
81. Atomic Energy of Canada Ltd., unpublished, 1964.

Section V

Reactor Materials

Special Fabrication Techniques

Melting, Casting, and Hot and Cold Working

The preparation of thin-walled tubing of W-Re and W-Re-Mo alloys is being investigated at General Electric Company.[1,2] The W–25 wt.% Re alloys with 0, 10, and 20 wt.% molybdenum added exhibited moderate loss in room-temperature ductility when heat-treated in the 2200 to 2600°C temperature range; whereas the W–25 wt.% Re alloy containing 30 wt.% molybdenum did not decrease in ductility as a result of the same heat-treatment. These studies also showed that the W–30 wt.% Re alloy with up to 20 wt.% molybdenum decreased in room-temperature ductility following heat-treatment at 1200 to 1600°C, whereas the alloy containing 30 wt.% molybdenum did not. The decrease in ductility exhibited by the low-molybdenum-content alloys is attributed to sigma-phase precipitation. All attempts to swage the W–25 wt.% Re–30 wt.% Mo alloy at room temperature have been unsuccessful, but hot swaging over mandrels appears promising. Since previous studies indicate that fabricability of the alloys is influenced by the grain size, and the grain size may be affected by the nitrogen content, studies to ascertain the effect of nitrogen on the grain size of sheet specimens have been initiated.

The Bureau of Mines[3] is interested in producing W–25 wt.% Re tubing. Consumable-electrode arc melting *in vacuo* has been used to produce 3-in.-diameter ingots. During these studies it was noted that sidewall conditions and ingot yield were improved by using high melting currents and increasing the strength of the stirring coil. Characterization of the W–25 wt.% Re prealloyed powder obtained from Curtiss-Wright Corp. showed that the majority of the particles are off composition. The 5-μ and larger particles are predominantly tungsten and contain only 7.7 to 10.5 wt.% rhenium; the 3-μ and smaller particles are rhenium rich. Some 2-μ particles contain as much as 83 wt.% rhenium. It is also reported that the powder is high in chromium, iron, and nickel.

Fused HfC is also being investigated at the Bureau of Mines.[3] Sixty-one tensile specimens containing 8 to 10.5 wt.% carbon have been cast, as have several ¼-in.-diameter by 3-in.-long rods. The latter were forwarded to Atomics International for zone-refining studies. Several ¼- by ½- by 3-in. slabs have been made for bend-rupture tests. While casting the above specimens, it was noted that the fluidity of the HfC was such as to produce 0.020- to 0.030-in.-diameter wire ½ to ⅝ in. long in the vent holes in the molds.

Allegheny Ludlum Steel Corp.[4] has completed a series of extrusions of TZM alloy using improved support tooling, with promising results. An extrusion ratio of 43 : 1, a billet temperature of 3200°F, and flame-sprayed zirconia dies yielded best results. Poor extrusions resulted when the billet temperature was increased to 3350°F.

An alloy with a density of 1.2 g/cm^3 or less, with good physical and mechanical properties, is being sought at Union Carbide Nuclear Co.[5] At the present time the Mg-Li alloy system is being studied. A Mg–40 wt.% Li alloy has been melted in a mild-steel crucible under an argon atmosphere. A Mg–25 wt.% Li alloy was melted at 700°C and held at temperature for 1 hr while stirring. This was then top poured into a zirconia-coated graphite mold under a pressure of 500 μ at 600°C. Other alloys in this system will be prepared.

National Lead Co. of Ohio[6] has reported the results of their studies concerned with the centrifugal casting of tubular uranium fuel cores.

Horizontal cast-iron molds coated with a zircon-based wash were employed in an effort to produce castings that would eliminate the extrusion step in the present process. Though some tubes were cast with bore tapers of less than $\frac{1}{8}$ in. in 68 in., the results were not reproducible and tapers of as much as $1\frac{1}{4}$ in. were obtained. A fast feed was superior to a slow feed in improving the billet surfaces and eliminating hairline cracks. A single beta heat-treatment of the billets yielded a FEDC grain size of 4.0 or finer, with some evidence of clustering. A mold speed of 1100 rpm produced the most uniform bore diameter and the soundest structure.

Static casting studies for the same purpose are in progress. At the present time a 14-in.-OD 9-cavity graphite mold 38 in. long is being employed. A melting cycle of $2\frac{1}{2}$ hr and a pour temperature of 2750 to 2800°F have proved most satisfactory. Future efforts will be directed toward improving the cast-tube surfaces and minimizing machining-stock removal.

A study of the effects of repeated quenching of uranium alloys of different compositions in cold water, boiling water, and Wood's metal was conducted by the Russians.[7] They noted that cracks occur in the process of quenching and not in the transformation process during tempering. An increase in the cooling rate during quenching promotes beta-phase retention and cracking. The cracking appears to be the result of stresses developed in the brittle beta phase at low temperatures. During quenching from the gamma region in an oil bath at 200°C, the cooling rate is such that even alloys containing 0.5 at.% chromium, 1 at.% silicon, or 0.5 at.% fissium do not crack. (N. E. Daniel)

Cladding

Pressure Bonding

Solid-state welding of refractory metals has been reviewed in a recent article.[8] Although the procedure was not detailed, it is apparent that the pressures were applied mechanically by the fixturing devices employed. The principal advantage of this technique over brazing is that solid-state welded structures can be subsequently heat-treated to attain optimum properties. The technique was employed in fabricating a tungsten rocket-motor case which involved the solid-phase bonding of two spun sections at the throat area. More recent work was devoted to the fabrication of sandwich structures to provide weight savings of $\frac{1}{3}$ lb/sq ft and greater. Conditions employed for solid-state joining of zirconium, beryllium, Cb-752, Mo–0.5 Ti, 90 Ta–10 W, titanium, and dissimilar metal combinations are described. Because of the relatively low pressures involved in this type of solid-state bonding, smooth surfaces that may be cleaned chemically or mechanically, depending on the subject materials, are recommended. Selection of fixturing materials was based on the thermal-expansion characteristics of the materials to be bonded and creep strengths at the temperature of interest. Reaction can be eliminated by pretreatment of the fixture surfaces.

High-density graphite bodies have been prepared by gas-pressure bonding.[9,10] High-purity artificial graphites and spectrographic graphites were densified to 99 and 98% of theoretical, respectively, by bonding for 1 hr at 23,500 psi and 4000°F. Representative samples were examined by neutron-activation analysis, and it was noted that the orientation of the isostatically pressed forms was less than that of the conventional extruded materials. Diametral compression tests revealed that the higher bonding temperatures, 4000°F, or higher pressures at 3000°F produced a higher strength material. It was also observed that impurities improved strength primarily by enhancing interparticle bonding.

Studies of zirconium solid-phase bonds with intermediate hydride layers were continued.[9,10] Structures bonded at 1400°F for 3 hr at 10,000 psi exhibited void-free bond areas with continuous grain growth across the original interface. It was apparent, however, that excess hydrogen was still present at the bond. Heat-treating for 2 hr in vacuum at 1650°F was conducted to effect removal of this hydrogen. The strength of the resulting self-bonds was determined to be 75% of that for high-purity zirconium. (S. W. Porembka)

Canning

Workers at Hanford Atomic Products Operation[11] fabricated 2000 UO_2–1.5 wt.% PuO_2 fuel rods for the Experimental Boiling Water Reactor (EBWR). The homogeneous, mixed-oxide fuel was prepared by pneumatically impacting to particle densities exceeding 98% of theoreti-

cal, crushing, sizing, and vibrationally compacting in Zircaloy-2 tubes, 9.2 mm in inside diameter by 10.8 mm in outside diameter. The core weight was 825 to 830 g, and the core length was 1.23 ± 0.002 m.

Two methods were used in compacting the EBWR fuel: the vertically excited plate and the transversely excited resonant-beam techniques. The former method allows a shorter compaction time (3 to 5 min), whereas the latter offers advantages in regard to versatility and amenability to multiple fabrication techniques. Pilot-scale capabilities of up to 30 fuel rods per day by vibrational compaction have been demonstrated with these units.

Several different types and configurations of metal-clad cermet cores with powdered-metal end caps were fabricated at Hanford in a "one-step" process utilizing pneumatic impaction. The tubing, metal and ceramic-matrix powder, and end-cap powder are loaded into a mild-steel die by cold pressing or vibratory compaction. The die and components are then heated and pneumatically impacted to densify the cermet matrix and bond the cladding, core, and end cap. The mild-steel die is then dissolved in acid, and this yields the finished part.

Fuel material and hood facilities have been prepared at Hanford[12] to permit fabrication of [UO_2–2 wt.% PuO_2, 91.5-cm (36 in.)-long by 1.28-cm (0.505 in.)-ID] fuel rods. The rods are vibrationally compacted in a vertical position, using a 25-in. extension piece that clamps to the lower end of the fuel rod and couples to a resonating plate. This system eliminates the cracking of rods encountered occasionally on a horizontal beam system because of the long vibration period and shifting of the rods on the horizontal system. (V. D. Linse)

Electroplating

Austrian researchers have reported[13] the deposition of thorium and uranium nitrates (hydrated) as thin (2 mg/cm^2), uniform films on stainless steel and other metals by an electrolytic process involving the migration of charged particles in an organic solvent and their discharge at cathode surfaces. The films are converted to oxides by heating and are comparable with films prepared by vacuum deposition. Thorium or uranium nitrate was dissolved in water mixed with acetone and/or isopropanol and electrolyzed at 100 to 600 volts to deposit the films. Yields were directly proportional to voltage and to time periods, up to about 10 min, and reached a maximum of 70% for thorium and 63% for uranium over stainless steel. Higher yields (to 82%) were obtained for uranium over aluminum and copper. Electropolishing of the cathodes and solution agitation from a rotating anode were important for obtaining a fine-grained structure.

Cerium, praseodymium, and other rare-earth elements were electrodeposited in compound form with good uniformity and adhesion on aluminum, copper, and stainless steel with yields[14] ranging from 96 to 100%. Thickness uniformity of the films was comparable with that of vacuum-deposited layers, but the electrolytic method was more efficient. Water solutions were mixed with butanol, isopropanol, ethanol, or acetone and electrolyzed with a potential of 50 to 600 volts. The water content of the solution affected adhesion. Films with a thickness of greater than 0.5 mg/cm^2 were prone to cracking if the cathode was deformed.

A method for electroplating tungsten was developed for circumventing heat-treatment after electrodeposition of a thin layer of nickel or other metal to form a diffusion alloy before plating the thicker coating needed for protection against oxidation at elevated temperatures.[15] The direct method includes deoxidation in a nitric-hydrofluoric acid mixture, anodic etching in a potassium hydroxide solution, and plating approximately 0.00002 in. (0.02 mil) of chromium and 0.00002 or 0.00003 in. (0.02 or 0.03 mil) of nickel in a nickel sulfate solution containing 40 g per liter of sulfuric acid. Heating to 980°C and distortion of tungsten-sheet specimens electroplated in this fashion caused no blistering or lifting of the electroplate. Specimens plated in an acid-iron solution before the nickel strike also resisted heating and bending, and there was no blistering or lifting of the electroplate.

The absorption of hydrogen by Zircaloy-2 during corrosion in organic media was reduced by electroplating copper and diffusing the copper by heat-treatment.[16]

Stress-corrosion cracking of U–10 wt.% Mo alloy, induced by static tension in air, has been delayed considerably by cladding the alloy with electrodeposited nickel.[5] Some specimens stressed at 96,000 or 98,000 psi showed no failures after 355 to 410 hr. Heating in air at 400°C was necessary to anneal the 5-mil-thick

electroplated nickel. Erratic results were obtained when the tensile specimens were not heated after being electroplated or when they were vacuum annealed.

Components of fast-burst reactors were electroclad with nickel after being electropolished and ferric chloride etched (or anodically etched). Procedures and precautionary measures for achieving good-quality electroplates were developed by Union Carbide workers.[5]

(W. H. Safranek)

Nonelectrolytic Chemical Plating

Increasing attention is being given to the use of metal-organic compounds as source materials in chemical vapor-deposition (CVD) processes. The main problem encountered is contamination of the deposits with carbon or other decomposition products. The results of work in progress on the use of metal-organic compounds for the deposition of boron, hafnium, molybdenum, and titanium are promising.[17]

The results of a number of investigations relating to procedures for vapor-forming structural members of tungsten and to the characteristics of the deposits are available. Details of the production of tungsten granules by hydrogen reduction of WF_6 in fluidized beds are described.[18] Granules in the size range of 200 to 400 μ, having less than 100 ppm total impurities, are commercially available. Gas-pressure bonding of these granules is employed to fabricate products with recrystallization temperatures above 1980°C. Summaries of the characteristics of CVD tungsten[19] and tungsten tubing[20,21] are presented. Further evidence of the excellent recrystallization resistance of this type of tungsten is also presented. Good-quality deposits of the alloy tungsten–2 to 37 wt.% rhenium can be made by CVD.[22] The as-deposited grain structure is less columnar with increasing rhenium content, but uniformity of composition has not yet been achieved in massive deposits. Consolidation and infiltration of various porous composite bodies consisting of wires, fibers, and spherical particles with tungsten and other refractory metals can be accomplished by CVD. Results of one series of investigations of this type are reported.[23] Advantage was taken of the normally occurring grain orientation of columnar tungsten deposits formed by CVD, and a thoriated tungsten emitter was prepared which had improved characteristics compared with those normally obtained from conventional thoriated tungsten emitters.[24]

Studies by Oak Ridge National Laboratory on the deposition of pyrolytic carbon (PyC) are reported.[25] The effects of deposition conditions and heat-treatment were evaluated in terms of anisotropy factors derived either directly from experimental data or indirectly by calculation from other experimental results.

Coatings of nickel can be successfully applied to small beryllium parts by electroless plating.[26] Uniform coverage can be achieved on complex shapes. Deposits contain 7.5 wt.% phosphorus. Electroless nickel coatings, 0.5 mil thick, on alloy specimens of Nb–1 wt.% Zr withstood 1500°F thermal-cycling tests during a 12-day period.[27]

McGuire[28] describes various ways in which tungsten coatings, obtained by pyrolysis of tungsten hexacarbonyl $[W(CO)_6]$, can be employed as protective, conductive, antigalling, or thermal-shielding media. The use of hydrogen or water vapor to minimize carbon content of the coating was discussed.

Study of mechanisms by which silicide diffusion type coatings either protect or fail to protect refractory-metal-alloy substrates was continued.[29,30] General problems encountered in devising protective coating systems for graphite are outlined.[31] Two classes of coatings for graphite which have been investigated are tungsten overlays[32] and transition and rare-earth metal oxides.[33] In the case of tungsten coatings, adherence is impaired by mismatch of thermal expansion between coating and substrate. The oxides are obtained by pyrolysis of compounds of the type $M(OR)_3$ and $M(OR)_4$, where M is titanium, zirconium, hafnium, thorium, yttrium, ytterbium, and dysprosium, and alkyl groups such as $C_4H_9^{2-}$ and $C_5H_{11}^{2-}$ are involved. This is discussed in somewhat more detail in Sec. IV under Ceramic Technology.

Coating of carbon filaments with PyC was carried out on a continuous basis.[34] The pyrolytic coating increased the strength-to-weight ratio of the filaments by a factor of 1.3 and acted as a sizing on the yarn to make weaving easier. It was noted that adherent metal coatings can be formed on ceramics using a gas discharge.[35] Films of titanium or chromium, in combination with copper or gold, were formed on high-alumina ceramics. Subsequent brazing

of these metallized ceramics yielded joint strengths of 3000 to 8000 psi.

(E. M. Sherwood)

Explosive Forming

A study has been conducted by the Martin Co.[36] in which the principles of dieless free forming using chemical explosives as an energy source have been developed. The basic fixture for dieless free forming is shown in Fig. V-1. Since this technique uses no female die to determine the final formed shape, the metal assumes a shape controlled by the combined interaction of the explosive charge, hold-down force, and mechanical properties of the metal. For a centrally located charge, this shape is always a fourth-degree paraboloid of revolution. It is possible to control the shape produced in a dieless forming process by controlling the nature of the impulsive loading on the metal blank and the material properties and dimensions of the blank.

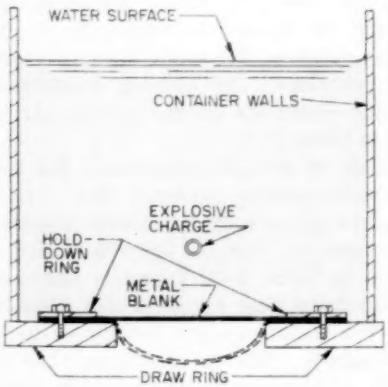

Fig. V-1 Dieless explosive forming.[36]

A modification of the dieless free-forming process, called the "plug-cushion" process, Fig. V-2, has also been developed at Martin.[37] This technique eliminates the excessive thickness gradient over the finished part normally experienced in dieless or closed-die forming and permits the forming of reliably shaped finished parts using dieless forming techniques. In the plug-cushion process, the shape that is produced is directly related to the mass of the plug cushion. The depth of draw that can be

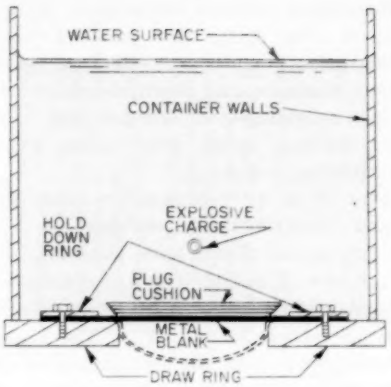

Fig. V-2 Plug-cushion dieless explosive forming.[37]

achieved is increased by the plug-cushion process since the blank is drawn into the die evenly from under the hold-down ring.

The parameters that must be controlled in the plug-cushion process are plug thickness, diameter, material, chamfer angle, and position with respect to the metal blank. In general, optimum forming takes place if (1) the plug is made of a ductile material whose thickness is twice that of the blank to be formed, (2) the diameter of the plug is slightly larger than that of the die, (3) the edges of the die are beveled between 30 and 60°, and (4) the charge is positioned at a distance of twice the plug thickness above the surface of the metal blank to be formed.

(C. C. Simons)

Welding and Brazing

As has been the case for some time, the joining of the refractory metals and their alloys is the subject of a large portion of recently acquired reports. All joining processes are covered.

The Infab chamber at Universal-Cyclops Steel Corporation has been shown adaptable to the fabrication of refractory-metal structures of virtually any size.[38] Personnel working within the chamber were able to adapt a single reliable procedure to the tungsten–inert-gas (TIG) welding process for TZM molybdenum, niobium (B-66), tantalum (90 Ta–10 W), tungsten, and pure molybdenum sheet 0.032 in. thick. They were not, however, able to use a single process for all alloys when the thickness was 0.125 in.

Out-of-position manual techniques were also developed. The study also covered process-variable effects such as: effect of work-to-electrode distance and electrode shape on penetration, shielding-gas composition, welding current, welding speed, weld shape, and other things affecting cracking.

Results of a weld-parameter study for the TIG and electron-beam welding of several refractory-metal alloys have been reported by Westinghouse Electric Corp. investigators.[39] The bend-test results on the work completed so far are shown in Fig. V-3. The study was also concerned with the properties of gloves used in welding chambers. Latex natural-rubber gloves were found to be inferior to neoprene gloves. They were subject to decomposition under vacuum bakeout (150 to 200°F) as evidenced by an unidentified tacky film that condensed on the cooler weld-box wall during bakeout. Oxygen permeability of the natural-rubber gloves was an order of magnitude worse than for neoprene gloves, whereas moisture permeability was about the same.

A method of cooling resistance-welding electrodes for welding refractory-metal alloys has been invented by Ling-Temco-Vought, Inc., engineers.[40] Copper electrodes are cooled with circulating liquid nitrogen and a nitrogen-gas envelope provided around the tip to prevent condensation of moisture. The technique is said to (1) prevent electrode sticking, (2) minimize damage to coatings, (3) reduce grain-growth problems, and (4) permit wider latitude when welding thin metals to thick metals.

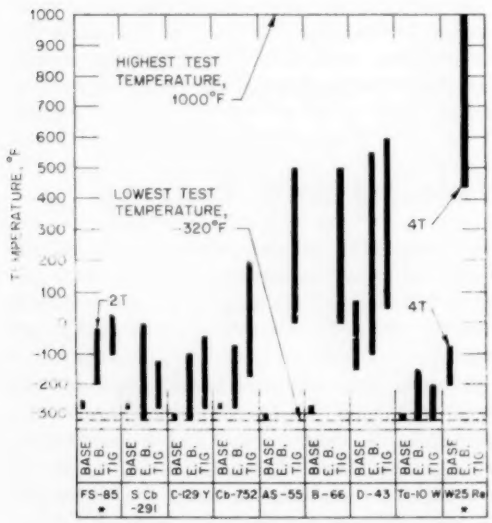

* All bends 1T radius except FS-85 electron-beam welds which are 2T radius and all W—25 Re tests which are 4T radius

Fig. V-3 Summary of current bend-test results for butt welds in 0.035-in. sheet.[39]

Union Carbide has published a report on their electron-beam-welding capabilities.[5] Table V-1 summarizes the welding parameters used on a number of alloys, including the refractory metals, and should be of general value to all users of this process.

A report on the diffusion bonding of three niobium alloys, a tantalum alloy, and TZM molybdenum in foil thicknesses has been published[41,42] by Solar Aircraft Co. The program also has included TD-nickel bonding.

Bonding processes were developed which require only a 20-sec cycle and which produce joints equal in strength to the base metal when coated for oxidation resistance. Joint resistance to oxidation approached that of the base metal.

The process involves rapid resistance heating of the joint area during the application of pressure. All joining is done under a protective atmosphere. Electrode materials present some problems. The bonding conditions and electrode materials for the several alloys are shown in Table V-2.

Methods of surface preparation and the use of an intermediate material that varied for each of the alloys considered were also studied. The results for niobium alloy B-66 are summarized in Table V-3. Tantalum intermediate foil was found best for D-43 and suitable for B-66. The tantalum-alloy bonding studies presented slightly different problems. The intermediate materials that showed the best peel strengths deteriorated when held at diffusion-annealing temperatures. This indicated a probable loss of strength at useful temperatures. Thin tantalum foil was also chosen as best for the bonding of tantalum. Delamination of the TZM-alloy foil prevented completely satisfactory results by the resistance-bonding process. Delamination of TD nickel when joints were tested at high temperature prevented the completion of a good system for this alloy too.

The program at Northrop Corp. to develop brazing alloys for molybdenum and tantalum has continued into the second year.[43] Work is now in progress on a series of hafnium-base

Table V-1 ELECTRON-BEAM-WELD STUDIES[5]

Material	Dimensions, in.	Welding parameters					Remarks
		kv	ma	Travel speed, in./min	Distance from heat shield, in.	Other	
Uranium	2 by 6 by 0.400	150	10 to 17.5	20 to 30	3	Deflection and circle	Preliminary welds for full penetration
Uranium	2 by 6 by 0.125	130 to 150	5 to 10	20 to 40	3	Deflection	Preliminary welds for full penetration
Type 1100 aluminum welded to uranium	2 by 2 by 1/16 2 by 2 by 1/8	120 to 140	2 to 6	30 to 40	3	Deflection and circle	This dissimilar-metal combination was not too successful
Tungsten	1 by 3 by 1/4	150	10 to 16.5	3 to 5	3		Poor weld and arcing; this grade of material was not weldable
20% nickel maraging steel	4 by 6 by 1/2	150	15	30	2 1/2		Full penetration; good appearance but no tests performed
B-66*	1/2 by 4 by 0.060	130	4.5	30	3	0.040-in. *L* deflection	Full penetration with optimum appearance on both sides
T-111†	1/2 by 4 3/4 by 0.066	120	6.8	30	3	0.040-in. *L* deflection	Full penetration with optimum appearance on both sides
Ta–10 wt.% W	4 1/2 by 8 by 0.200	150	17	20	2 3/4		Full penetration
Ta–10 wt.% W		130	10	20	2 3/4	0.020-in. ϕ circle	Second pass to smooth up surface
D-43‡	1/2 by 5 by 0.060	130	6.5	30	3	0.060-in. *L* deflection	Full penetration with optimum appearance on both sides
C-129Y§	1/2 by 3 by 0.028	130	3.5	30	3	0.060-in. *L* deflection	Full penetration with optimum appearance on both sides
Be-Cu	2 by 6 by 3/8	100	6.0	30	2 7/8		0.075-in. penetration
Be-Cu	2 by 6 by 3/8	130	5.0	30	3		0.110-in. penetration
Armco iron	2 dia. by 8 high by 2 1/8 thick	100	5.0	20	3	0.040-in. *L* deflection	Seal-weld required; excess outgassing caused difficulty
Type 6061 aluminum	8.6-dia. parts with 0.5 wall	120	5.0	30	3	0.030-in. *T* deflection	Partial penetration (0.050 min.) required with minimum distortion
Copper	4 by 10 by 0.090	100 to 130	5 to 12	16 to 30	3	0.040- to 0.080-in. *L* deflection	Preliminary welds for full penetration with good appearance
Type 304 stainless steel	2 by 4 by 0.007	70	0.40	30	3	0.010-in. ϕ circle	Full penetration; fit-up and hold-down critical
Be-Cu	3 by 7 by 0.145	130	6.5	30	3		0.118-in.-thick beryllium for backup; about 90% penetration obtained
Be-Cu	3 by 7 by 0.145	130	7.5	30	3		0.118-in.-thick beryllium for backup; full penetration obtained
Copper	1.5 dia. by 0.085 step joint	100	9.5	12.7	7 1/8	0.060-in. *L* deflection	Test samples for full penetration

*B-66 nominal: niobium 5, vanadium 5, molybdenum 1, zirconium.
†T-111 nominal: tantalum 8, tungsten 2, hafnium.
‡D-43 nominal: niobium 10, tungsten 1, zirconium 0.1, carbon.
§C-129Y nominal: niobium 10, tungsten 10, hafnium 0.1, yttrium.

Table V-2 ELECTRODES USED FOR RESISTANCE-HEATED BONDING[41]

Alloy	Bonding conditions	Electrode material
Niobium-base D-36, D-43, and B-66	2450°F 12,000 psi 20 sec	Tungsten alloys: 1% thoriated; 2% thoriated; 3% rhenium; all perform equally well
Tantalum-base T-111	2600°F 24,000 psi 20 sec	Tungsten–3 wt.% rhenium distinctly superior to thoriated alloys; approximately 30 bonds without refacing; cost is 40 times greater than for thoriated electrodes
Molybdenum-base TZM	2450°F 12,000 psi 20 sec	Electrode problems are not critical with the bonding of either molybdenum or tungsten alloys; 1% thoriated tungsten was used; approximately 50 bonds without refacing
Nickel-base TD nickel	2100°F 12,000 psi 20 sec	Severe electrode problem; tungsten-alloy electrodes useful only below 1700°F; can be used to 2200°F with film of graphite parting agent on face; approximately 10 bonds without refacing

Table V-3 RESISTANCE BONDING OF B-66 ALLOY[41]

Parent Material: 0.012-in. B-66 Alloy
Joint Area: 0.050 by 0.375 in.
Total Heating Time: 18 sec
Atmosphere: Vacuum-Purged Argon from 2×10^{-4} torr

Surface preparation	Intermediate foil	Specimens	Temp., °F	Pressure, 1000 psi	Peel, lb/in. Average	Peel, lb/in. Deviation	Parent material failure in peel, %
Etched	Tantalum, 0.0003 in.	2	2400	12	211*		
		1	2500	12	304*		
		2	2600	12	283	52	71
		9	2600	15	295	32	92
Etched	Niobium, 0.0005 in.	2	2400	12	181*		
		2	2500	12	128*		
Etched	Vanadium, 0.001 in.	2	2400	12	121*		
		2	2500	12	370*		
		4	2600	12	280	77	82
Pennsalt degreased	Tantalum	2	2600	12	429	19	70
	Vanadium	2	2600	12	402	16	35
Abraded and Pennsalt degreased	Tantalum	1	2600	12	419		50
	Vanadium	2	2600	12	306	18	25
Abraded and Pennsalt degreased	None	8	2700	12	445	40	74
		9	2700	12	434	68	98

*Tested in shear prior to peel test.

alloys containing relatively low concentrations of the offending melting-point depressants. The braze-alloy systems being considered are: Hf–40 Ta, Hf–10 Mo, Hf–10 Mo–(5 to 15 Zr), Hf–7 Mo–5 V, and Hf–25 Nb–15 Zr.

The objective of a continuing steel-welding program at Thompson Ramo Wooldridge Inc. is to find procedures and filler metals that will permit production of 95% efficient joints with the ductility and toughness of certain HY-180/200 steels.[44] The work covers the following alloys in the martensitic condition: HP 9-4-20, HP 9-4-25, and Vasco Jet X-2. The bainitic alloys, HP 9-4-45 and D6ac, are also included. Conclusions drawn so far are as follows:

1. Tensile tests conducted on Vasco Jet material quenched and triple tempered at 1075°F resulted in yield strengths of 186,000 to 191,000 psi, well within the desired 180,000 to 200,000-psi range.

2. Modified HP 9-24-20 filler wires of basic composition with a 0.05% titanium addition gave yield strengths of 190,000 to 202,000 psi. However, some loss in ductility resulted from the titanium addition.

3. The TIG welds made in Vasco Jet plate with filler wire of matching composition had ultimate and yield strengths below those desired.

4. The HP 9-4-45 alloy as ½-in. plate that was transformed to bainite at 590°F for 7 hr did not have desirable strength.

5. The D6ac material that was transformed to bainite at 625°F for 4 hr did not have desirable strength.

6. The TIG welds made in HP 9-4-45 plate with matching filler wire provided did not give the desired properties.

7. Specimens consisting entirely of weld deposit from weldments in D6ac material were marginal when a postheat of 575°F for 2 hr was used. Specimens tested from welds made using postheats of 625°F for 4 hr gave strengths that were too low.

This work on high-strength steels is a continuation of an earlier program in which good procedures and filler metals were found for use when HP 9-4-20 is TIG welded.[45] But welds made by the metal-arc–inert-gas (MIG) process had poor properties because of the loss of carbon during welding.

Some rather broad conclusions have been published by Douglas Aircraft Co. as a result of their studies of the welding of 18 Ni–7 Co–5 Mo maraging steel.[46] These are:

1. "High energy" MIG welding techniques are adequate for welding 0.75-in. plate.

2. The standard mechanical properties of welds containing 1.0% titanium are less sensitive to aging-cycle variations than welds made with the nominal titanium content (0.5%).

3. The fracture toughness of welds is relatively insensitive to variations in welding technique and weld composition where aging is at 900°F for 12 hr.

4. The welds have poorer fracture toughness than the base metal. Fracture appears to be associated with an unidentified phase in the weld metal.

5. Welds and base metal of the 18 Ni–7 Co–4 Mo alloy are more resistant to delayed failure than AISI type 4340 steel at equivalent strength levels.

There are two relatively new publications that should be of value to those interested in metals-joining technology relative to reactor fabrication.[47,48] (R. M. Evans)

Nondestructive Testing

Ultrasonic Techniques

A frequent question concerning ultrasonic techniques of nondestructive testing is, "Are there any established ultrasonic test specifications?" A report compiled at Savannah River Laboratory[47] contains a useful section on ultrasonic techniques, a small part of which discusses ultrasonic test specifications, including military standards, ASTM specifications, and commercial specifications. Although the report would be more useful if it were updated and more thorough, it does provide information that would aid in training personnel and in locating specifications. As the report states, acceptance standards are subject to agreement between purchaser and supplier.

According to researchers at Hanford,[49] preliminary experiments with ultrasonic critical-angle techniques indicate that fatigue can be detected before the cracks initiate. Two samples each of AISI 304L and 4340 stainless steel and A-212 carbon steel were tested prior to being subjected to fatigue. One sample of each metal was retained as a standard, and the others were fatigued to 80 to 90% of fatigue life. Beam-shift signal changes ranged from a factor of 2.3 to 10 when signals after fatigue were compared with those before fatigue.

(D. Ensminger)

NDT Techniques Other Than Ultrasonic

A neutron-image intensification system is under development by investigators at Argonne.[27,50–52] The system employs an image-intensifier tube constructed by The Rauland Corp. The output phosphor of the intensifier tube can be observed directly, or with a closed-circuit television system to bring the image out of the radiation area. The threshold sensitivity of the intensifier appears to exceed the predicted value of 10^5 thermal neutrons/(cm^2)(sec) when observed directly, with further improvement offered by the TV system. Initial investigations of the new system's ability to discriminate thickness changes in metals[50] indicate

that 8 to 10% changes can be detected in natural uranium 2 to 4 cm thick. Investigations to measure the brightness of the output phosphor of the intensifier in response to neutrons and high-energy gamma radiation are being conducted,[52] and the characteristics of the system in regard to contrast sensitivity (4%) and speed of response (minimum blurring at 20 m/min)[51] are being determined. When the system was used for a postirradiation annealing study of an irradiated fuel pin, motion-picture and videotape records were made over a 5-hr period.[27] Improved resolution is expected from a new intensifier on order that will provide reduced target-to-window spacing.

(A. F. Leatherman)

References

1. General Electric Company, Advanced Technology Services, Fourth Annual Report, High-Temperature Materials and Reactor Component Development Programs, Vol. I, Materials, USAEC Report GEMP-334A, Feb. 26, 1965.
2. General Electric Company, Advanced Technology Services, High-Temperature Materials Program, Progress Report No. 43, Part A, USAEC Report GEMP-43A, Jan. 29, 1965.
3. Bureau of Mines, Albany Metallurgy Research Center, Metallurgical Quarterly Progress Report No. 25, October 1–December 31, 1964, USAEC Report USBM-RC-1150.
4. P. A. Santoli, Extruding and Drawing Molybdenum to Complex Thin H-Section, First Interim Technical Engineering Report, July 1–September 30, 1963, Report RTD-TR-8-112, Allegheny Ludlum Steel Corp., October 1963.
5. Union Carbide Nuclear Co., Y-12 Development Activities Progress Report November 1963–January 1964, USAEC Report Y-1477, Feb. 3, 1965. (Classified)
6. National Lead Co. of Ohio, Summary Technical Report for the Period October 1–December 31, 1964, USAEC Report NLCO-940, Feb. 10, 1965.
7. A. T. Semenchenkov and O. S. Ivanov, Effect of Repeated Tempering on Cracking of Uranium Alloys, USAEC Report WAPD-Trans-11, translated from *Stroenie i Svoistva Splavov Urana, Toriya i Tsirkoniya*, pp. 47-60, Gosatomizdat, Moscow (Russian), 1963.
8. M. J. Albom, Solid State Welding of Reactive and Refractory Metals, *Mater. Design Eng.*, 61(4): 106-109 (April 1965).
9. R. W. Dayton and S. J. Paprocki, Progress Relating to Civilian Applications During January 1965, USAEC Report BMI-1711, Battelle Memorial Institute, Feb. 1, 1965. (Classified)
10. R. W. Dayton and S. J. Paprocki, Progress Relating to Civilian Applications During December 1964, USAEC Report BMI-1707, Battelle Memorial Institute, Jan. 1, 1965. (Classified)
11. J. K. Green (Ed.), Research and Development Programs Executed for the Division of Reactor Development, Quarterly Progress Report, January–March 1964, USAEC Report HW-81984, Hanford Atomic Products Operation, September 1964.
12. Hanford Atomic Products Operation, Ceramics Research and Development Operation, Quarterly Report, July–September 1964, USAEC Report HW-81602.
13. W. Parker, H. Bildstein, and N. Getoff, Electrodeposition of Thorium and Uranium, *Nucl. Instr. Methods*, 26: 55-60 (February–March 1964).
14. W. Parker et al., A Rapid Quantitative Method for the Electrodeposition of the Rare-Earth Elements, *Nucl. Instr. Methods*, 26: 61-65 (February–March 1964).
15. C. Marzano, Plating of Tungsten, *Plating*, 51: 207-271 (March 1964).
16. E. Caretta, R. Di Pietro, and R. Sesini, Electroplating of Zircaloy-2 with Copper, *Energia Nucl. (Milan)*, 11: 505-508 (September 1964).
17. R. L. Mack, J. Kozikowski, R. D. Stevenson, and L. M. Niebylski, Metal-Organic Compounds for Vapor-Plating Applications, Report GR 65-16, Ethyl Corp. Research Laboratories, Jan. 31, 1965.
18. J. H. Oxley, E. A. Beidler, J. M. Blocher, Jr., C. J. Lyons, R. S. Park, and J. H. Pearson, Fluoride Tungsten, *Trans. Am. Nucl. Soc.*, 7(2): 426 (November 1964).
19. General Atomic Division, General Dynamics Corp., and John Jay Hopkins Laboratory for Pure and Applied Science, Vapor-Deposited Tungsten, Report NASA CR-54266 (GA-5640; N65-15591), Oct. 6, 1964.
20. R. G. Mills, J. R. Lindgren, and A. F. Weinberg, An Evaluation of Vapor-Deposited Tungsten Tubing, Report NASA CR-54277 (GA-5721), General Atomic Division, General Dynamics Corp., Oct. 19, 1964.
21. A. F. Weinberg, N. B. Elsner, R. G. Mills and J. R. Lindgren, Grain-Growth Characteristics of Vapor-Deposited Tungsten at Temperatures up to 2500°C, *Trans. Am. Nucl. Soc.*, 7(2): 427 (November 1964).
22. J. I. Federer and C. F. Leitten, Jr., Vapor Deposition of Tungsten-Rhenium Alloys, *Trans. Am. Nucl. Soc.*, 7(2): 425 (November 1964).
23. A. C. Nyce, B. L. Vondra, R. Cline, and L. P. Pepkowitz, Applications and Properties of the Tungsten Cementation Process, *Trans. Am. Nucl. Soc.*, 7(2): 427-428 (November 1964).
24. I. Weissman, Improved Thermionic Emitter: Thorium on Grain-Oriented Polycrystalline Tungsten, *J. Appl. Phys.*, 36(2): 406-411 (February 1965).
25. J. Y. Chang, Studies on Effects of Deposition Conditions and Heat Treatment on the Properties of Pyrolytic Carbon, USAEC Report ORNL-3764, Oak Ridge National Laboratory, March 1965.
26. W. H. Roberts, Coating Beryllium with Electroless Nickel, USAEC Report RFP-478, Dow Chemical Co., Dec. 29, 1964.
27. Argonne National Laboratory, Reactor Development Program Progress Report, February 1965, USAEC Report ANL-7017, Mar. 18, 1965.
28. J. C. McGuire, Simple Experimental Techniques for Deposition of Tungsten from Tungsten Hexacarbonyl, *Trans. Am. Nucl. Soc.*, 7(2): 426-427 (November 1964).
29. R. W. Bartlett and P. R. Gage, Investigation of Mechanisms for Oxidation Protection and Failure of Intermetallic Coatings for Refractory Metals,

Report ASD-TDR-63-753 (Pt. II), Philco Corporation, Aeronutronic Division, July 1964.
30. R. W. Bartlett, Investigation of Mechanisms for Oxidation Protection and Failure of Intermetallic Coatings for Refractory Metals, Tenth Quarterly Progress Report, Philco Corporation, Aeronutronic Division, Jan. 15, 1965.
31. J. M. Criscione, R. A. Mercuri, E. P. Schram, A. W. Smith, and H. F. Volk, High-Temperature Protective Coatings for Graphite, Report ML-TDR-64-173 (Pt. I), Union Carbide Corporation, December 1964.
32. V. A. Nieberlein, Vapor-Deposited Tungsten Coatings on Graphite, *Am. Ceram. Soc. Bull.*, 44: 14-17 (January 1965).
33. K. S. Mazdiyasni and C. T. Lynch, An Approach to the Preparation of Powders, Fibers, and Films of Ultra-High-Purity Ceramics, Report ML-TDR-64-269, Research and Technology Division, Air Force Materials Laboratory, August 1964.
34. Union Carbide Corporation, Pyrolytic Coating of Carbon Filaments, Report ML-TDR-64-297, November 1964.
35. D. M. Mattox, Metallizing Ceramics Using a Gas Discharge, USAEC Report SC-R-64-1330, Sandia Corp., September 1964.
36. N. N. Ida and A. A. Ezra, Die-Less, Explosive Forming of One-Piece Thin Shells of Revolution, presented at The American Society of Tool and Manufacturing Engineers, Creative Manufacturing Seminars, 1962–1963, Paper No. SP-63-27.
37. N. N. Ida and J. T. Snyder, Explosive Forming by Use of the Plug-Cushion Technique, presented at The American Society of Tool and Manufacturing Engineers, Creative Manufacturing Seminars, 1962–1963, Paper No. SP-63-32.
38. L. M. Bianchi, W. A. McNeish, and F. D. Seaman, Welding of Refractory Metals, Final Report to U.S. Navy Bureau of Weapons, Universal-Cyclops Steel Corporation, Refractomet Division, July 1964.
39. G. G. Lessmann and D. R. Stoner, Determination of the Weldability and Elevated-Temperature Stability of Refractory Metal Alloys, Report WANL-PR-(P)-005, Westinghouse Electric Corp., Astronuclear Laboratory, September 1964.
40. Uses Cryogenics in Refractory Joining, *Metalworking News*, 6(242): (Mar. 22, 1965).
41. A. G. Metcalfe, F. K. Rose, and J. S. Dunning, Final Report on Diffusion Bonding of Refractory Metals and TD Nickel, Vol. I, Development of Diffusion Bonding Processes, Report AFML-TR-64-394 (Vol. I), Solar Aircraft Co., Division of International Harvester Co., December 1964.
42. A. G. Metcalfe, F. K. Rose, and A. Zumbrunnen, Final Report on Diffusion Bonding of Refractory Metals and TD Nickel, Vol. II, Evaluation of Bonding Processes, Report AFML-TR-64-394 (Vol. II), Solar Aircraft Co., Division of International Harvester Co., December 1964.
43. Northrop Corp., Tantalum and Molybdenum Brazing Techniques, 5th Quarterly Progress Report, Report NOR-65-3, January 1965.
44. J. M. Faulkner and G. L. Hanna, Development of Welding Processes and Filler Materials for Joining High-Strength Low-Alloy Steels, 6th Quarterly Progress Report, Thompson Ramo Wooldridge Inc., Dec. 31, 1964.
45. J. M. Faulkner, G. L. Hanna, and J. V. Peck, Development of Welding Processes and Filler Materials for Joining High-Strength Low-Alloy Steels, Report ML-TDR-64-255, Thompson Ramo Wooldridge Inc., August 1964.
46. Z. P. Saperstein and B. V. Whiteson, The Properties of Welded 18 Ni-7 Co-5 Mo Plate, Report AD-604052 (SM-45959), Douglas Aircraft Co., Inc., Apr. 30, 1964.
47. W. C. Rion, Jr. (Comp.), Stainless Steel Information Manual for Savannah River Plant, Vol. II, Fabrication, USAEC Report DP-860, Savannah River Laboratory, July 1964.
48. G. M. Slaughter, Welding and Brazing Techniques for Nuclear Reactor Components, An AEC–ASM Monograph, Rowman and Littlefield, Inc., New York, 1964.
49. Hanford Atomic Products Operation, Research and Development Programs Executed for the Division of Reactor Development, Quarterly Progress Report, April–June, 1964, USAEC Report HW-83298, November 1964.
50. Argonne National Laboratory, Reactor Development Program, Progress Report, November 1964, USAEC Report ANL-6977, Dec. 21, 1964.
51. Argonne National Laboratory, Reactor Development Program, Progress Report, January 1965, USAEC Report ANL-7003, Feb. 18, 1965.
52. Argonne National Laboratory, Reactor Development Program, Progress Report, December 1964, USAEC Report ANL-6997, Jan. 18, 1965.

LEGAL NOTICE

This journal was prepared under the sponsorship of the U. S. Atomic Energy Commission. Neither the United States, nor the Commission, nor any person acting on behalf of the Commission:

A. Makes any warranty or representation, expressed or implied, with respect to the accuracy, completeness, or usefulness of the information contained in this journal, or that the use of any information, apparatus, method, or process disclosed in this journal may not infringe privately owned rights; or

B. Assumes any liabilities with respect to the use of, or for damages resulting from the use of any information, apparatus, method, or process disclosed in this journal.

As used in the above, "person acting on behalf of the Commission" includes any employee or contractor of the Commission, or employee of such contractor, to the extent that such employee or contractor of the Commission, or employee of such contractor prepares, disseminates, or provides access to, any information pursuant to his employment or contract with the Commission, or his employment with such contractor.

NUCLEAR SCIENCE ABSTRACTS

The U. S. Atomic Energy Commission, Division of Technical Information, publishes *Nuclear Science Abstracts (NSA)*, a semimonthly journal containing abstracts of the literature of nuclear science and engineering.

NSA covers (1) research reports of the U. S. Atomic Energy Commission and its contractors; (2) research reports of government agencies, universities, and industrial research organizations on a world-wide basis; and (3) translations, patents, books, and articles appearing in technical and scientific journals.

Complete indexes covering subject, author, source, and report number are included in each issue. These are cumulated quarterly, semiannually, and annually providing a detailed and convenient key to the literature.

Availability of *NSA*

SALE *NSA* is available on subscription from the Superintendent of Documents, U. S. Government Printing Office, Washington, D. C., 20402, at $30.00 per year for the semimonthly abstract issues and $22.00 per year for the four cumulated-index issues. Subscriptions are postpaid within the United States, Canada, Mexico, and all Central and South American countries, except Argentina, Brazil, British and French Guiana, Surinam, and British Honduras. Subscribers in these Central and South American countries, and in all other countries throughout the world, should remit $37.00 per year for subscriptions to semimonthly abstract issues and $25.00 per year for the four cumulated-index issues.

EXCHANGE *NSA* is also available on an exchange basis to universities, research institutions, industrial firms, and publishers of scientific information. Inquiries should be directed to the Division of Technical Information Extension, U. S. Atomic Energy Commission, P. O. Box 62, Oak Ridge, Tennessee, 37831.

TECHNICAL PROGRESS REVIEWS may be purchased from Superintendent of Documents, U. S. Government Printing Office, Washington, D. C., 20402. *Isotopes and Radiation Technology* at $2.00 per year for each subscription or $0.55 per issue; the other four journals at $2.50 per year and $0.70 per issue. The use of the coupon below will facilitate the handling of your order.

POSTAGE AND REMITTANCE: Postpaid within the United States, Canada, Mexico, and all Central and South American countries except as hereinafter noted. Add $0.50 per year or $0.15 per single issue for the *Isotopes and Radiation Technology* journal and $0.75 per year or $0.20 per single issue for the other four journals for postage to all other countries, including Argentina, Brazil, British and French Guiana, Surinam, and British Honduras. Payment should be by check, money order, or document coupons and MUST accompany order. Remittances from foreign countries should be made by international money order or draft on an American bank, payable to the Superintendent of Documents, or by UNESCO book coupons.

order form

SUPERINTENDENT OF DOCUMENTS
U. S. GOVERNMENT PRINTING OFFICE
WASHINGTON, D. C., 20402

Enclosed:
document coupons ☐ check ☐ money order ☐

Charge to Superintendent of Documents No. _____

Please send a one-year subscription to

☐ NUCLEAR SAFETY

☐ POWER REACTOR TECHNOLOGY

☐ REACTOR FUEL PROCESSING

☐ REACTOR MATERIALS

(Each subscription $2.50 per year; $0.70 per issue.)

☐ ISOTOPES AND RADIATION TECHNOLOGY

(Each subscription $2.00 a year; $0.55 per issue.)

SUPERINTENDENT OF DOCUMENTS
U. S. GOVERNMENT PRINTING OFFICE
WASHINGTON, D. C., 20402

(Print clearly)

_____
Name

_____
Street

_____
City, State, ZIP Code